NASA TR R-111

NATIONAL AERONAUTICS AND SPACE ADMINISTRATION

TECHNICAL REPORT
R-111

THEORETICAL PERFORMANCE OF HYDROGEN-OXYGEN ROCKET THRUST CHAMBERS

By GILBERT K. SIEVERS, WILLIAM A. TOMAZIC,
and GEORGE R. KINNEY

1961

For sale by the Superintendent of Documents, U.S. Government Printing Office, Washington 25, D.C. Yearly subscription, $15; foreign, $19; single copy price varies according to size --------- Price 65 cents

19980227353 IR

NASA TR R-111
National Aeronautics and Space Administration.
THEORETICAL PERFORMANCE OF HYDROGEN-OXYGEN ROCKET THRUST CHAMBERS. Gilbert K. Sievers, William A. Tomazic, and George R. Kinney. 1961. i, 75 p. diagrs., tabs. GPO price 65 cents. (NASA TECHNICAL REPORT R-111.)

Data are presented for liquid-hydrogen—liquid-oxygen thrust chambers at chamber pressures from 15 to 1200 pounds per square inch absolute, area ratios to approximately 300, and percent fuel from about 8 to 34 for both equilibrium and frozen composition during expansion. Specific impulse in vacuum, specific impulse, combustion-chamber temperature, nozzle-exit temperature, characteristic velocity, and the ratio of chamber-to-nozzle-exit pressure are included. The data are presented in convenient graphical forms to allow quick calculation of theoretical nozzle performance with over- or underexpansion, flow separation, and introduction of the propellants at various initial conditions or heat loss from the combustion chamber.

(Initial NASA distribution: 39, Propulsion systems, liquid-fuel rockets; 44, Propulsion systems, theory.)
Copies obtainable from Supt. of Docs., GPO, Washington

I. Sievers, Gilbert K.
II. Tomazic, William A.
III. Kinney, George R.
IV. NASA TR R-111

NASA

NASA TR R-111
National Aeronautics and Space Administration.
THEORETICAL PERFORMANCE OF HYDROGEN-OXYGEN ROCKET THRUST CHAMBERS. Gilbert K. Sievers, William A. Tomazic, and George R. Kinney. 1961. i, 75 p. diagrs., tabs. GPO price 65 cents. (NASA TECHNICAL REPORT R-111.)

Data are presented for liquid-hydrogen—liquid-oxygen thrust chambers at chamber pressures from 15 to 1200 pounds per square inch absolute, area ratios to approximately 300, and percent fuel from about 8 to 34 for both equilibrium and frozen composition during expansion. Specific impulse in vacuum, specific impulse, combustion-chamber temperature, nozzle-exit temperature, characteristic velocity, and the ratio of chamber-to-nozzle-exit pressure are included. The data are presented in convenient graphical forms to allow quick calculation of theoretical nozzle performance with over- or underexpansion, flow separation, and introduction of the propellants at various initial conditions or heat loss from the combustion chamber.

(Initial NASA distribution: 39, Propulsion systems, liquid-fuel rockets; 44, Propulsion systems, theory.)
Copies obtainable from Supt. of Docs., GPO, Washington

I. Sievers, Gilbert K.
II. Tomazic, William A.
III. Kinney, George R.
IV. NASA TR R-111

NASA

NASA TR R-111
National Aeronautics and Space Administration.
THEORETICAL PERFORMANCE OF HYDROGEN-OXYGEN ROCKET THRUST CHAMBERS. Gilbert K. Sievers, William A. Tomazic, and George R. Kinney. 1961. i, 75 p. diagrs., tabs. GPO price 65 cents. (NASA TECHNICAL REPORT R-111.)

Data are presented for liquid-hydrogen—liquid-oxygen thrust chambers at chamber pressures from 15 to 1200 pounds per square inch absolute, area ratios to approximately 300, and percent fuel from about 8 to 34 for both equilibrium and frozen composition during expansion. Specific impulse in vacuum, specific impulse, combustion-chamber temperature, nozzle-exit temperature, characteristic velocity, and the ratio of chamber-to-nozzle-exit pressure are included. The data are presented in convenient graphical forms to allow quick calculation of theoretical nozzle performance with over- or underexpansion, flow separation, and introduction of the propellants at various initial conditions or heat loss from the combustion chamber.

(Initial NASA distribution: 39, Propulsion systems, liquid-fuel rockets; 44, Propulsion systems, theory.)
Copies obtainable from Supt. of Docs., GPO, Washington

I. Sievers, Gilbert K.
II. Tomazic, William A.
III. Kinney, George R.
IV. NASA TR R-111

NASA

NASA TR R-111
National Aeronautics and Space Administration.
THEORETICAL PERFORMANCE OF HYDROGEN-OXYGEN ROCKET THRUST CHAMBERS. Gilbert K. Sievers, William A. Tomazic, and George R. Kinney. 1961. i, 75 p. diagrs., tabs. GPO price 65 cents. (NASA TECHNICAL REPORT R-111.)

Data are presented for liquid-hydrogen—liquid-oxygen thrust chambers at chamber pressures from 15 to 1200 pounds per square inch absolute, area ratios to approximately 300, and percent fuel from about 8 to 34 for both equilibrium and frozen composition during expansion. Specific impulse in vacuum, specific impulse, combustion-chamber temperature, nozzle-exit temperature, characteristic velocity, and the ratio of chamber-to-nozzle-exit pressure are included. The data are presented in convenient graphical forms to allow quick calculation of theoretical nozzle performance with over- or underexpansion, flow separation, and introduction of the propellants at various initial conditions or heat loss from the combustion chamber.

(Initial NASA distribution: 39, Propulsion systems, liquid-fuel rockets; 44, Propulsion systems, theory.)
Copies obtainable from Supt. of Docs., GPO, Washington

I. Sievers, Gilbert K.
II. Tomazic, William A.
III. Kinney, George R.
IV. NASA TR R-111

NASA

TECHNICAL REPORT R-111

THEORETICAL PERFORMANCE OF HYDROGEN-OXYGEN ROCKET THRUST CHAMBERS

By GILBERT K. SIEVERS, WILLIAM A. TOMAZIC, and GEORGE R. KINNEY

Lewis Research Center
Cleveland, Ohio

TECHNICAL REPORT R-111

THEORETICAL PERFORMANCE OF HYDROGEN-OXYGEN ROCKET THRUST CHAMBERS

By GILBERT K. SIEVERS, WILLIAM A. TOMAZIC, and GEORGE R. KINNEY

SUMMARY

Theoretical rocket performance data for the propellant combination of liquid hydrogen and liquid oxygen are presented in convenient graphical forms to permit rapid determination of specific impulse, vacuum specific impulse, and characteristic velocity. Data are presented for both frozen and equilibrium composition during expansion for chamber pressures of 15, 30, 60, 150, 300, 600, 900, and 1200 pounds per square inch absolute over a wide range of percent fuel from approximately 8 to 34 and area ratios to approximately 300. For rapid calculation of the theoretical nozzle performance with over- or underexpansion, separated flow, and introduction of propellants at different initial conditions or heat loss from the combustion chamber, the following theoretical data are also presented: combustion-chamber temperature, nozzle-exit temperature, and the ratio of chamber-pressure to nozzle-exit pressure. An easy method is given for estimating theoretical specific impulse at chamber pressures other than those presented.

INTRODUCTION

Interest in hydrogen-oxygen as a rocket propellant combination for a wide variety of applications including stages for launch vehicles and outer space probes has increased the need for theoretical performance data over a wider range of chamber pressures than has been generally available (60, 150, 300, and 600 lb/sq in. abs, ref. 1). To answer this need, data for chamber pressures of 15, 30, 900, and 1200 pounds per square inch absolute were calculated.

Generally, rocket performance parameters (I_{vac}, I, c^*) have been tabulated or presented graphically as a function of pressure ratio. In this report, specific impulse data are presented in a convenient graphical form as functions of the ratio of nozzle-exit to nozzle-throat area. Characteristic velocity data are presented as functions of chamber pressure. These plots, which may be obtained in large working sizes (by using the request form in back of report), eliminate tedious time-consuming interpolation. The following conditions are considered:

(1) Eight chamber pressures (15, 30, 60, 150, 300, 600, 900, and 1200 lb/sq in. abs)
(2) A wide range of percent fuel by weight (7.749 to 33.51)
(3) Equilibrium and frozen composition during expansion
(4) A wide range of area ratio (1 to approx. 300)

Methods are described for using these data to obtain quick calculations or estimates of theoretical performance at the following conditions:

(1) Over- or underexpanded flow in nozzle flowing full
(2) Flow separation in nozzle
(3) Introduction of the propellants at different initial conditions or heat loss from the combustion chamber
(4) Chamber pressures other than those presented

SYMBOLS

A nozzle area, sq in.

C_F coefficient of thrust, $C_F = g_c I / c^* = F / P_c A_t$

c^* characteristic velocity, $g_c P_c A_t / w$, ft/sec

c_p specific heat at constant pressure, $(\partial h / \partial T)_p$, cal/(g)(°K)

F thrust, lb

g_c gravitational conversion factor, $32.174 \left(\frac{\text{lb mass}}{\text{lb force}}\right)\left(\frac{\text{ft}}{\text{sec}^2}\right)$

H_T° sum of sensible enthalpy and chemical energy at temperature T, cal/mole

h sum of sensible enthalpy and chemical energy per unit mass,

$$\sum_i x_i(H_T^\circ)_i/M, \text{ cal/g}$$

I specific impulse with ambient and nozzle-exit pressures equal, (lb force) (sec)/lb mass

I_{vac} specific impulse in vacuum, (lb force) (sec)/lb mass

M molecular weight, $\sum_i x_i M_i$, g/g-mole or lb/lb-mole

O/F oxidant-fuel weight ratio

P static pressure (sum of partial pressures), lb/sq in. abs

R equivalence ratio, ratio of two times the number of oxygen atoms to the number of hydrogen atoms, 2(O)/(H)

T temperature, °K

w mass-flow rate, lb/sec

x mole fraction

ϵ ratio of nozzle-exit area to nozzle-throat area, A_e/A_t

ϵ_s ratio of nozzle-separation area to nozzle-throat area, A_s/A_t

Subscripts:

a ambient

c combustion chamber

e nozzle exit

i product of combustion

m mean, after flow separation

o at initial or calculated theoretical conditions

p constant pressure

s at separation point

t nozzle throat

1 corrected for over- or underexpansion of flow in nozzle

2 corrected for change in initial heat content of propellants or heat loss from combustion chamber

3 corrected for change in initial heat content of propellants or heat loss from combustion chamber and over- or underexpansion of nozzle

4 corrected for flow separation in nozzle

METHOD OF CALCULATION

Theoretical rocket performance data for liquid hydrogen—liquid oxygen at chamber pressures of 60, 150, 300, and 600 pounds per square inch absolute were obtained directly from reference 1. Additional theoretical performance data at chamber pressures of 15, 30, 900, and 1200 pounds per square inch absolute, assuming both frozen and equilibrium composition during expansion, were furnished by the authors of reference 1.

The calculations were based on the assumptions used in reference 1 and are as follows: perfect gas law, adiabatic combustion at constant pressure, isentropic expansion, no friction, homogeneous mixing, and one-dimensional flow. The products of combustion were assumed to be the following ideal gases: atomic hydrogen, H; hydrogen, H_2; water, H_2O; atomic oxygen, O; oxygen, O_2; and the hydroxyl radical, OH. The propellants at injection were assumed to be at the boiling points as given in table I (from ref. 1).

THEORETICAL PERFORMANCE DATA

Three theoretical performance parameters, c^*, I_{vac}, and I, are plotted in figures 1 to 3 for both frozen and equilibrium composition during expansion for chamber pressures of 15, 30, 60, 150, 300, 600, 900, and 1200 pounds per square inch absolute with a range of percent fuel by weight from 7.749 to 33.51 as a parameter.

Figure 1 is a plot of characteristic velocity against chamber pressure. Figures 2 and 3 are plots of vacuum specific impulse and specific impulse, respectively, against the ratio of nozzle exit-to-throat area.

SUPPLEMENTAL DATA

In order to calculate theoretical performance at conditions other than those presented in this report, the following supplemental data are presented:

(1) Combustion-chamber temperature and specific heat for the given chamber pressures and percent fuel by weight, table II

(2) Nozzle-exit temperature, figure 4

(3) Ratio of chamber pressure to nozzle-exit pressure, figure 5

The parameters of figures 4 and 5 are presented as functions of nozzle area ratio.

METHODS OF USING SUPPLEMENTAL DATA

The methods and formulas presented herein are helpful in using the supplemental data to obtain

theoretical performance of nozzles being operated at the following conditions:

(1) Over- or underexpanded flow in nozzle flowing full (case A)
(2) Change in initial heat content of propellants or heat loss from the combustion chamber (case B)
(3) Combination of conditions (1) and (2) (case C)
(4) Flow separation in nozzle (case D)
(5) Chamber pressures other than those presented (case E)

These methods and formulas apply equally well to either frozen or equilibrium composition during expansion.

CASE A

OVER- OR UNDEREXPANSION OF FLOW IN NOZZLE FLOWING FULL

The specific impulse corrected for over- or underexpansion of flow in a nozzle flowing full is

$$I_1=I_o+\frac{P_e-P_a}{w}A_e \tag{1}$$

where

$$w=\frac{P_c A_t g_c}{c_o^*} \tag{2}$$

Therefore,

$$I_1=I_o+\frac{P_e-P_a}{P_c}\left(\frac{A_e}{A_t}\right)\left(\frac{c_o^*}{g_c}\right)$$

$$=I_o+\left(\frac{1}{P_c/P_e}-\frac{1}{P_c/P_a}\right)(\epsilon)\left(\frac{c_o^*}{g_c}\right) \tag{3}$$

For example, consider a thrust chamber using liquid hydrogen with liquid oxygen as a propellant. The nozzle has an area ratio of 6 and is to be operated at 300 pounds per square inch absolute chamber pressure and 13.6 percent fuel with an ambient pressure of 14.7 pounds per square inch absolute. The theoretical specific impulse with frozen composition during expansion is desired.

The values of the parameters needed for equation (3) are as follows:

$$\epsilon=6$$

$$P_c/P_a=20.41$$

I_o=343 lb-sec/lb from fig. 3(j)

P_c/P_e=43 from fig. 5(j)

c_o^*=7237 from fig. 1(b)

Therefore,

$$I_1=343+(1/43-1/20.41)\ (6)\ (7237/32.17)$$
$$=308 \text{ lb-sec/lb}$$

CASE B

CHANGE IN INITIAL HEAT CONTENT OF PROPELLANTS OR HEAT LOSS FROM THE COMBUSTION CHAMBER

The results presented in this report are computed for adiabatic combustion with propellants at the initial temperatures indicated in table I. A change in heat content of the combustion gases in the combustion chamber would result, for example, from heat loss in the combustion chamber or from the introduction of the propellants at a temperature other than the one indicated. The corrected specific impulse assuming isentropic expansion and the same combustion and exit pressures as in the initial calculations may be closely approximated by the following equation:

$$I_2^2=I_o^2+87\left(1-\frac{T_e}{T_c}\right)_0\Delta h_c \tag{4}$$

where Δh_c is the change in heat content of the combustion gases in the combustion chamber and the subscript o indicates the original values of the parameters. This equation is derived exactly in reference 2 for these conditions (isentropic expansion and constant pressure ratio) and contains a second-order term. Actually, if pressure ratio is held constant, a change in heat content of the combustion gases generally will require a change in area ratio; and conversely, if area ratio is held constant, the pressure ratio will change. However, numerous calculations have been made to compare the approximate values of specific impulse as given by equation (4) and the true theoretical values. These calculations indicate that by dropping the second-order term and assuming pressure ratio and area ratio to be constant, the error involved is about one impulse unit. This order of error should hold as long as Δh_c is no more than several hundred calories per gram of propellant. The accuracy of plotting and reading the curves is probably no greater than this.

Characteristic velocity c^* is also affected by a change in the heat content of the combustion gases. From

$$c^*=\frac{Ig_c}{C_F} \tag{5}$$

the corrected c_2^* becomes:

$$c_2^*=c_o^* \frac{I_2}{I_o} \frac{C_{F,o}}{C_{F,2}} \tag{6}$$

The ratio $C_{F,o}/C_{F,2}$ has been calculated and found to deviate from unity by less than 0.001 over a wide range of conditions. Therefore, for all practical purposes the ratio can be taken as equal to unity, and equation (6) reduces to

$$c_2^*=c_o^* \frac{I_2}{I_o} \tag{7}$$

As an illustration, a thrust chamber using gaseous hydrogen at 25° C with liquid oxygen as a propellant is considered. The nozzle has an area ratio of 10 and is to be operated at a chamber pressure of 150 pounds per square inch absolute and 15.24 percent fuel. The ambient pressure is that necessary for ideal expansion. The theoretical characteristic velocity and specific impulse with equilibrium composition during expansion are desired.

The parameter values necessary for equation (4) are as follows:

$(T_c)_o$=3231° K from table II
$(T_e)_o$=1895° K from fig. 4(g)
I_o=385 lb-sec/lb from fig. 3(g)

For this example, Δh_c is the enthalpy required to convert liquid hydrogen at its boiling point to gas at 25° C per gram of propellant. From table I,

$$\Delta H_T^\circ=1894 \text{ cal/mole}$$

For 15.25 percent hydrogen by weight,

$$M=\frac{2.016}{0.1525}=13.22 \text{ g/mole}$$

and

$$\Delta H_c=\frac{\Delta H_T^\circ}{M}=\frac{1894}{13.22}=143.3 \text{ cal/g}$$

The corrected specific impulse can now be obtained by substituting the preceding values into equation (4); therefore,

$$I_2^2=(385)^2+87\left(1-\frac{1895}{3231}\right)(143.3)$$

or

$$I_2=392 \text{ lb-sec/lb}$$

The corrected characteristic velocity c_2^* is determined by substituting the values of I_o, I_2, and c_o^* (7577 ft/sec from fig. 1(a)) into equation (7); therefore,

$$c_2^*=(7577)\left(\frac{392}{385}\right)=7690 \text{ ft/sec}$$

CASE C

COMBINATION OF CHANGE IN INITIAL HEAT CONTENT OF PROPELLANTS OR HEAT LOSS FROM THE COMBUSTION CHAMBER AND OVER- OR UNDEREXPANDED FLOW IN NOZZLE

The specific impulse corrected for change in initial heat content of propellants and for over- or underexpansion of flow is

$$I_3=I_2+\frac{P_e-P_a}{w_2} A_e \tag{8}$$

where I_2 is obtained from equation (4). Combining equations (2) and (7) gives

$$w_2=\left(\frac{P_c A_t g_c}{c_o^*}\right)\left(\frac{I_o}{I_2}\right) \tag{9}$$

By the use of equation (9), equation (8) becomes

$$\begin{aligned} I_3&=I_2+\frac{P_e-P_a}{P_c}\left(\frac{A_e}{A_t}\right)\left(\frac{c_o^*}{g_c}\right)\left(\frac{I_2}{I_o}\right) \\ &=I_2+\left(\frac{1}{P_c/P_e}-\frac{1}{P_c/P_a}\right)_o (\epsilon)\left(\frac{c_o^*}{g_c}\right)\left(\frac{I_2}{I_o}\right) \end{aligned} \tag{10}$$

The example given in case B is used to illustrate the use of this equation. All conditions are the same with the exception that the ambient pressure is 5.0 pounds per square inch absolute. The theoretical specific impulse with equilibrium composition during expansion is desired.

From case B,

I_o=385 lb-sec/lb
ϵ=10
P_c/P_a=30
I_2=392 lb-sec/lb
c_o^*=7577 ft/sec

The remaining value necessary for equation (10) is

P_c/P_e=73 from fig. 5(g)

Substituting into equation (10) gives the specific impulse corrected for change in initial heat content of propellants and for overexpansion of flow:

$$I_3=392+\left(\frac{1}{73}-\frac{1}{30}\right)(10)\left(\frac{7577}{32.17}\right)\left(\frac{392}{385}\right)$$

$$=345 \text{ lb-sec/lb}$$

CASE D

FLOW SEPARATION IN NOZZLE

The specific impulse corrected for flow separation in the nozzle is

$$I_4=I_s+\frac{P_s-P_a}{w}A_s+\frac{P_m-P_a}{w}(A_e-A_s) \quad (11)$$

where I_s is the theoretical specific impulse corresponding to the separation area ratio ϵ_s, which is determined by the separation pressure ratio P_c/P_s.

Much experimental work has been conducted to determine the values of P_s and P_m (see refs. 3, 4, and 5). Reference 3 states that the separation pressure for a nozzle is a function only of both ambient pressure and nozzle geometry. Data from various sources indicate that separation pressure is insensitive to other flow parameters including fluid properties and composition.

By rearranging terms and by the use of equation (2), equation (11) becomes

$$I_4=I_s+\left(\frac{c_o^*}{g_c}\right)\left[\epsilon_s\left(\frac{P_s}{P_c}-\frac{P_m}{P_c}\right)+\epsilon\left(\frac{P_m}{P_c}-\frac{P_a}{P_c}\right)\right] \quad (12)$$

To illustrate the use of this equation, a liquid-hydrogen—liquid-oxygen thrust chamber with a conical nozzle having a 15° half-angle divergence and an area ratio of 6 is considered. The thrust chamber is to be operated at a chamber pressure of 150 pounds per square inch absolute at 17.35 percent fuel with an ambient pressure of 10.0 pounds per square inch absolute. The specific impulse with frozen composition is desired.

The value of P_s, obtained from reference 4, is 3.56 pounds per square inch absolute. Therefore, $P_c/P_s=150/3.56=42.1$. By use of this value and figure 5(h), $\epsilon_s=5.8$. With this value and reference 4, P_m can be obtained and is 4.76 pounds per square inch absolute. Using the value of ϵ_s and figure 3(h) gives

$$I_s=359 \text{ lb-sec/lb}$$

From figure 1(b), $c_o^*=7621$ feet per second. Therefore, the corrected specific impulse for nozzle separation from equation (12) is

$$I_4=359+\left(\frac{7621}{32.17}\right)\left[5.8\left(\frac{3.56}{150}-\frac{4.76}{150}\right)+6\left(\frac{4.76}{150}-\frac{10.0}{150}\right)\right]$$

$$=298 \text{ lb-sec/lb}$$

CASE E

ESTIMATION OF THEORETICAL SPECIFIC IMPULSE AT CHAMBER PRESSURES OTHER THAN THOSE PRESENTED

There are many methods and procedures that can be used to estimate accurately the theoretical specific impulse at chamber pressures other than those presented in this report. One method of using the data is described herein. This method is valid over the entire range of pressure presented but is illustrated only for a particular range of pressure.

As an example, a liquid-hydrogen—liquid-oxygen thrust chamber is considered. The nozzle has an area ratio of 5 and is to be operated at a chamber pressure of 350 pounds per square inch absolute and 15.25 percent fuel with an ambient pressure of 14.7 pounds per square inch absolute. The theoretical specific impulse with equilibrium composition during expansion is desired.

By use of equation (3), the theoretical specific impulse can be calculated at 15.25 percent fuel at chamber pressures of 150, 300, and 600 pounds per square inch absolute. The necessary data are obtained from the appropriate curves and are as follows:

Parameter	Chamber pressure, lb/sq in. abs		
	150	300	600
ϵ	5	5	5
P_c/P_a	10. 21	20. 41	40. 83
I_0	351	352	354
P_c/P_e	28. 4	29. 0	29. 5
c_o^*	7577	7669	7669

Inserting these data into equation (3) gives

$$(I_1)_{150}=277 \text{ lb-sec/lb}$$

$$(I_1)_{300}=335 \text{ lb-sec/lb}$$

$$(I_1)_{600}=365 \text{ lb-sec/lb}$$

A plot of theoretical specific impulse against chamber pressure with percent fuel as a param-

eter can then be made on semilog paper as follows:

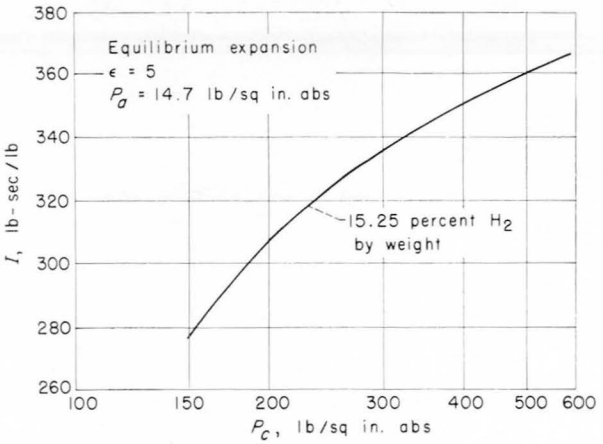

From this plot the specific impulse at the desired chamber pressure of 350 pounds per square inch absolute is found to be 343 pounds per second per pound.

This same procedure can be carried out for other percentages of fuel so that a cross plot of specific impulse against percent fuel can be obtained for any chamber pressure within the range of 150 to 600 pounds per square inch absolute. This is particularly useful and timesaving when test data are obtained with the same thrust chamber at various chamber pressures.

CONCLUDING REMARKS

This report contains theoretical data on hydrogen-oxygen as a rocket propellant combination over a wide range of chamber pressures (15 to 1200 lb/sq in. abs). Conventional rocket performance parameters are presented primarily as functions of expansion area ratio, so that the performance is related to engine geometry rather than to thermochemical parameters as is usually done. This form of presentation allows rapid and accurate calculation of theoretical performance for any hydrogen-oxygen rocket thrust chamber being operated at any chamber pressure within this range at design or off-design conditions. The off-design conditions include over- or underexpanded flow in nozzle, flow separation in nozzle, introduction of the propellants at a different level of heat content or heat loss from the combustion chamber.

LEWIS RESEARCH CENTER
NATIONAL AERONAUTICS AND SPACE ADMINISTRATION
CLEVELAND, OHIO, *March 13, 1961*

REFERENCES

1. Gordon, Sanford, and McBride, Bonnie J.: Theoretical Performance of Liquid Hydrogen with Liquid Oxygen as a Rocket Propellant. NASA MEMO 5–21–59E, 1959.
2. Gordon, Sanford, and Huff, Vearl N.: Theoretical Performance of Liquid Hydrazine and Liquid Fluorine as a Rocket Propellant. NACA RM E53E12, 1953.
3. Eisenklam, P., and Wilkie, D.: On Jet Separation in Supersonic Rocket Nozzles. 1—The Characteristics of Flow. JRL 29, Imperial College of Sci. and Tech. (London), May 1955.
4. Campbell, C. E., and Farley, J. M.: Performance of Several Conical Convergent-Divergent Rocket-Type Exhaust Nozzles. NASA TN D–467, 1960.
5. Farley, John M., and Campbell, Carl E.: Performance of Several Method-of-Characteristics Exhaust Nozzles. NASA TN D–293, 1960.

TABLE I.—PROPERTIES OF LIQUID PROPELLANTS

Properties	Hydrogen	Oxygen
Molecular weight, M	2.016	32.00
Density, g/cc	0.0709 at −252.7° C	1.1414 at −182.0° C
Freezing point, °C	−259.20	−218.76
Boiling point, °C (propellant temperature used in this report)	−252.77	−182.97
Enthalpy required to convert liquid at boiling point to gaseous elements at 25° C, kcal/mole	1.894	3.081
Enthalpy of vaporization, kcal/mole	0.216 at −252.77° C	1.630 at −182.97° C
Enthalpy of fusion, kcal/mole	0.028 at −259.20° C	0.106 at −218.76° C

TABLE II.—THEORETICAL COMBUSTION-CHAMBER TEMPERATURES AND SPECIFIC HEATS

H_2, percent	R	O/F	Chamber pressure, lb/sq in. abs															
			15		30		60		150		300		600		900		1200	
			$c_{p,c}$	T_c	$c_{p,c}$	T_c	$c_{p,c}$	T_c	$c_{p,c}$	T_c	$c_{p,c}$	T_c	$c_{p,c}$	T_c	$c_{p,c}$	T_c	$c_{p,c}$	T_c
7. 749	1. 5	11. 905	2. 8271	2961	2. 5501	3038	2. 2973	3116	1. 9992	3219	1. 8003	3297	1. 6233	3374	1. 5295	3417	1. 4672	3448
11. 19	1. 0	7. 937	4. 4128	3039	4. 0070	3127	3. 6327	3217	3. 1852	3341	2. 8811	3437	2. 6053	3534	2. 4567	3591	2. 3567	3632
12. 28	. 9	7. 143	4. 5829	3036	4. 1544	3123	3. 7588	3213	3. 2851	3336	2. 9626	3430	2. 6696	3526	2. 5113	3582	2. 4047	3622
13. 6	. 8	6. 349	4. 4645	3016	4. 0221	3101	3. 6135	3188	3. 1245	3304	2. 7921	3393	2. 4909	3481	2. 3289	3532	2. 2202	3568
15. 25	. 7	5. 556	3. 9719	2971	3. 5484	3049	3. 1609	3128	2. 7036	3231	2. 3992	3307	2. 1301	3381	1. 9888	3422	1. 8957	3451
17. 35	. 6	4. 762	3. 2346	2885	2. 8811	2951	2. 5641	3015	2. 2005	3097	1. 9667	3155	1. 7671	3208	1. 6656	3236	1. 6001	3255
20. 12	. 5	3. 968	2. 4943	2735	2. 2390	2783	2. 0170	2828	1. 7727	2881	1. 6231	2915	1. 5012	2944	1. 4415	2959	1. 4040	2969
21. 87	. 45	3. 571	2. 1634	2627	1. 9612	2663	1. 7899	2696	1. 6077	2733	1. 5003	2755	1. 4156	2773	1. 3752	2782	1. 3502	2788
23. 95	. 4	3. 175	1. 8704	2487	1. 7255	2511	1. 6075	2531	1. 4879	2553	1. 4207	2565	1. 3697	2574	1. 3460	2579	1. 3316	2581
26. 47	. 35	2. 778	1. 6400	2308	1. 5552	2320	1. 4897	2329	1. 4271	2339	1. 3936	2344	1. 3691	2347	1. 3579	2349	------	------
29. 57	. 3	2. 381	1. 5172	2083	1. 4829	2086	1. 4578	2089	1. 4348	2092	1. 4230	2093	1. 4145	2094	1. 4108	2095	------	------
33. 51	. 25	1. 984	1. 5219	1815	1. 5143	1816	1. 5088	1816	1. 5040	1816	1. 5015	1817	1. 4998	1817	1. 4990	1817	------	------

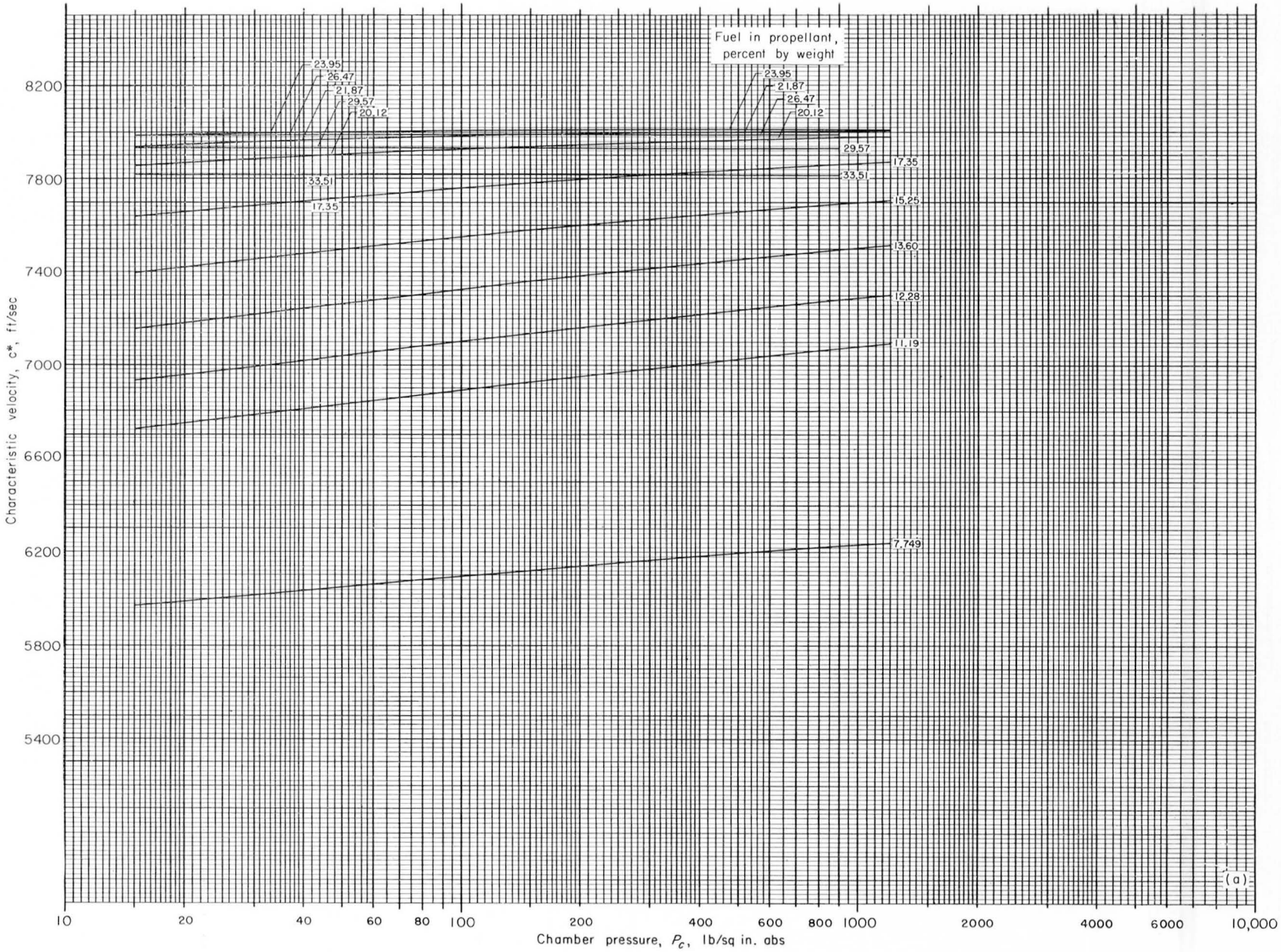

(a) Equilibrium composition during expansion.

FIGURE 1.—Theoretical characteristic velocity of liquid hydrogen and liquid oxygen. (A complete set of 66 large working charts for figs. 1 to 5 can be obtained by using the request form in the back of this report.)

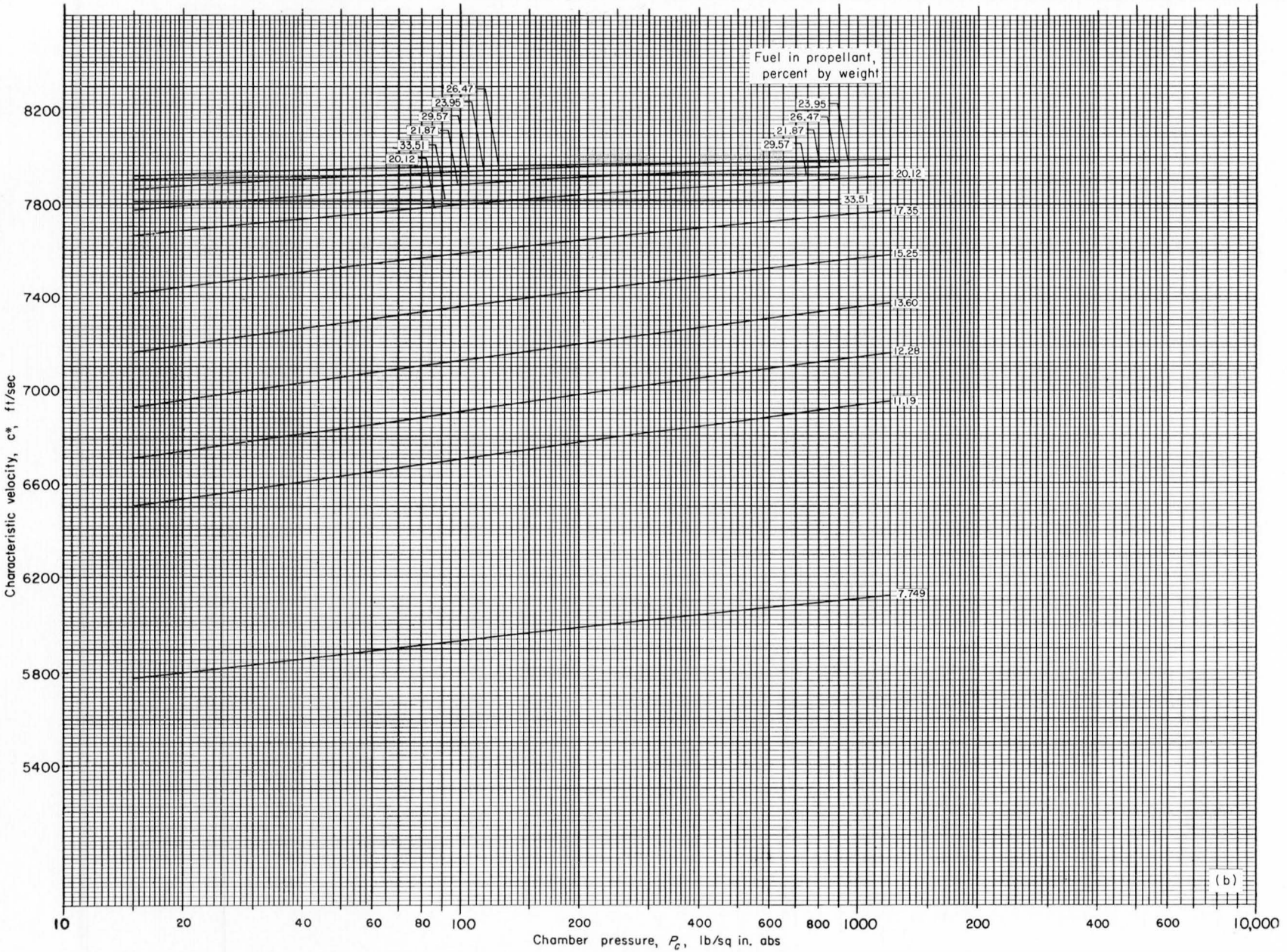

(b) Frozen composition during expansion.

FIGURE 1.—Concluded. Theoretical characteristic velocity of liquid hydrogen and liquid oxygen.

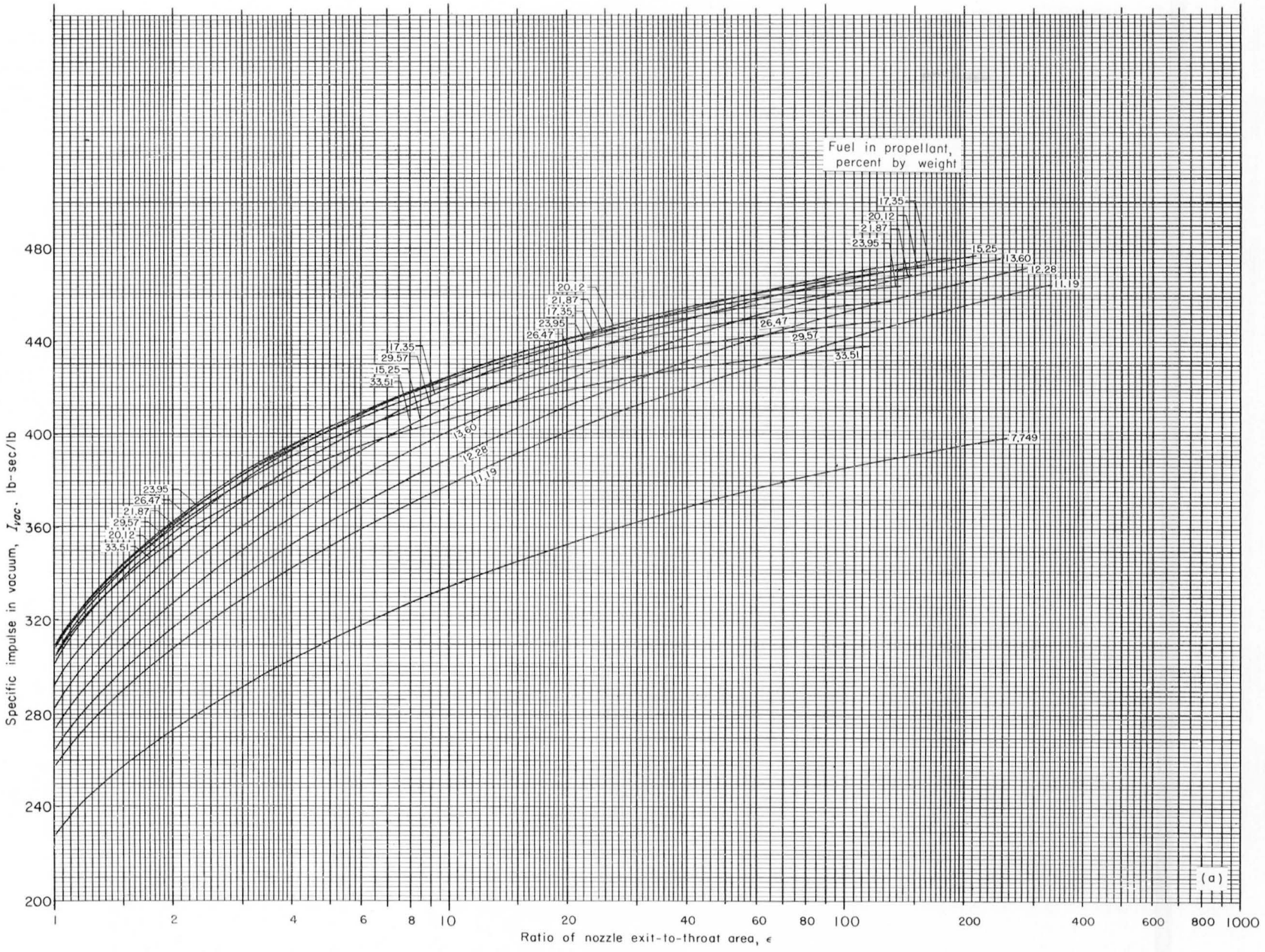

(a) Chamber pressure, 15 pounds per square inch absolute; equilibrium composition during isentropic expansion to area ratio indicated.

FIGURE 2.—Theoretical specific impulse in vacuum of liquid hydrogen and liquid oxygen.

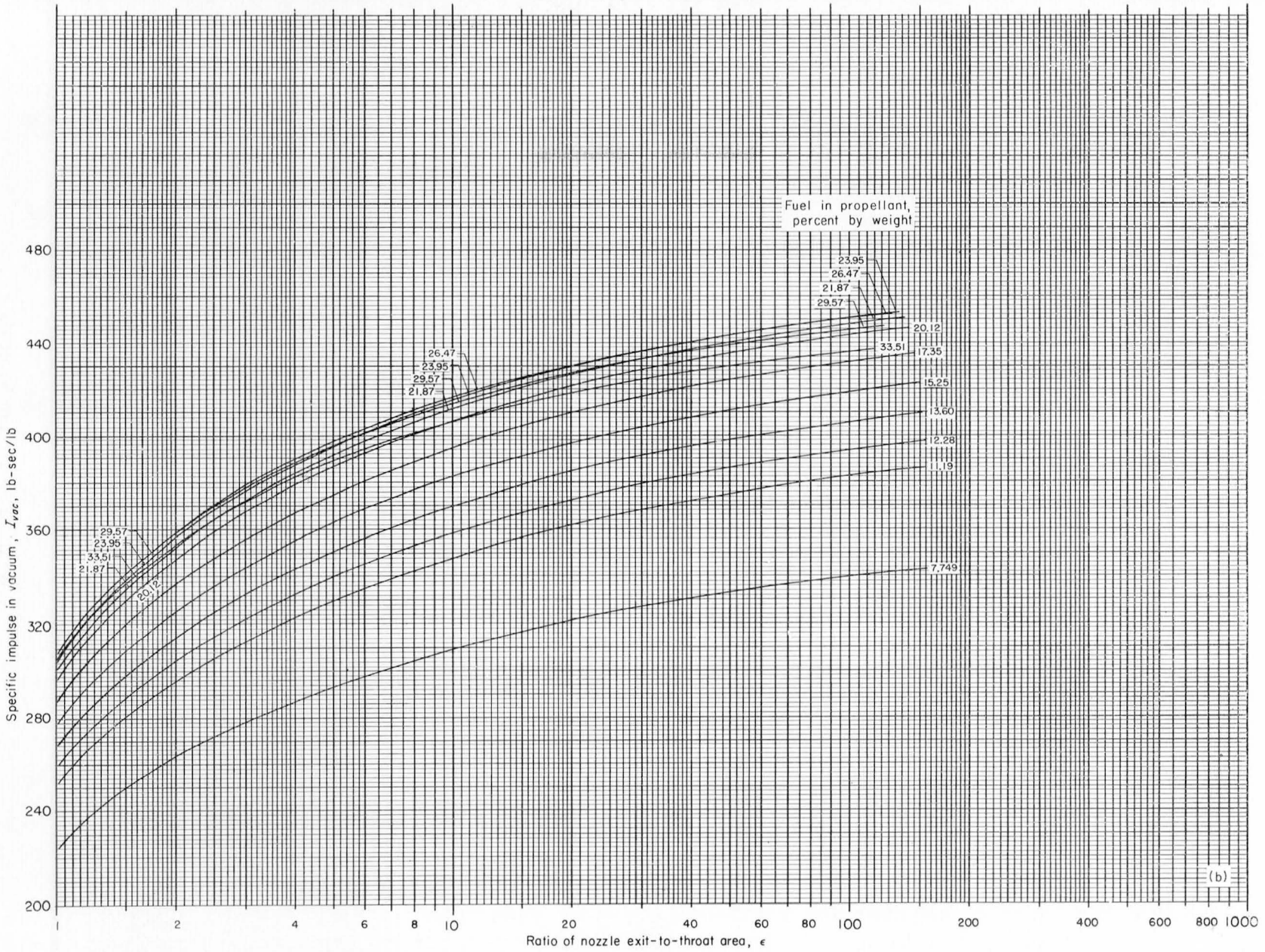

(b) Chamber pressure, 15 pounds per square inch absolute; frozen composition during isentropic expansion to area ratio indicated.

FIGURE 2.—Continued. Theoretical specific impulse in vacuum of liquid hydrogen and liquid oxygen.

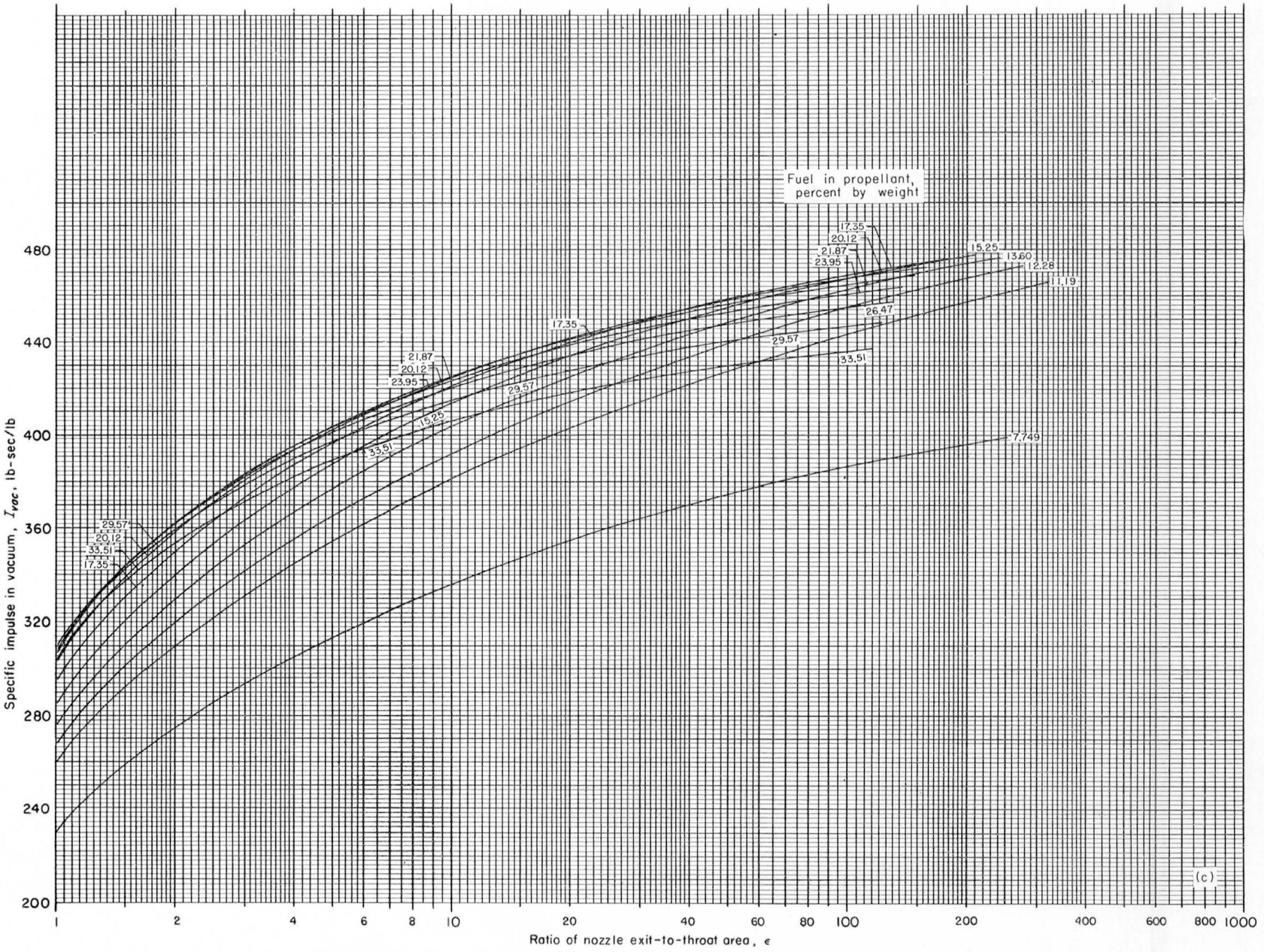

(c) Chamber pressure, 30 pounds per square inch absolute; equilibrium composition during isentropic expansion to area ratio indicated.

FIGURE 2.—Continued. Theoretical specific impulse in vacuum of liquid hydrogen and liquid oxygen.

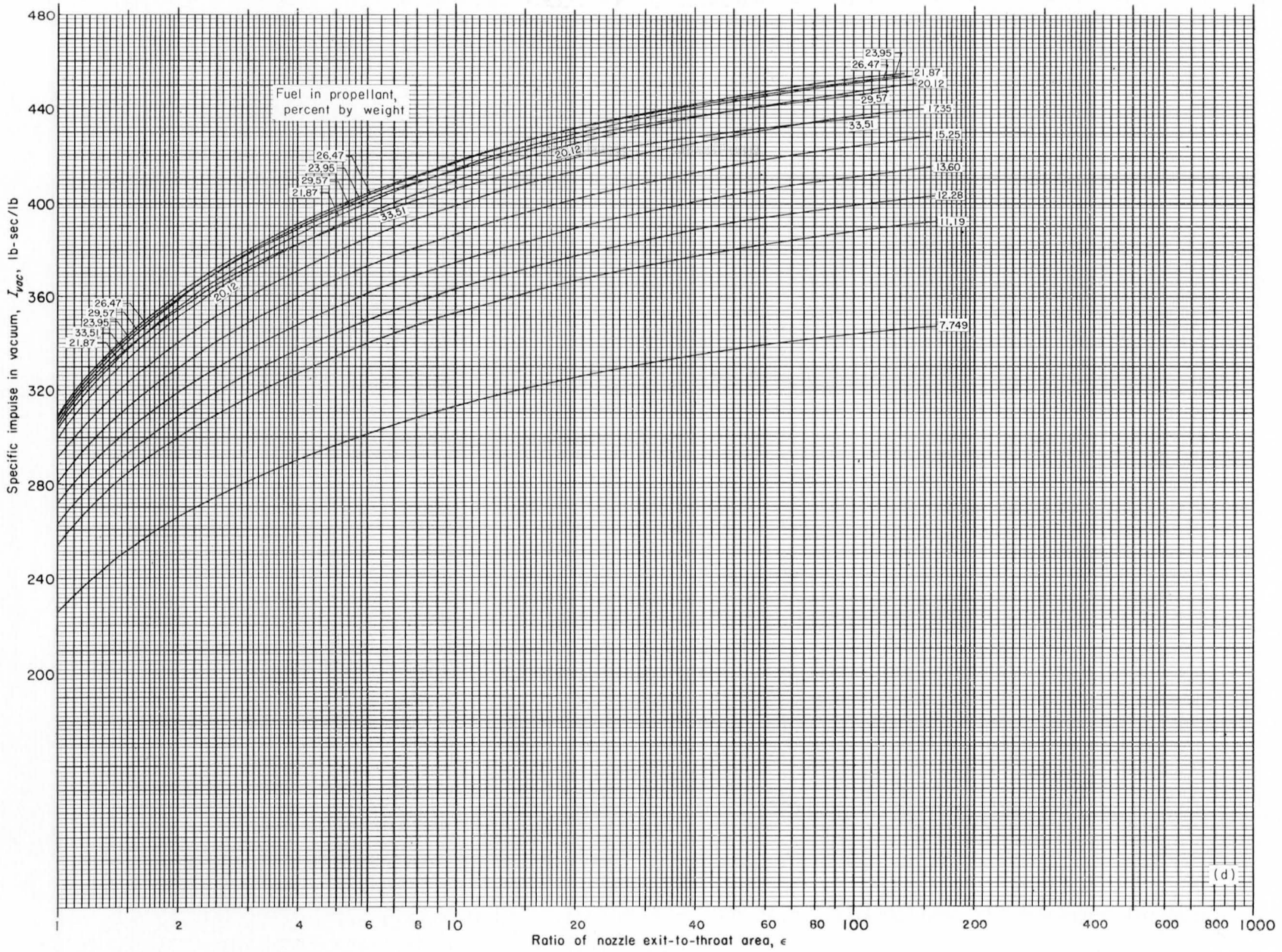

(d) Chamber pressure, 30 pounds per square inch absolute; frozen composition during isentropic expansion to area ratio indicated.

FIGURE 2.—Continued. Theoretical specific impulse in vacuum of liquid hydrogen and liquid oxygen.

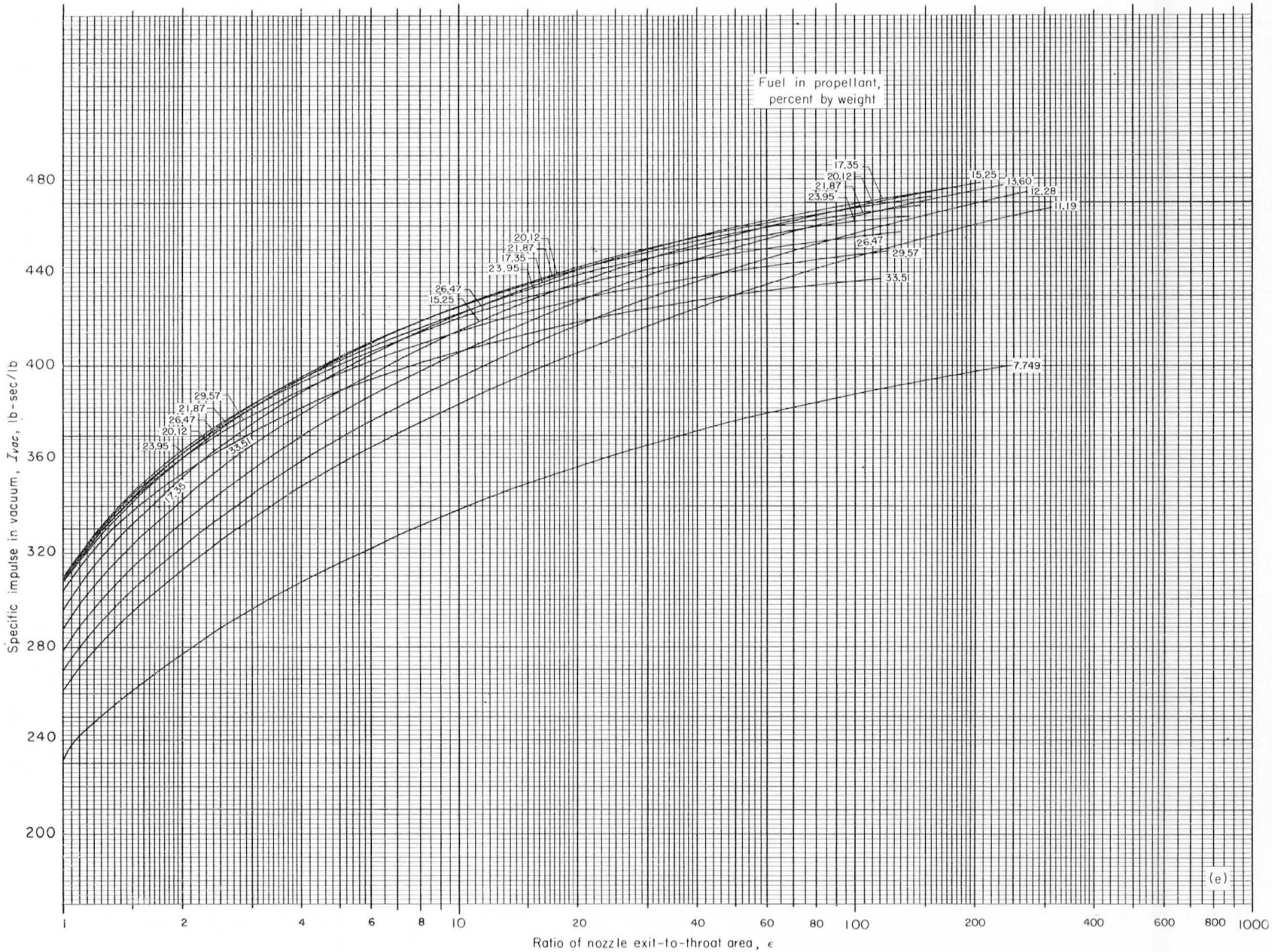

(e) Chamber pressure, 60 pounds per square inch absolute; equilibrium composition during isentropic expansion to area ratio indicated.

FIGURE 2.—Continued. Theoretical specific impulse in vacuum of liquid hydrogen and liquid oxygen.

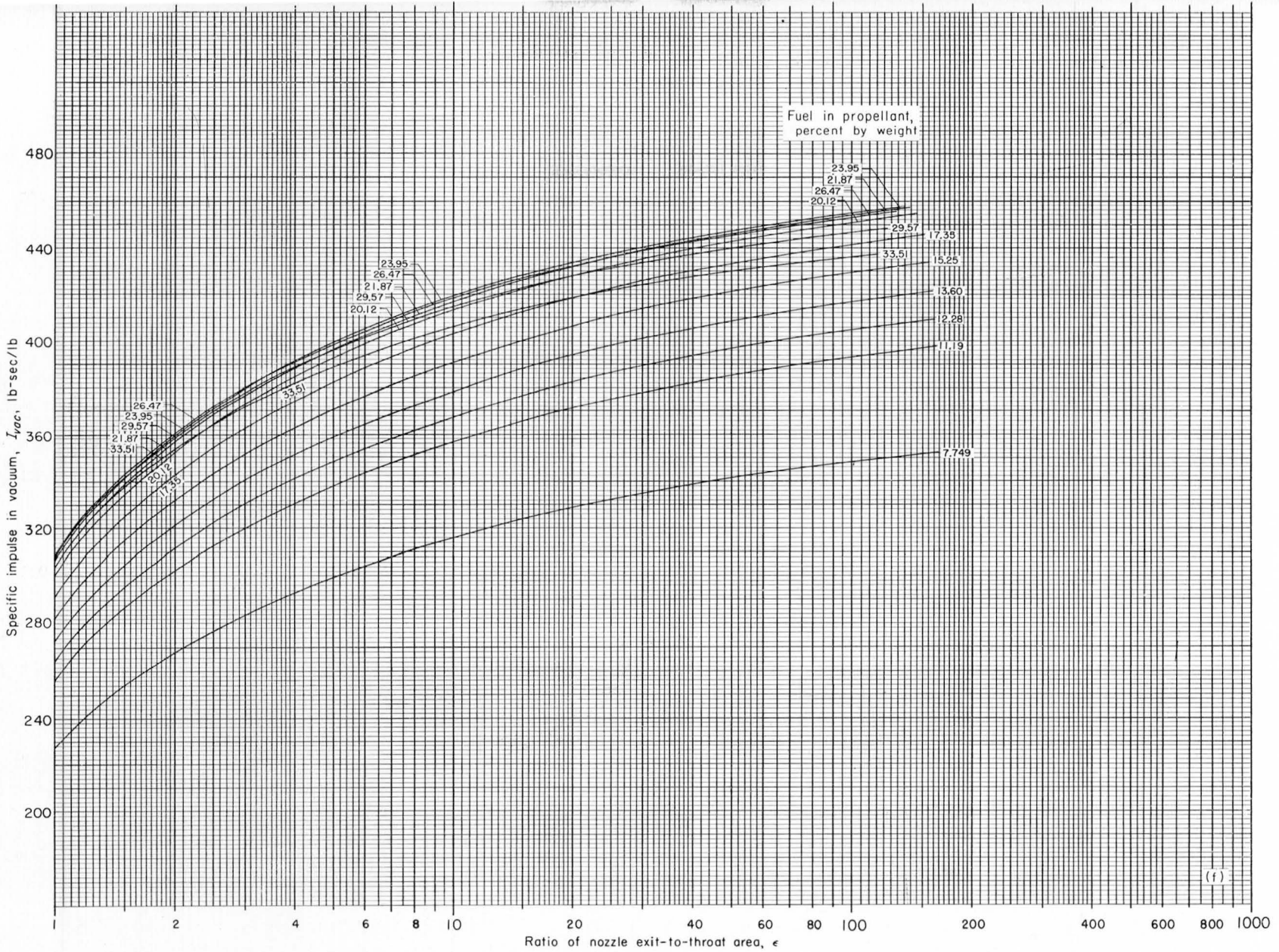

(f) Chamber pressure, 60 pounds per square inch absolute; frozen composition during isentropic expansion to area ratio indicated.

FIGURE 2.—Continued. Theoretical specific impulse in vacuum of liquid hydrogen and liquid oxygen.

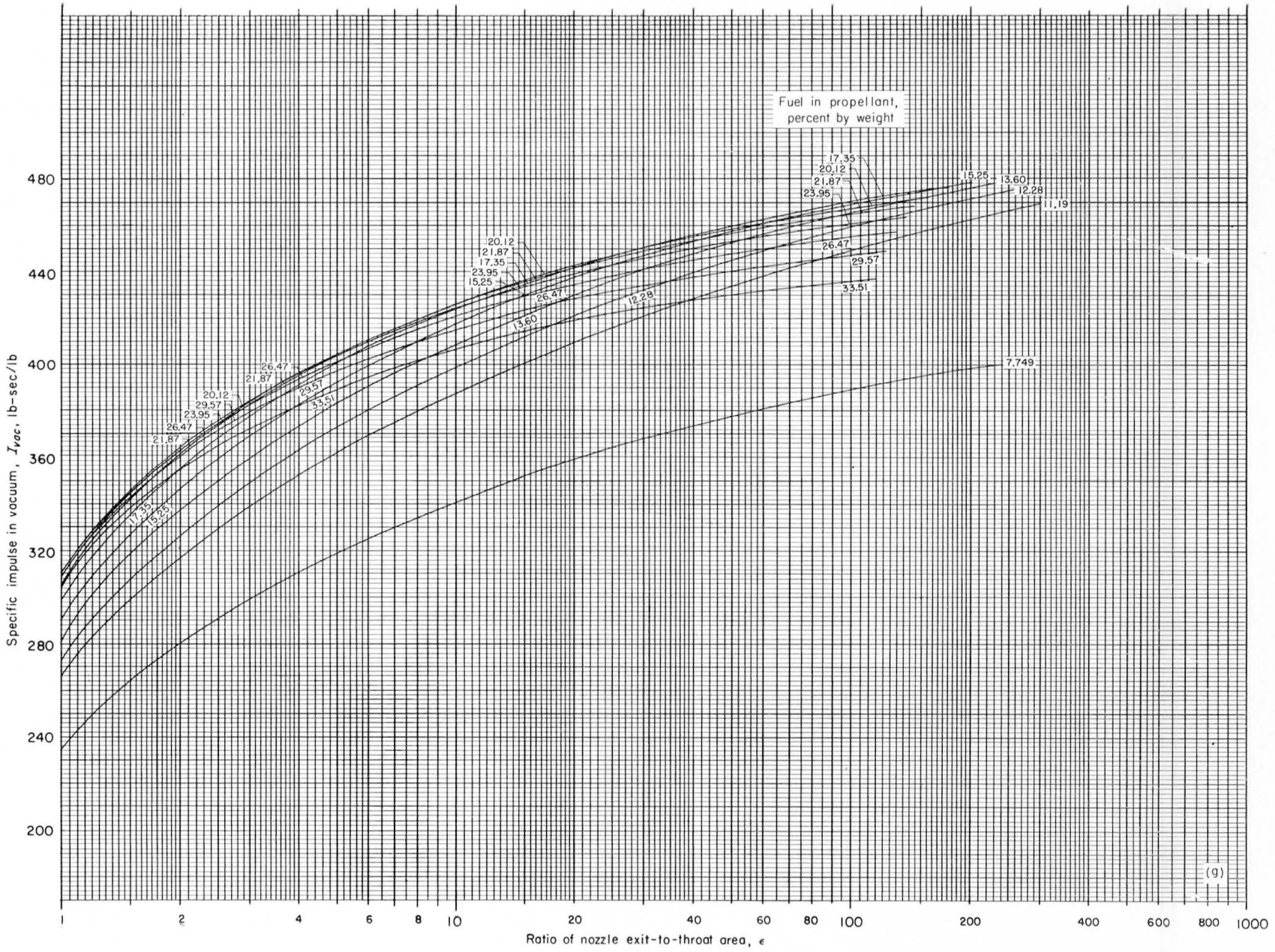

(g) Chamber pressure, 150 pounds per square inch absolute; equilibrium composition during isentropic expansion to area ratio indicated.

FIGURE 2.—Continued. Theoretical specific impulse in vacuum of liquid hydrogen and liquid oxygen.

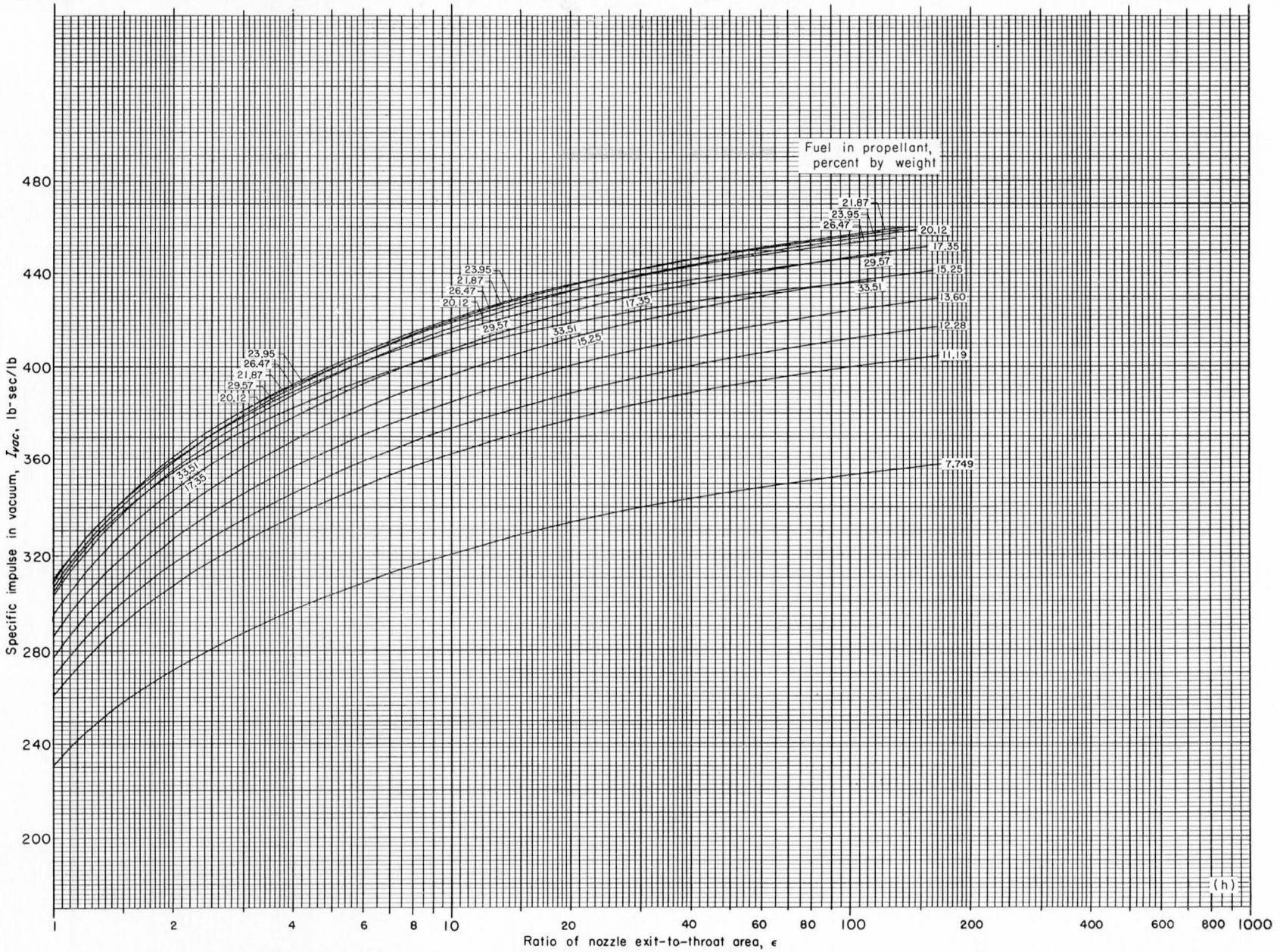

(h) Chamber pressure, 150 pounds per square inch absolute; frozen composition during isentropic expansion to area ratio indicated.

FIGURE 2.—Continued. Theoretical specific impulse in vacuum of liquid hydrogen and liquid oxygen.

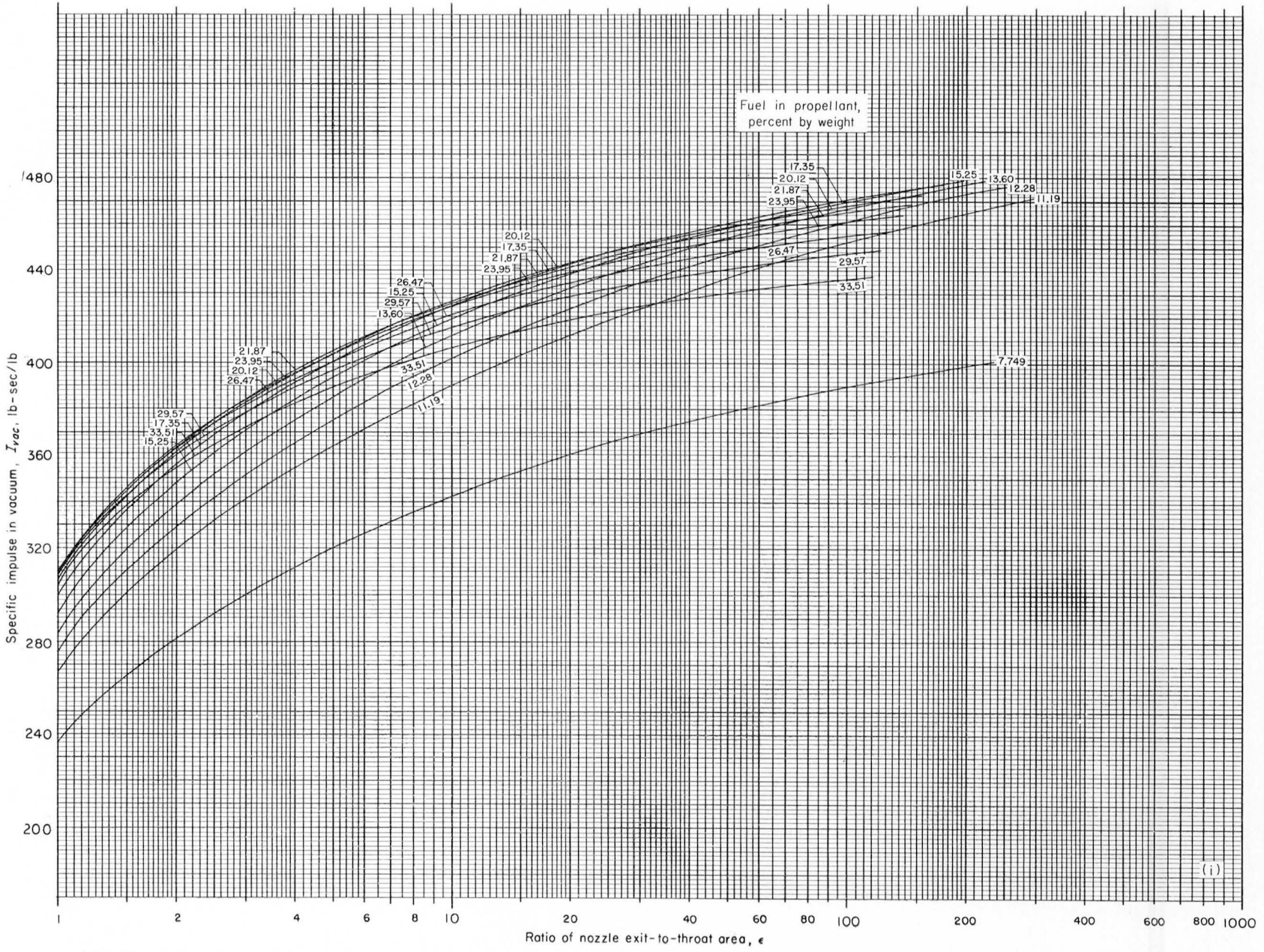

(i) Chamber pressure, 300 pounds per square inch absolute; equilibrium composition during isentropic expansion to area ratio indicated.

FIGURE 2.—Continued. Theoretical specific impulse in vacuum of liquid hydrogen and liquid oxygen.

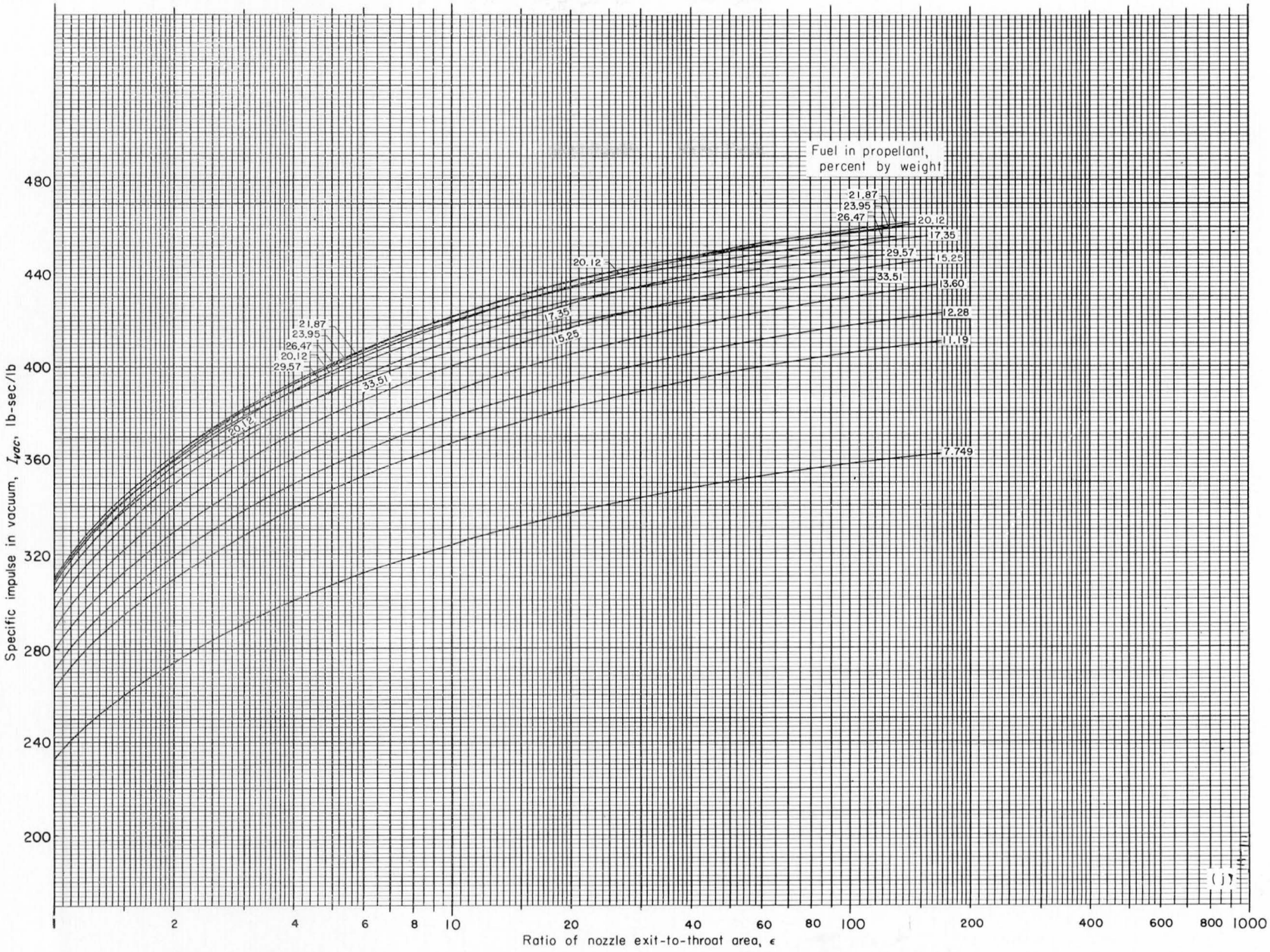

(j) Chamber pressure, 300 pounds per square inch absolute; frozen composition during isentropic expansion at area ratio indicated.

FIGURE 2.—Continued. Theoretical specific impulse in vacuum of liquid hydrogen and liquid oxygen.

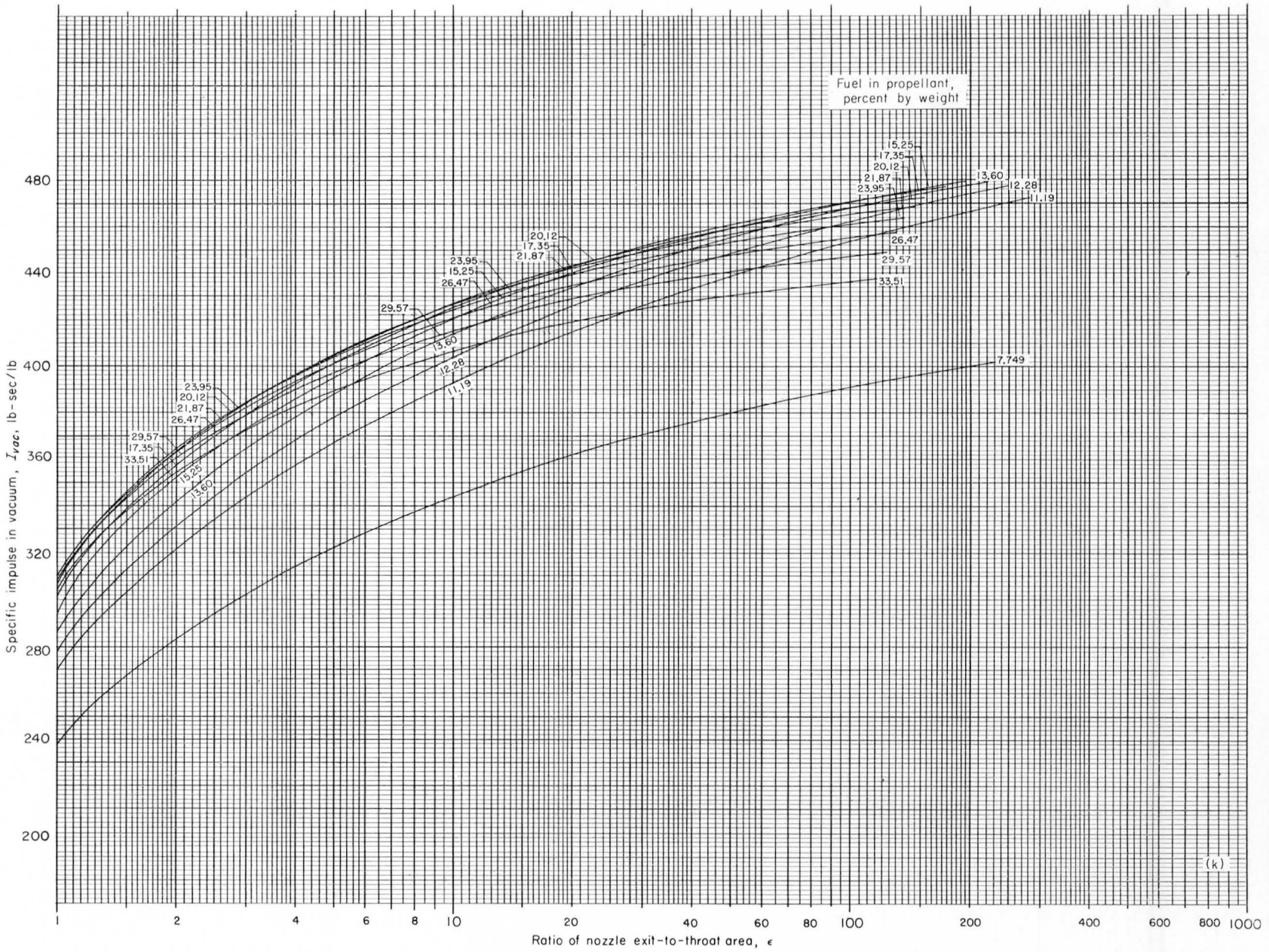

(k) Chamber pressure, 600 pounds per square inch absolute; equilibrium composition during isentropic expansion to area ratio indicated.

FIGURE 2.—Continued. Theoretical specific impulse in vacuum of liquid hydrogen and liquid oxygen.

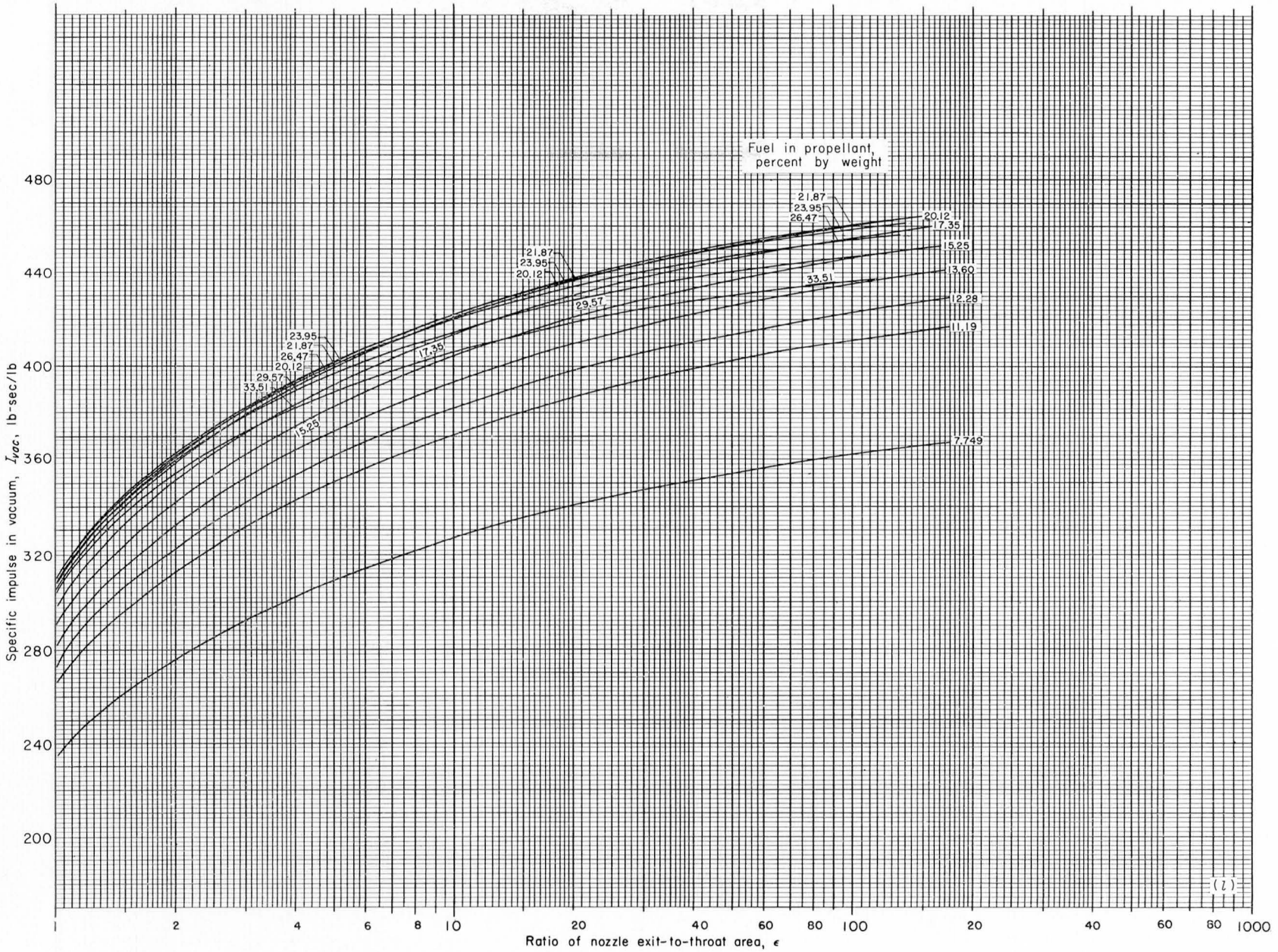

(l) Chamber pressure, 600 pounds per square inch absolute; frozen composition during isentropic expansion to area ratio indicated.

FIGURE 2.—Continued. Theoretical specific impulse in vacuum of liquid hydrogen and liquid oxygen.

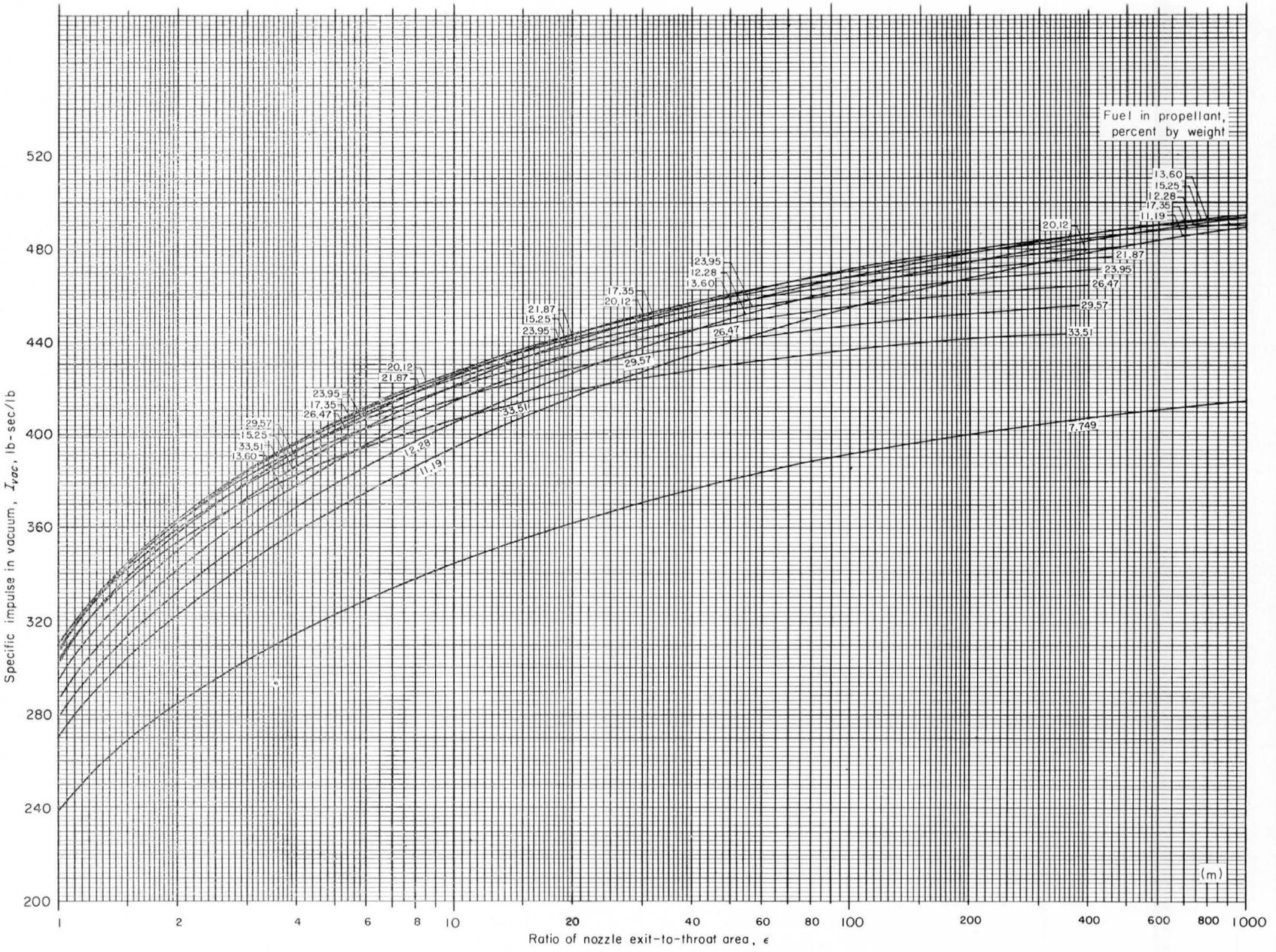

(m) Chamber pressure, 900 pounds per square inch absolute; equilibrium composition during isentropic expansion to area ratio indicated.

FIGURE 2.—Continued. Theoretical specific impulse in vacuum of liquid hydrogen and liquid oxygen.

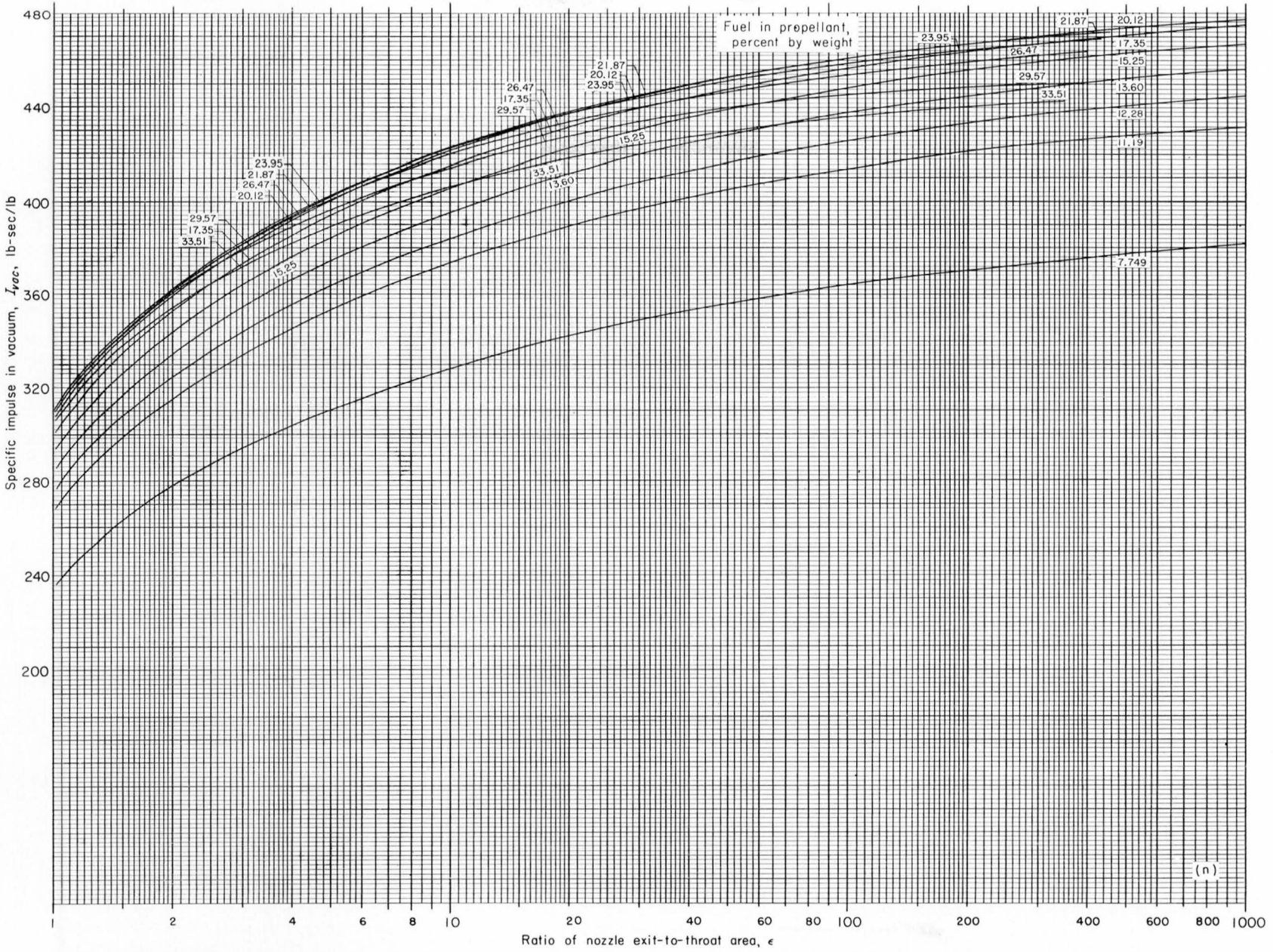

(n) Chamber pressure, 900 pounds per square inch absolute; frozen composition during isentropic expansion to area ratio indicated.

FIGURE 2.—Continued. Theoretical specific impulse in vacuum of liquid hydrogen and liquid oxygen.

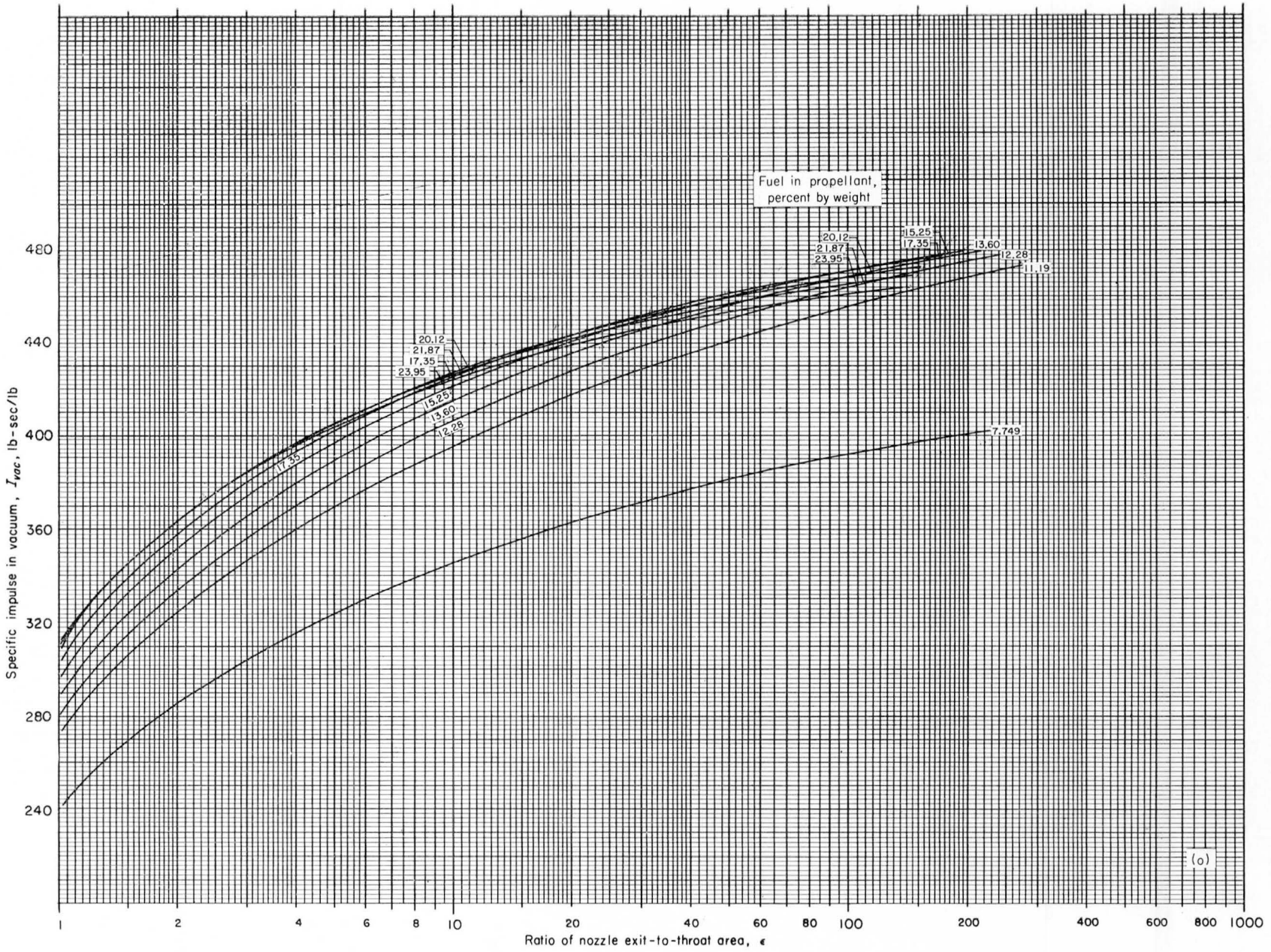

(o) Chamber pressure, 1200 pounds per square inch absolute; equilibrium composition during isentropic expansion to area ratio indicated.

FIGURE 2.—Continued. Theoretical specific impulse in vacuum of liquid hydrogen and liquid oxygen.

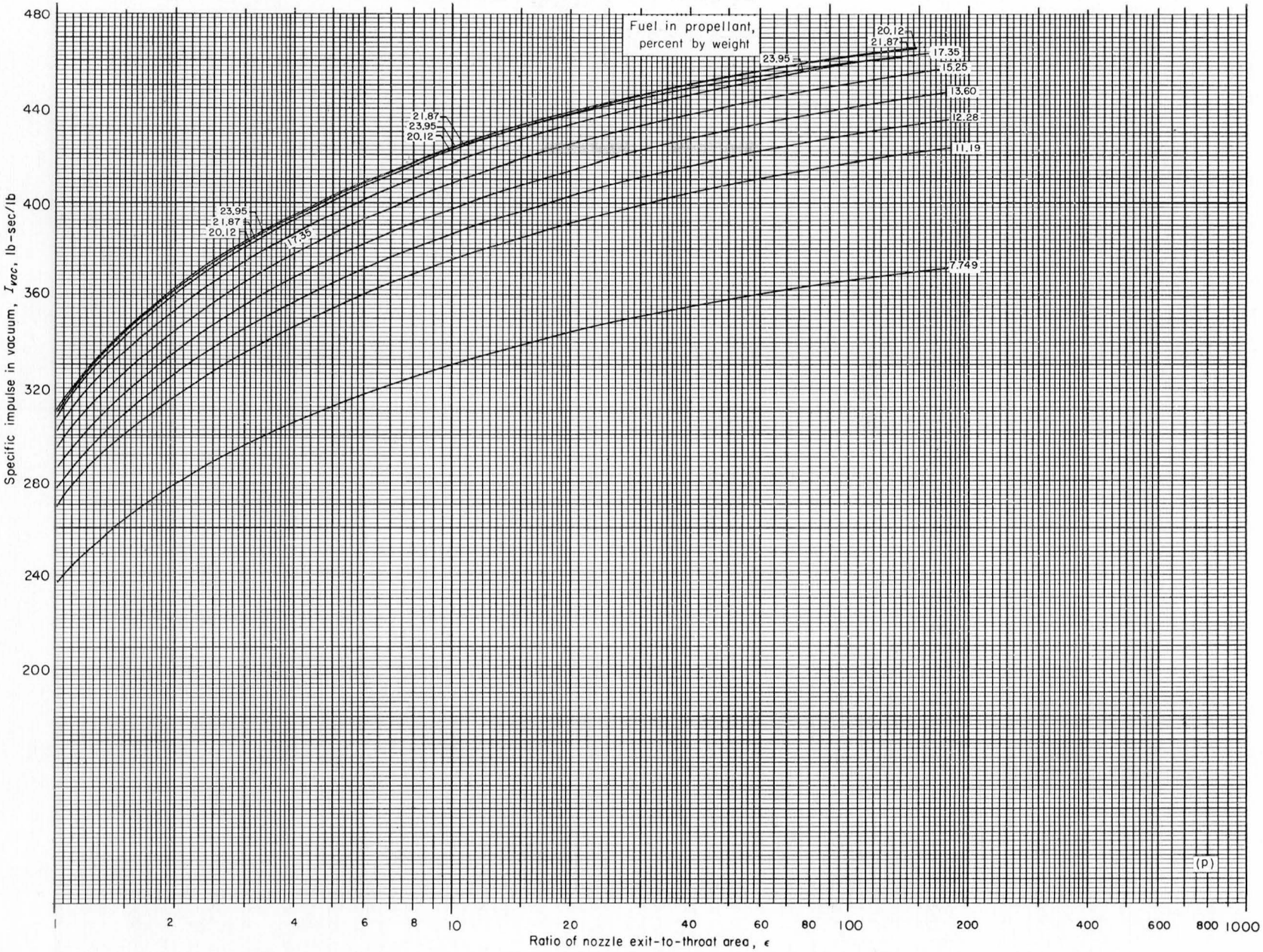

(p) Chamber pressure, 1200 pounds per square inch absolute; frozen composition during isentropic expansion to area ratio indicated.

FIGURE 2.—Concluded. Theoretical specific impulse in vacuum of liquid hydrogen and liquid oxygen.

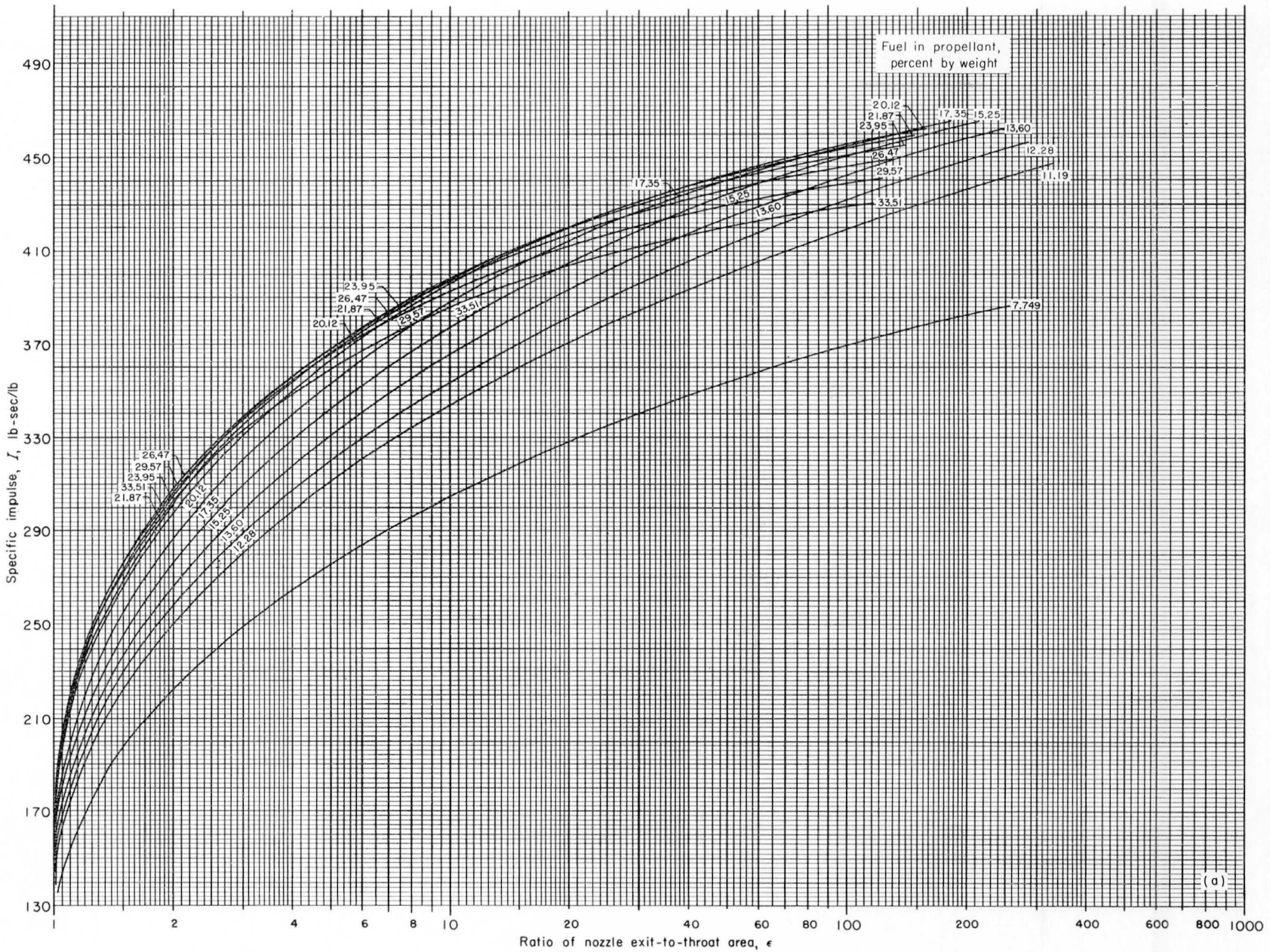

(a) Chamber pressure, 15 pounds per square inch absolute; equilibrium composition during isentropic expansion to area ratio indicated.

FIGURE 3.—Theoretical specific impulse of liquid hydrogen and liquid oxygen.

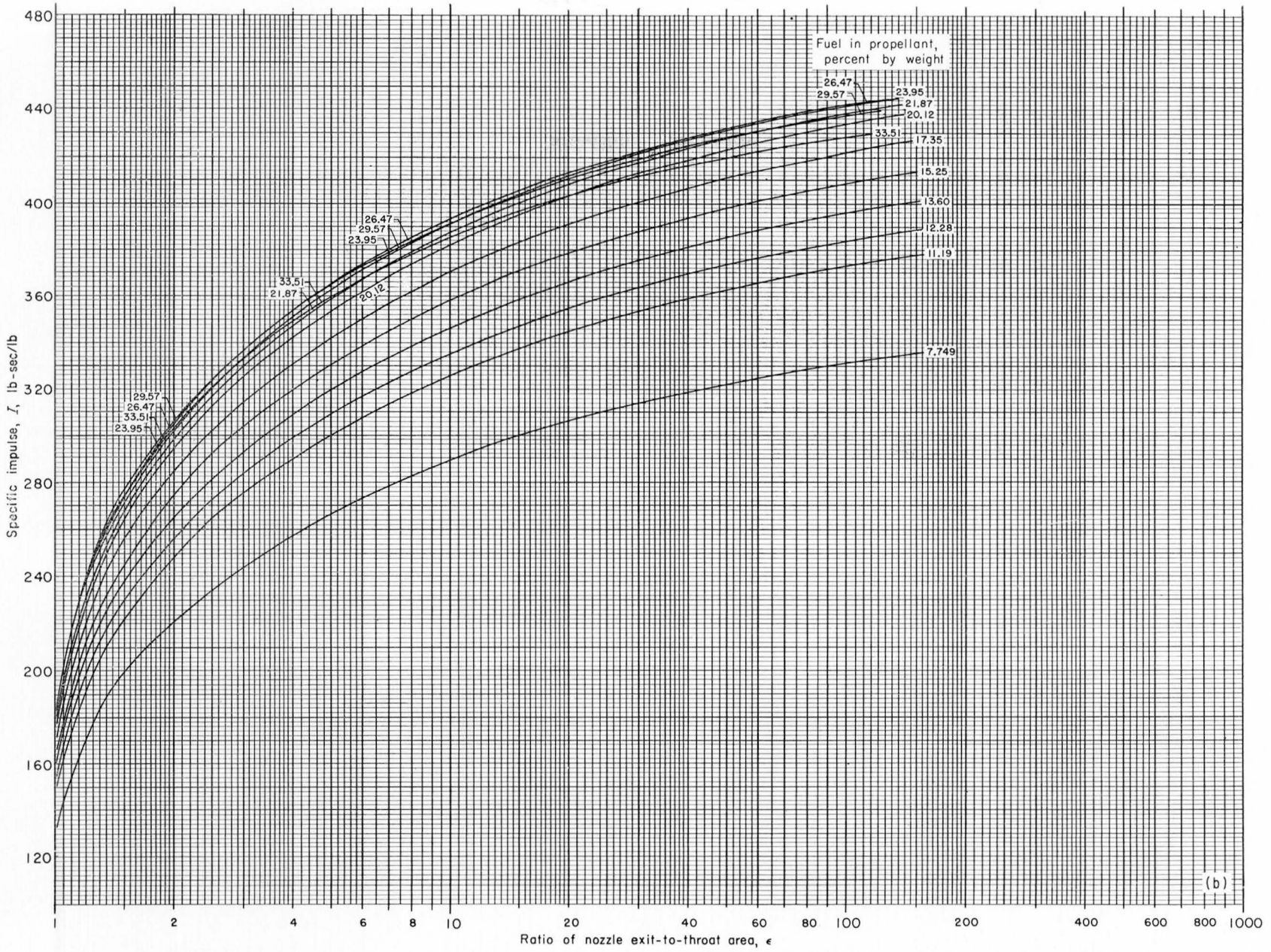

(b) Chamber pressure, 15 pounds per square inch absolute; frozen composition during isentropic expansion to area ratio indicated.

FIGURE 3.—Continued. Theoretical specific impulse of liquid hydrogen and liquid oxygen.

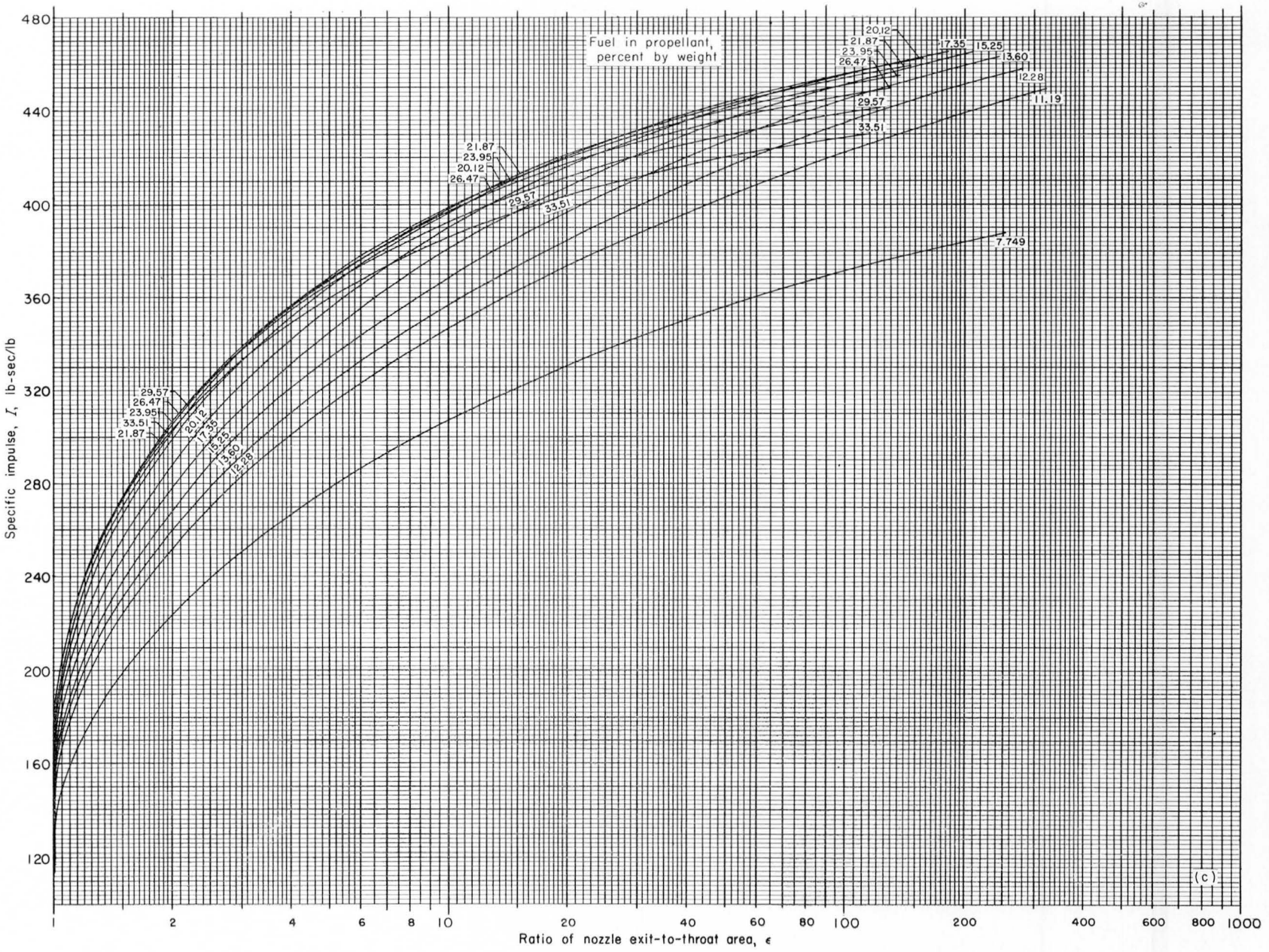

(c) Chamber pressure, 30 pounds per square inch absolute; equilibrium composition during isentropic expansion to area ratio indicated.

FIGURE 3.—Continued. Theoretical specific impulse of liquid hydrogen and liquid oxygen.

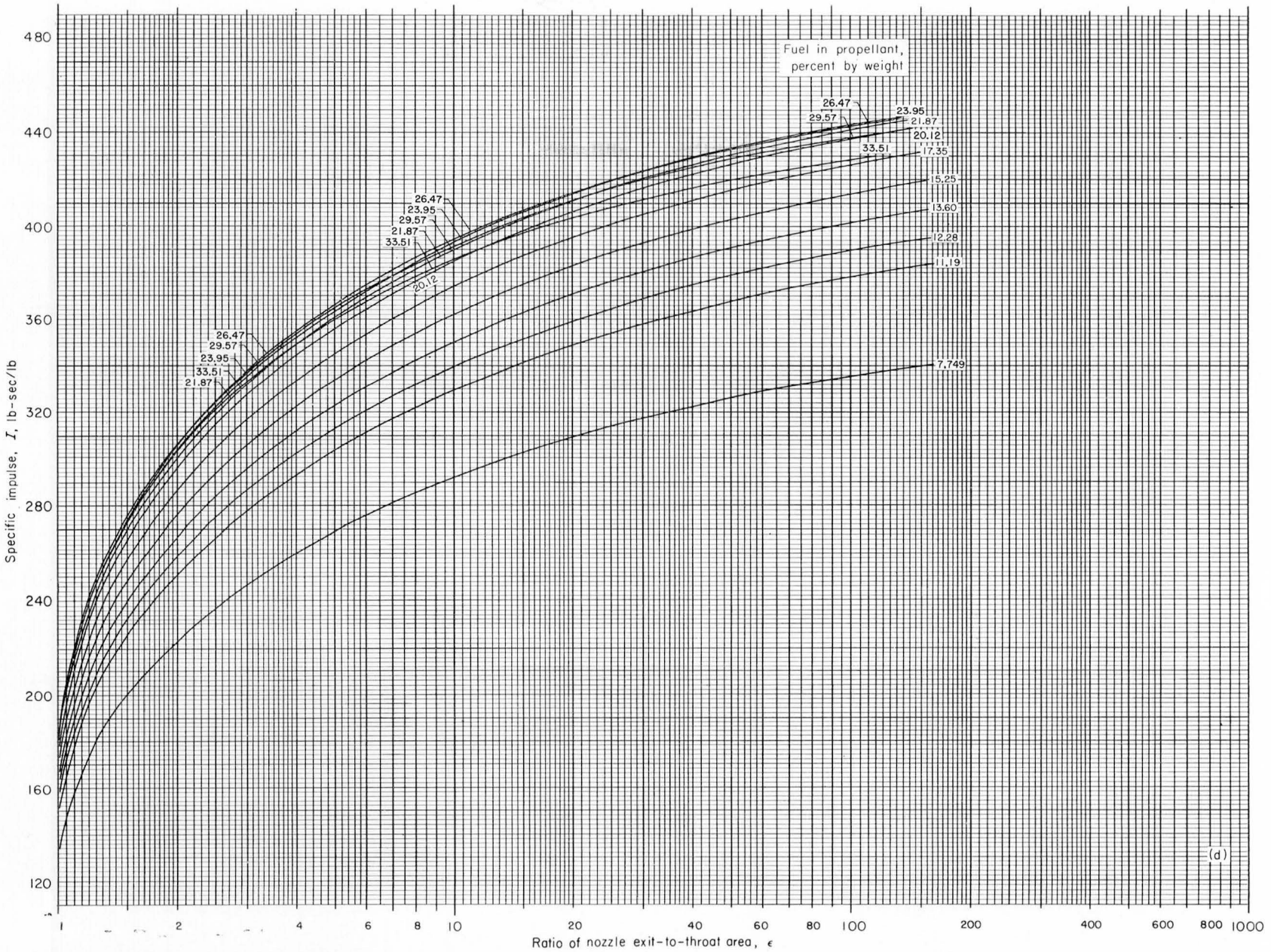

(d) Chamber pressure, 30 pounds per square inch absolute; frozen composition during isentropic expansion to area ratio indicated.

FIGURE 3.—Continued. Theoretical specific impulse of liquid hydrogen and liquid oxygen.

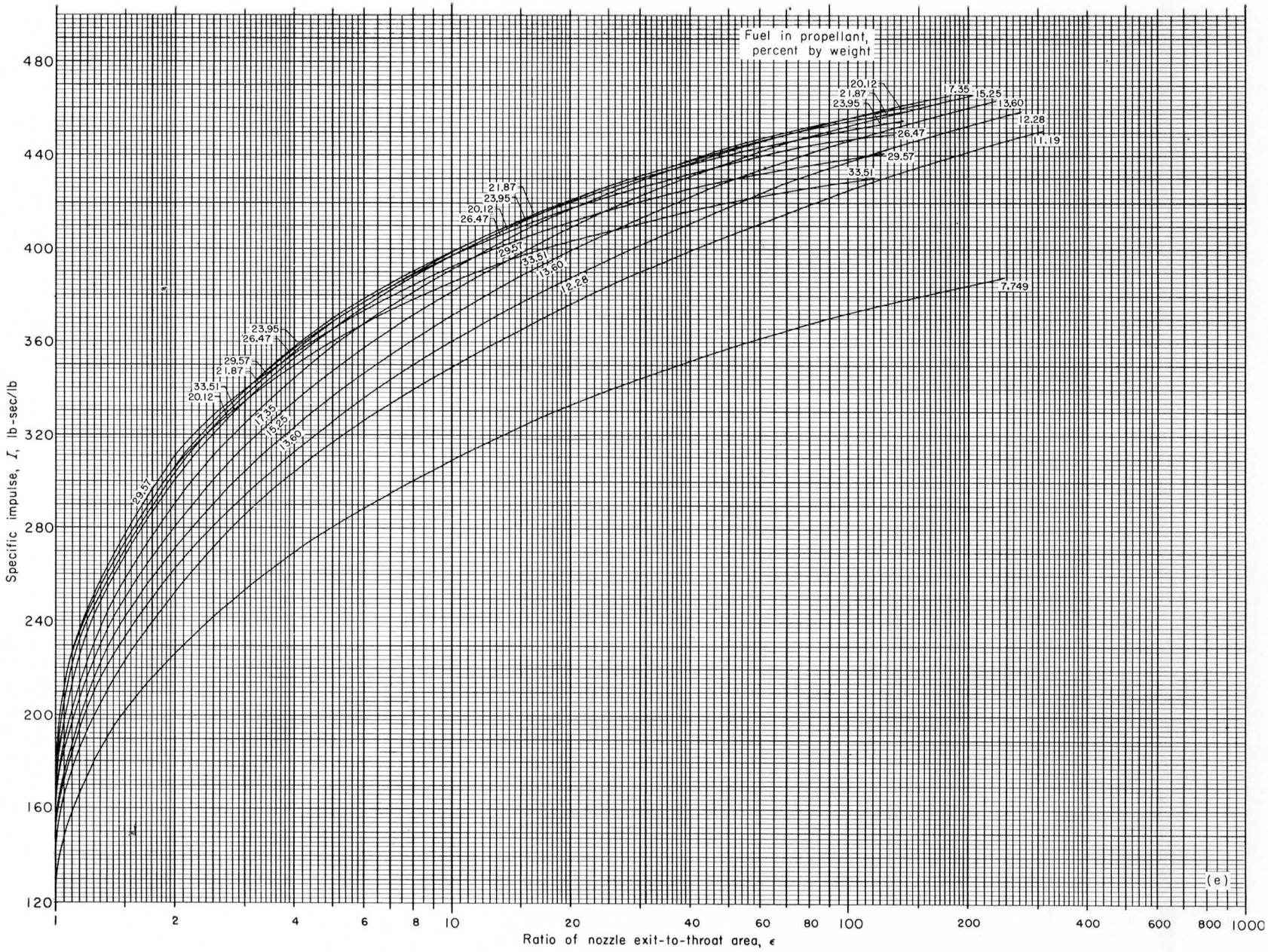

(e) Chamber pressure, 60 pounds per square inch absolute; equilibrium composition during isentropic expansion to area ratio indicated.

FIGURE 3.—Continued. Theoretical specific impulse of liquid hydrogen and liquid oxygen.

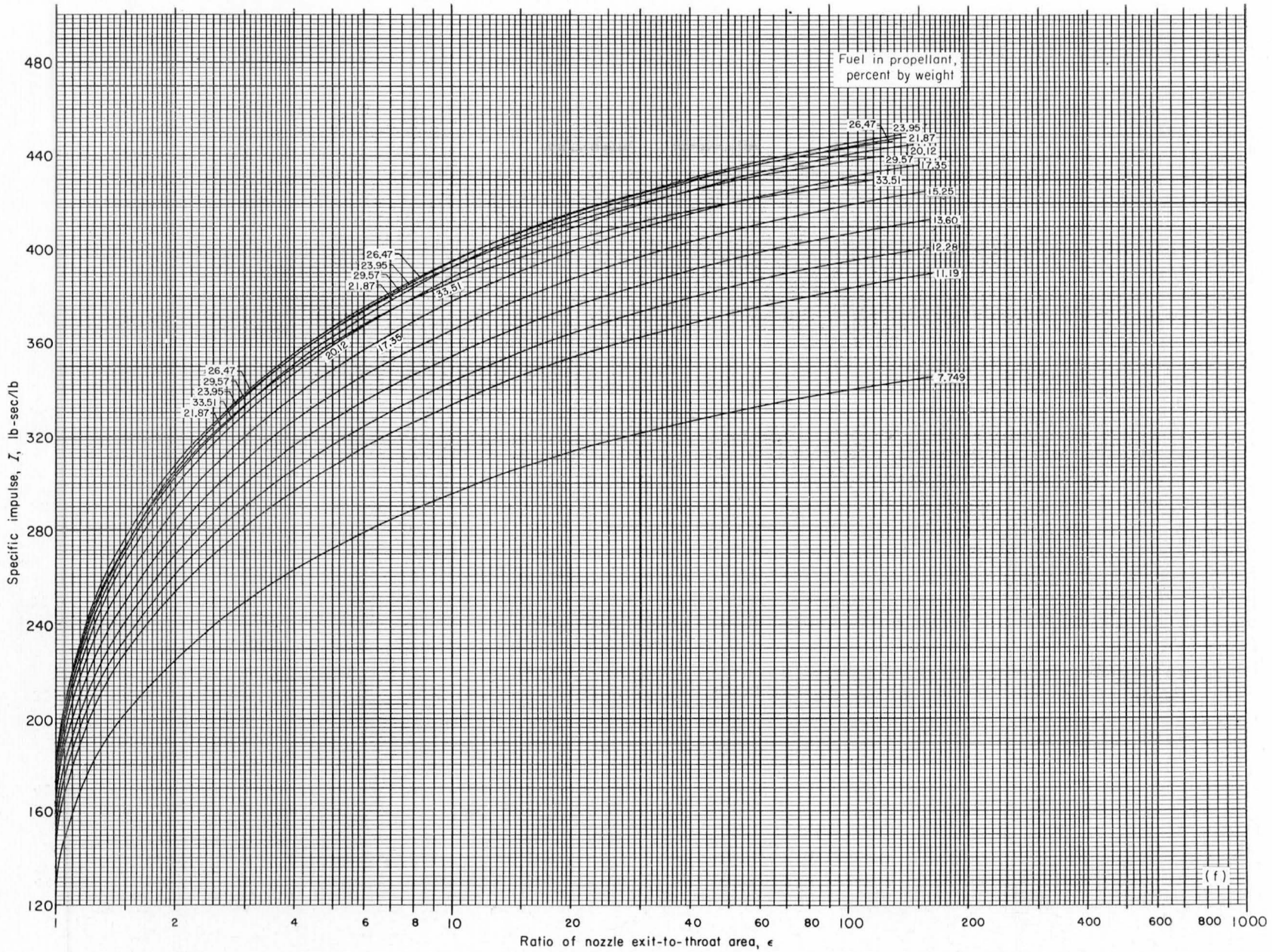

(f) Chamber pressure, 60 pounds per square inch absolute; frozen composition during isentropic expansion to area ratio indicated.

FIGURE 3.—Continued. Theoretical specific impulse of liquid hydrogen and liquid oxygen.

618157—62——5

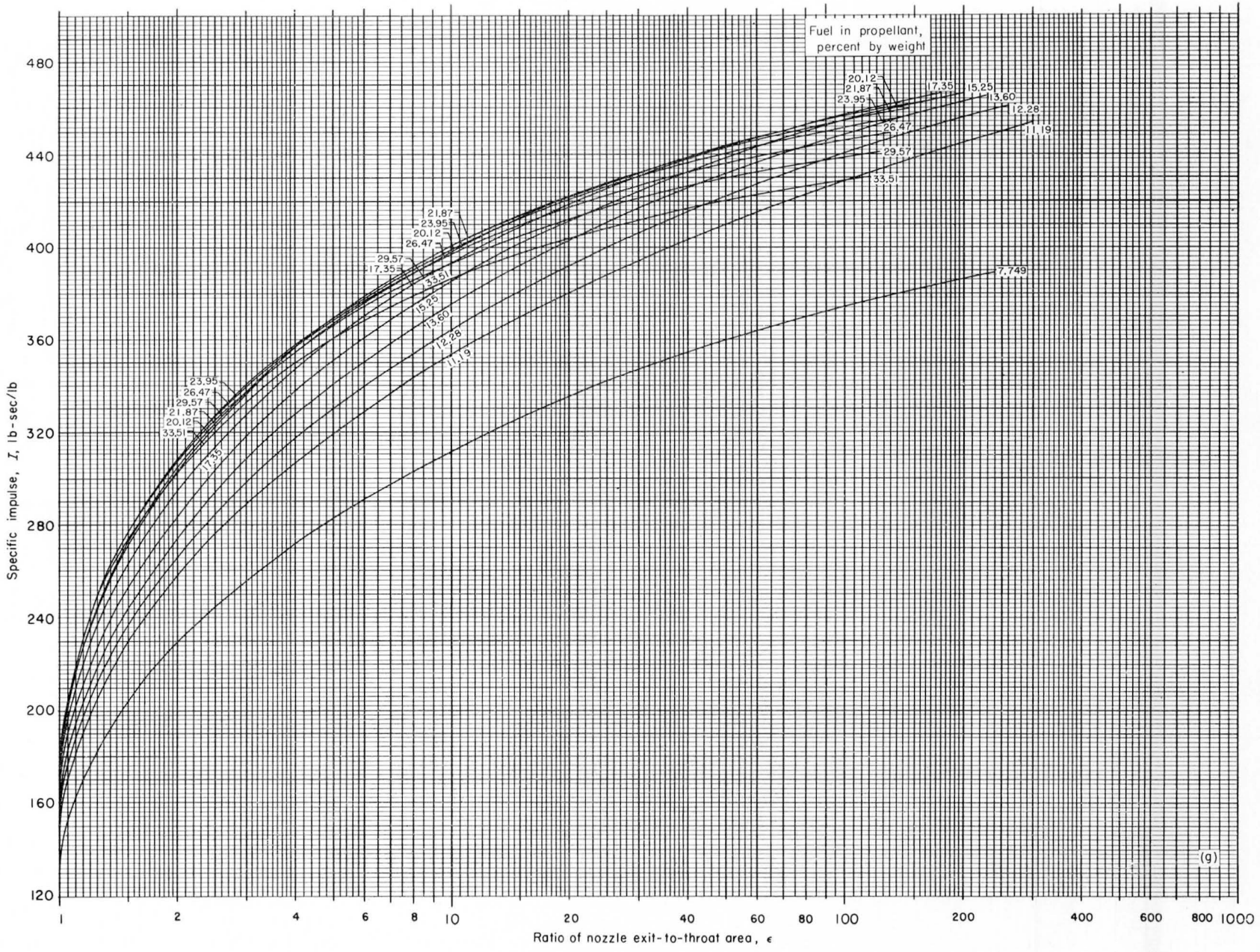

(g) Chamber pressure, 150 pounds per square inch absolute; equilibrium composition during isentropic expansion to area ratio indicated.

FIGURE 3.—Continued. Theoretical specific impulse of liquid hydrogen and liquid oxygen.

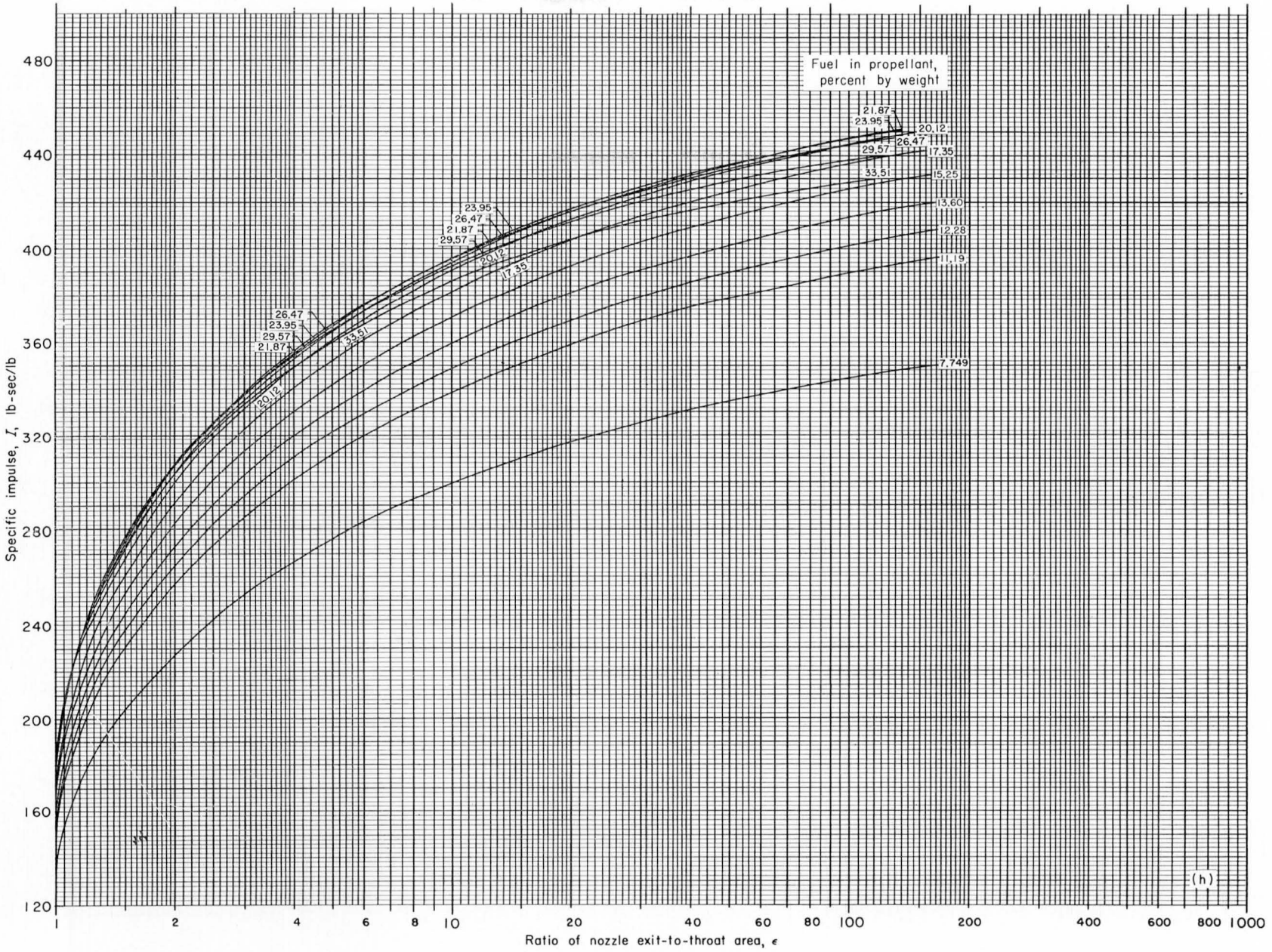

(h) Chamber pressure, 150 pounds per square inch absolute; frozen composition during isentropic expansion to area ratio indicated.

FIGURE 3.—Continued. Theoretical specific impulse of liquid hydrogen and liquid oxygen.

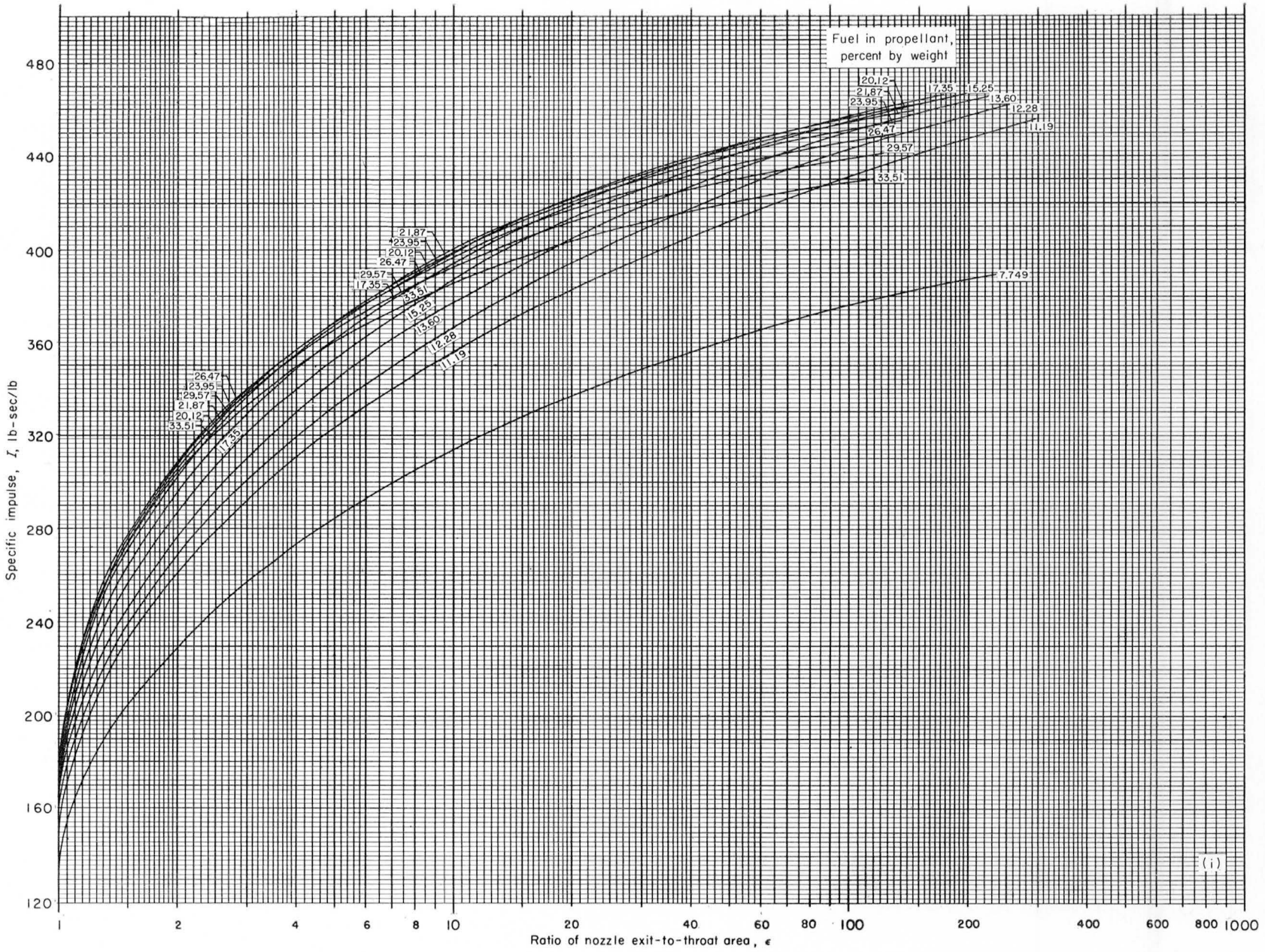

(i) Chamber pressure, 300 pounds per square inch absolute; equilibrium composition during isentropic expansion to area ratio indicated.

FIGURE 3.—Continued. Theoretical specific impulse of liquid hydrogen and liquid oxygen.

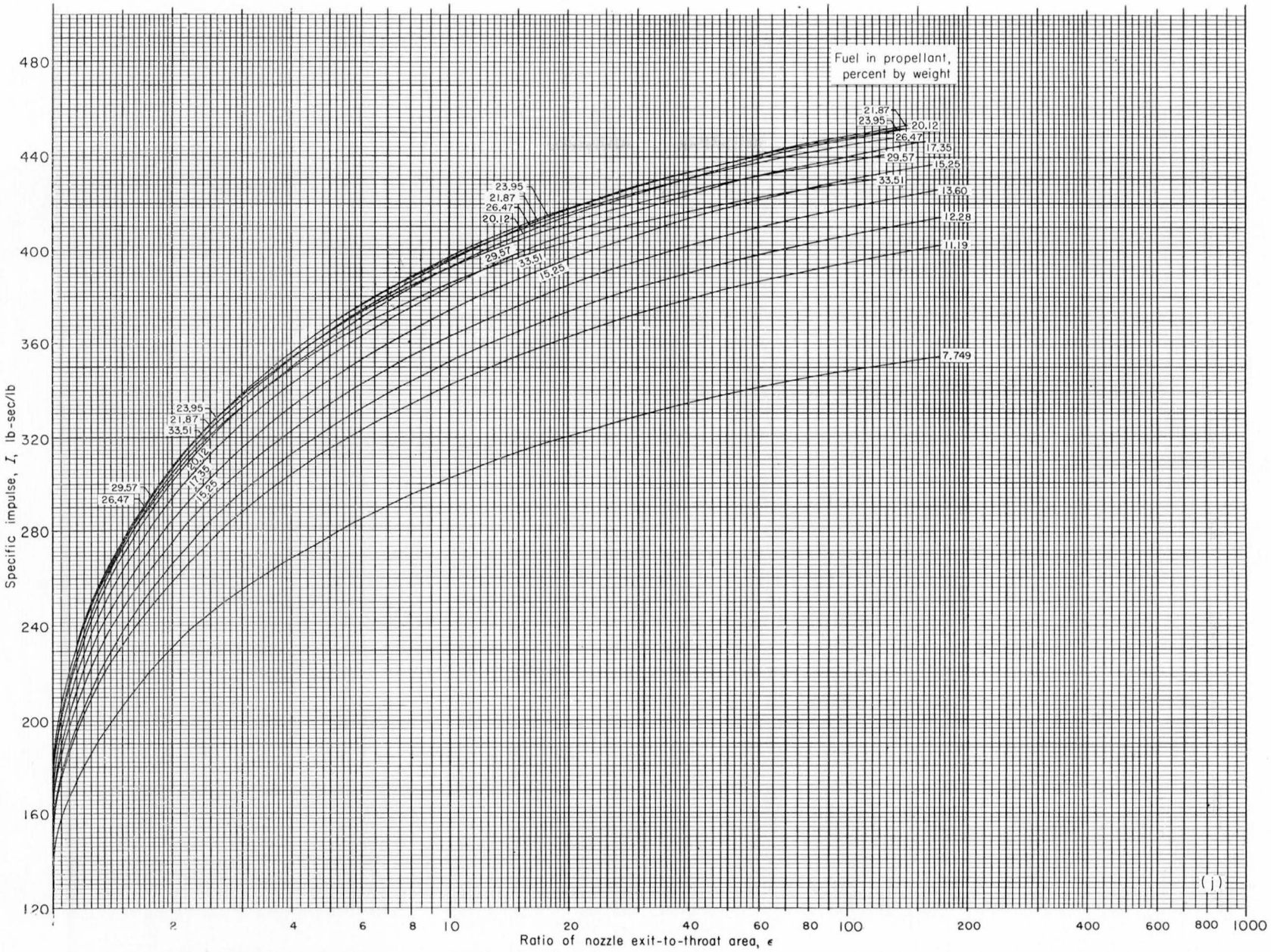

(j) Chamber pressure, 300 pounds per square inch absolute; frozen composition during isentropic expansion to area ratio indicated.

FIGURE 3.—Continued. Theoretical specific impulse of liquid hydrogen and liquid oxygen.

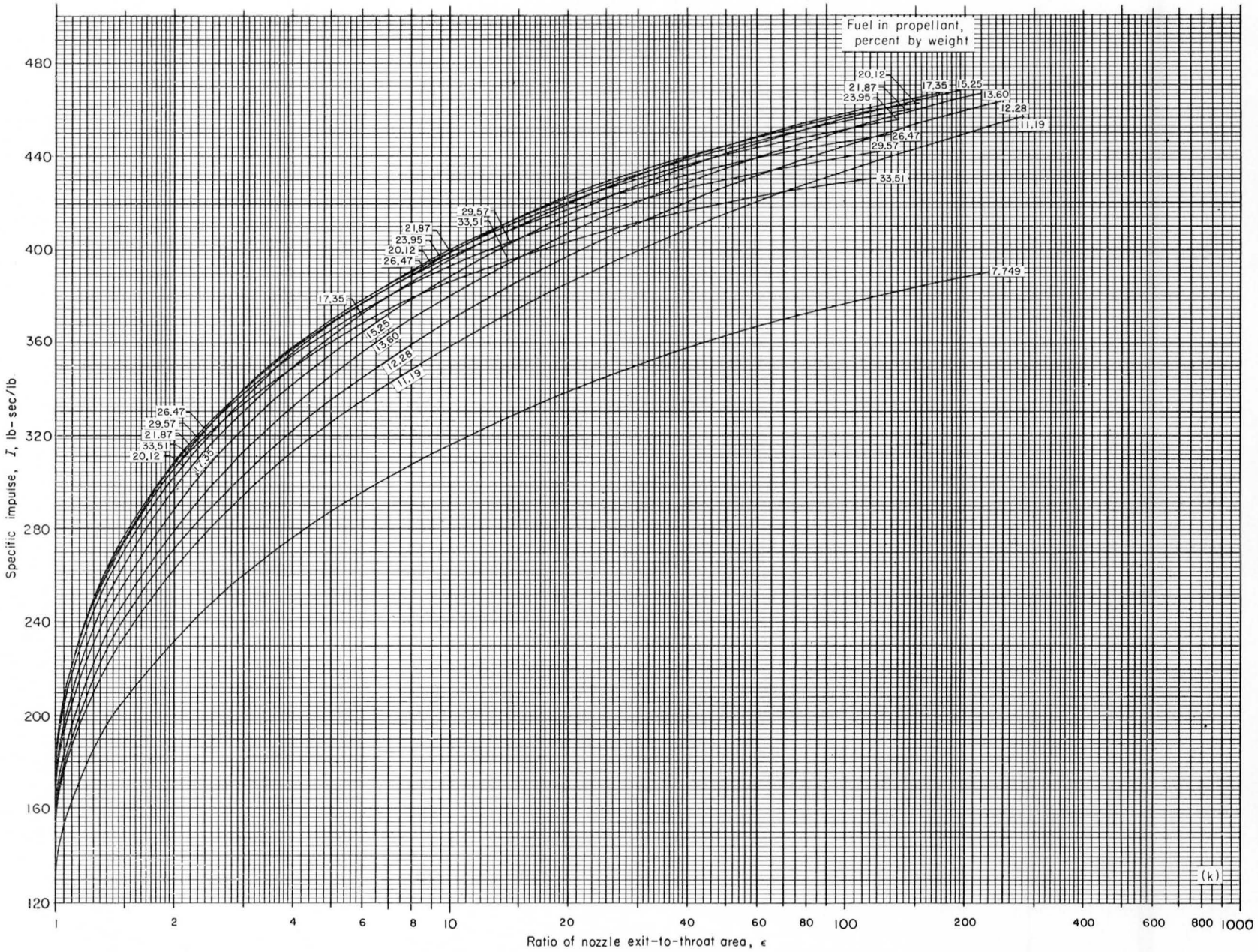

(k) Chamber pressure, 600 pounds per square inch absolute; equilibrium composition during isentropic expansion to area ratio indicated.

FIGURE 3.—Continued. Theoretical specific impulse of liquid hydrogen and liquid oxygen.

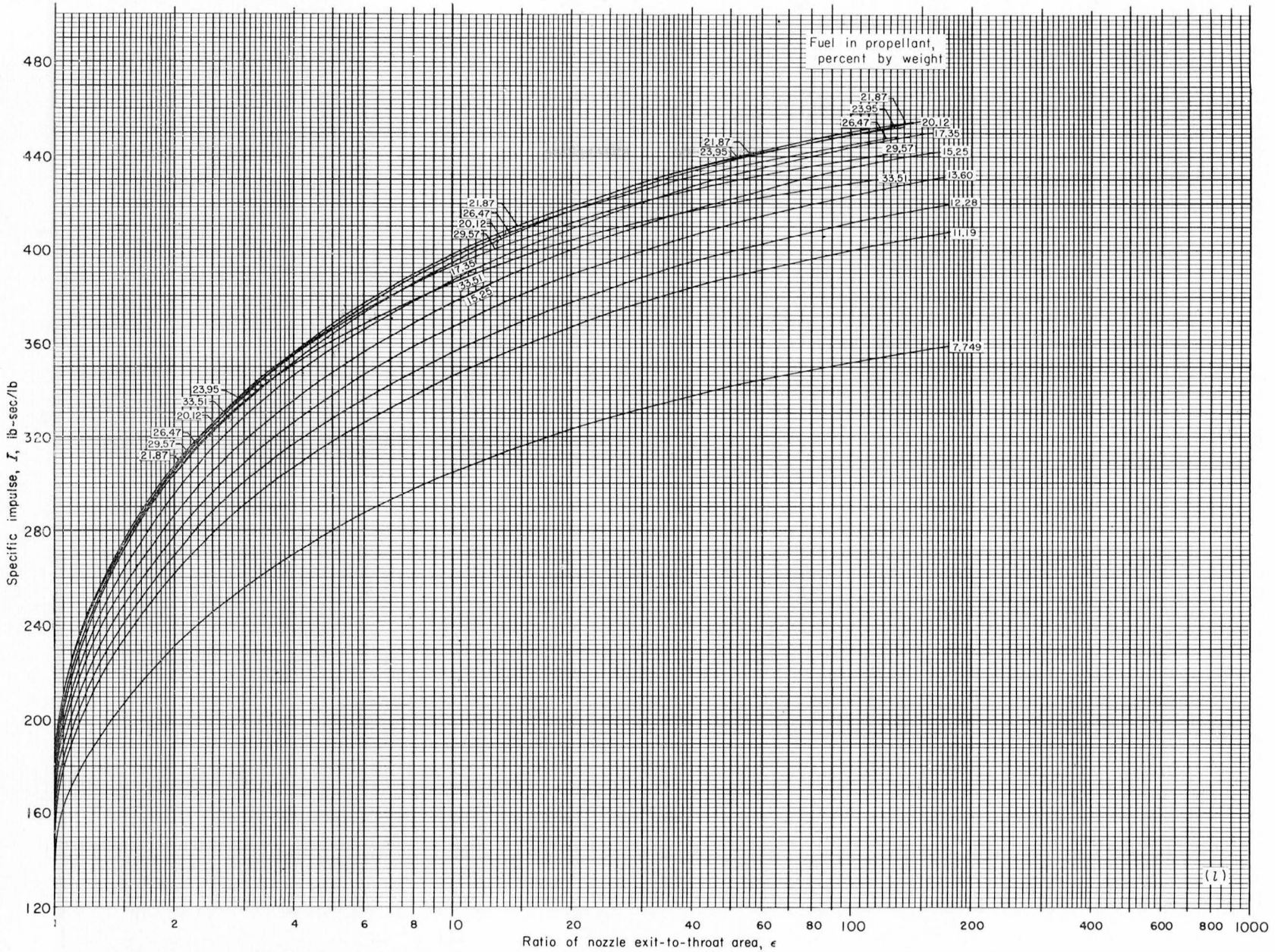

(1) Chamber pressure, 600 pounds per square inch absolute; frozen composition during isentropic expansion to area ratio indicated.

FIGURE 3.—Continued. Theoretical specific impulse of liquid hydrogen and liquid oxygen.

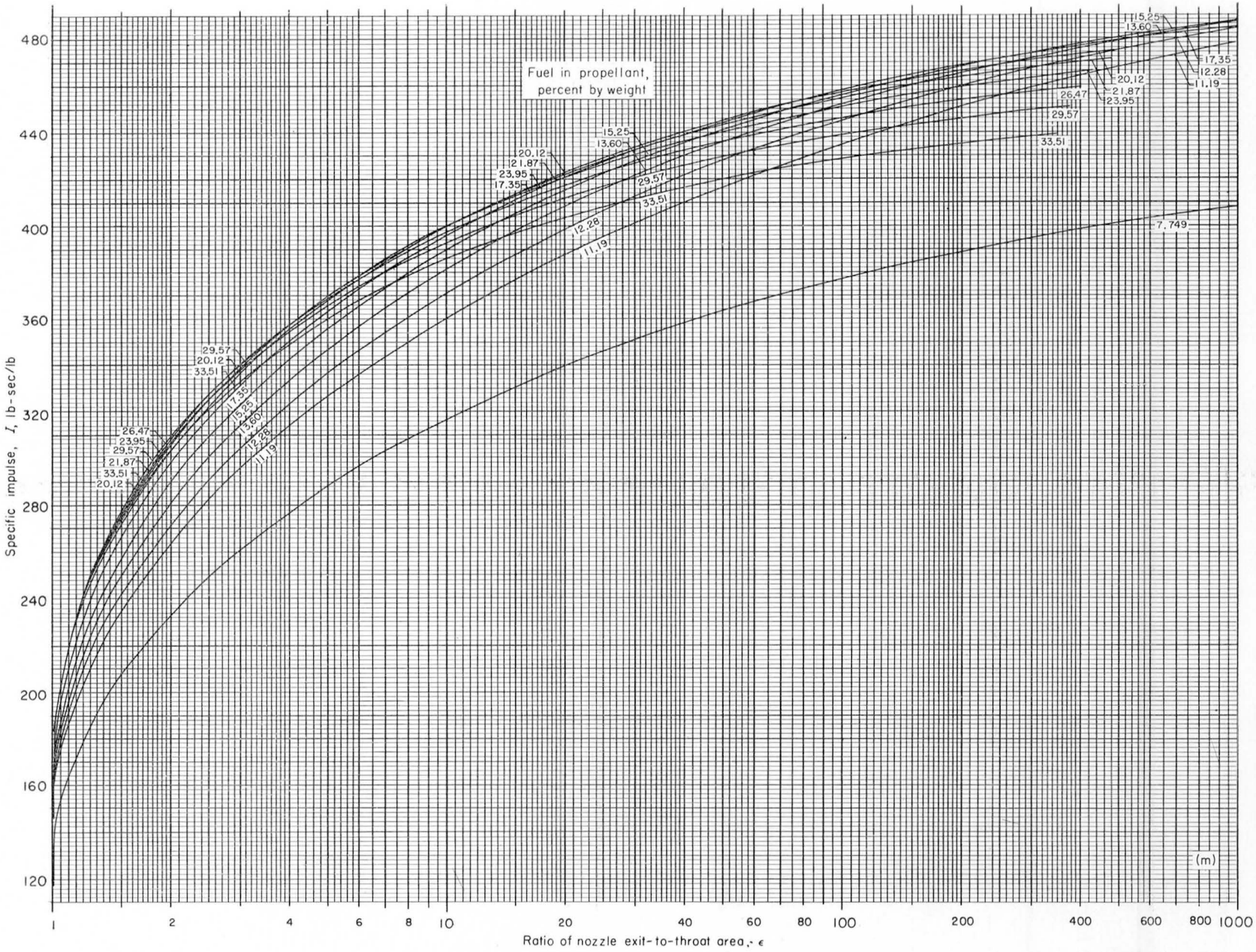

(m) Chamber pressure, 900 pounds per square inch absolute; equilibrium composition during isentropic expansion to area ratio indicated.

FIGURE 3.—Continued. Theoretical specific impulse of liquid hydrogen and liquid oxygen.

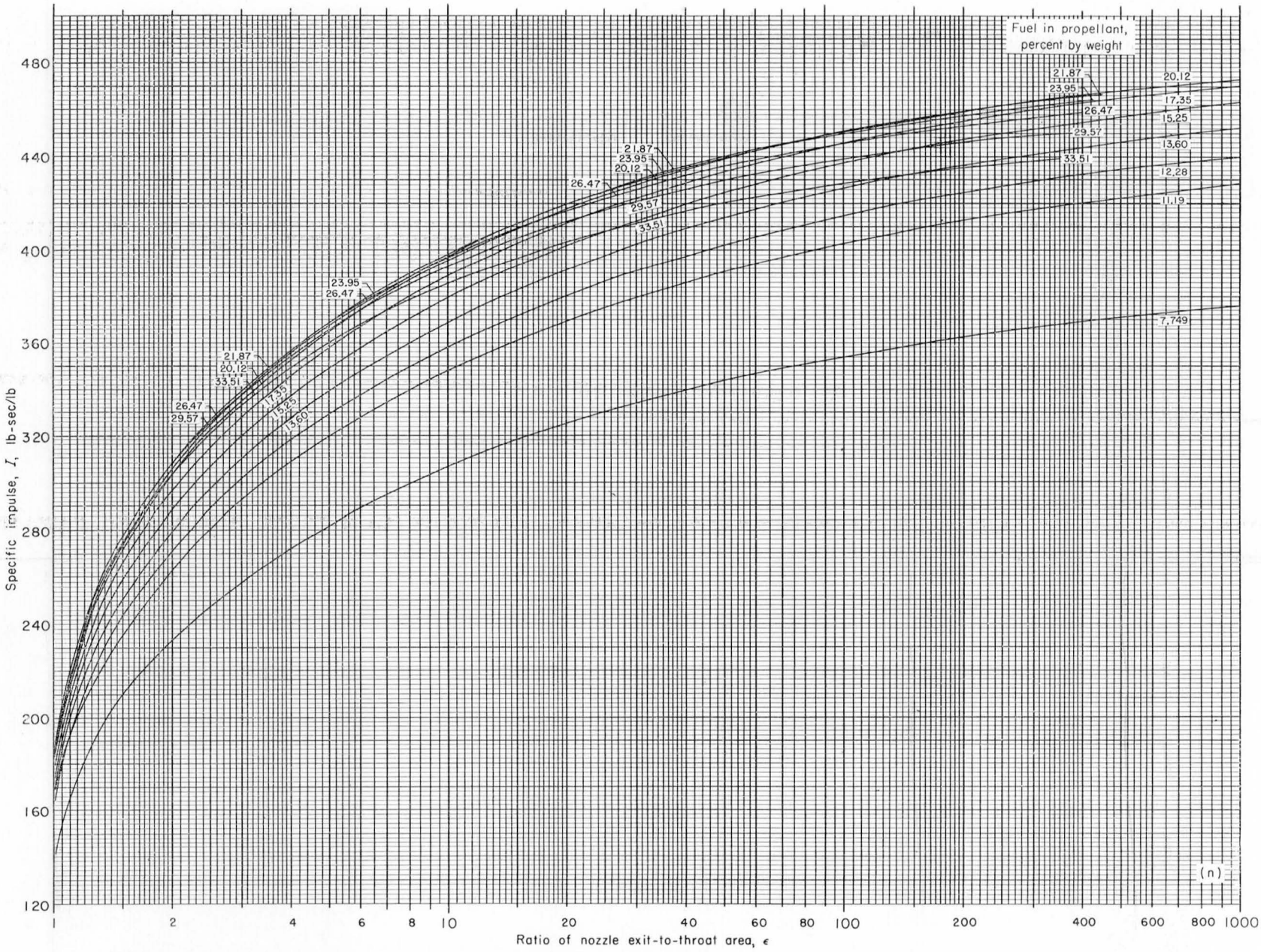

(n) Chamber pressure, 900 pounds per square inch absolute; frozen composition during isentropic expansion to area ratio indicated.

FIGURE 3.—Continued. Theoretical specific impulse of liquid hydrogen and liquid oxygen.

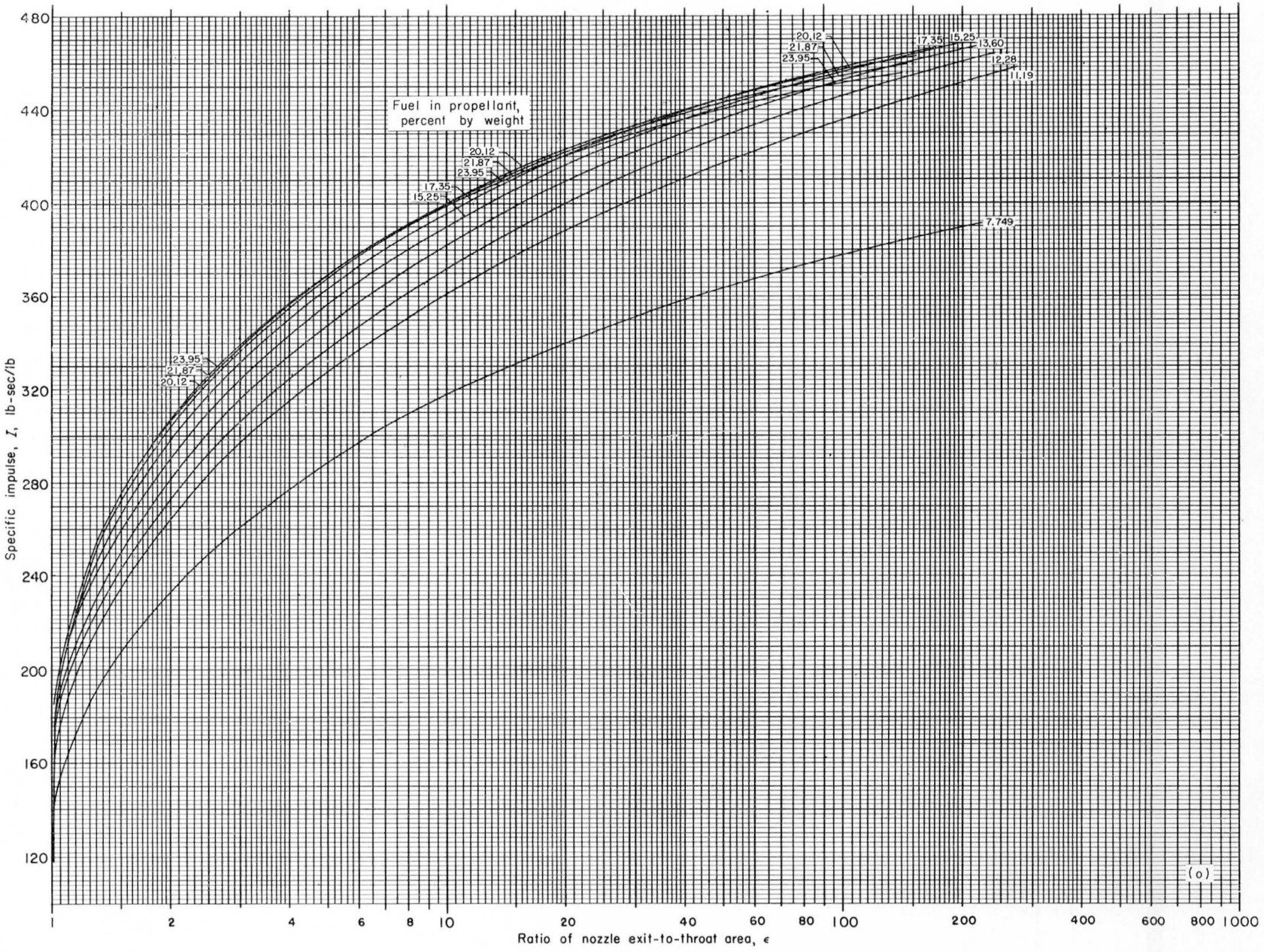

(o) Chamber pressure, 1200 pounds per square inch absolute; equilibrium composition during isentropic expansion to area ratio indicated.

FIGURE 3.—Continued. Theoretical specific impulse of liquid hydrogen and liquid oxygen.

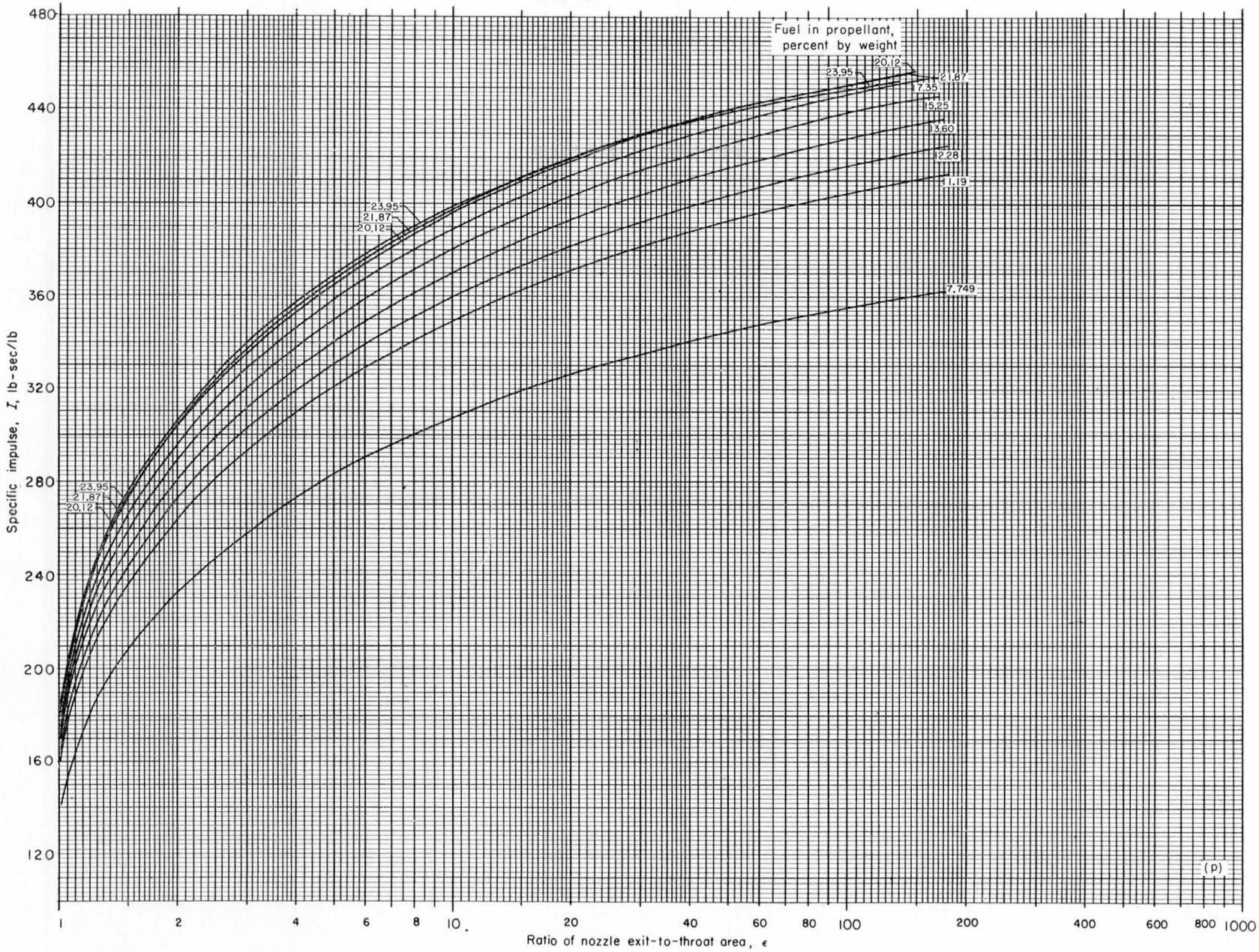

(p) Chamber pressure, 1200 pounds per square inch absolute; frozen composition during isentropic expansion to area ratio indicated.

FIGURE 3.—Concluded. Theoretical specific impulse of liquid hydrogen and liquid oxygen.

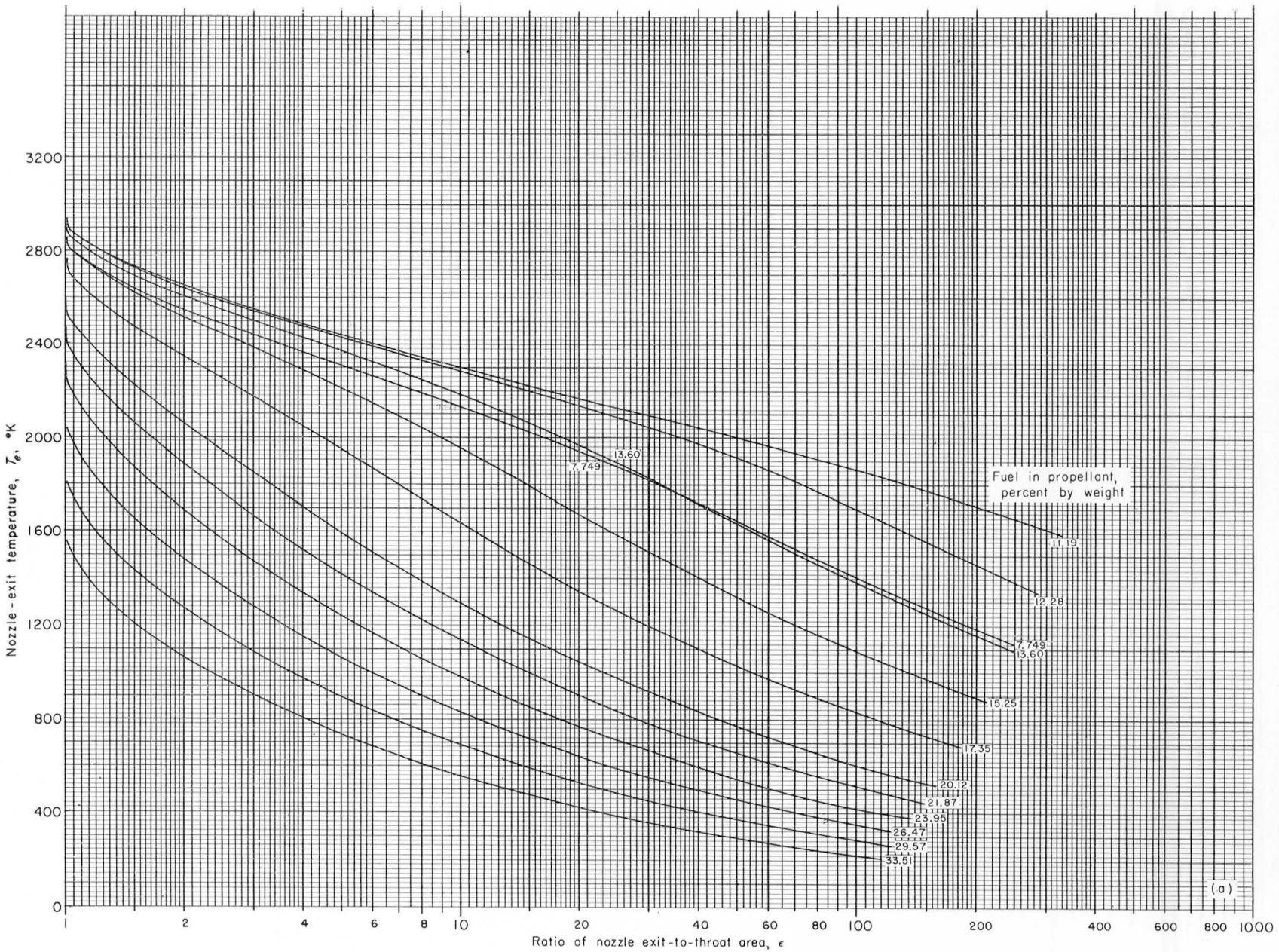

(a) Chamber pressure, 15 pounds per square inch absolute; equilibrium composition during isentropic expansion to area ratio indicated.

FIGURE 4.—Theoretical nozzle-exit temperatures of liquid hydrogen and liquid oxygen.

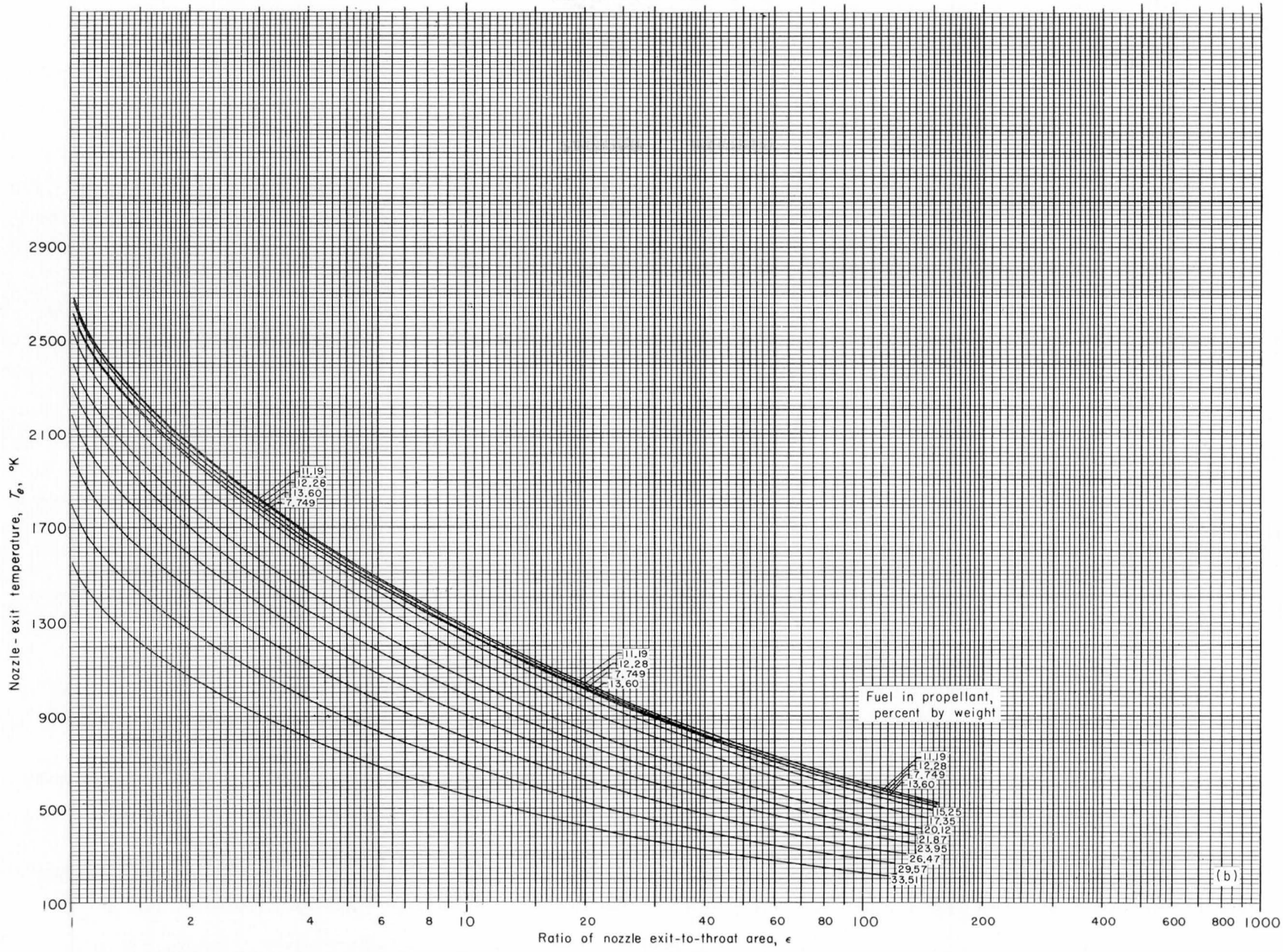

(b) Chamber pressure, 15 pounds per square inch absolute; frozen composition during isentropic expansion to area ratio indicated.

FIGURE 4.—Continued. Theoretical nozzle-exit temperatures of liquid hydrogen and liquid oxygen.

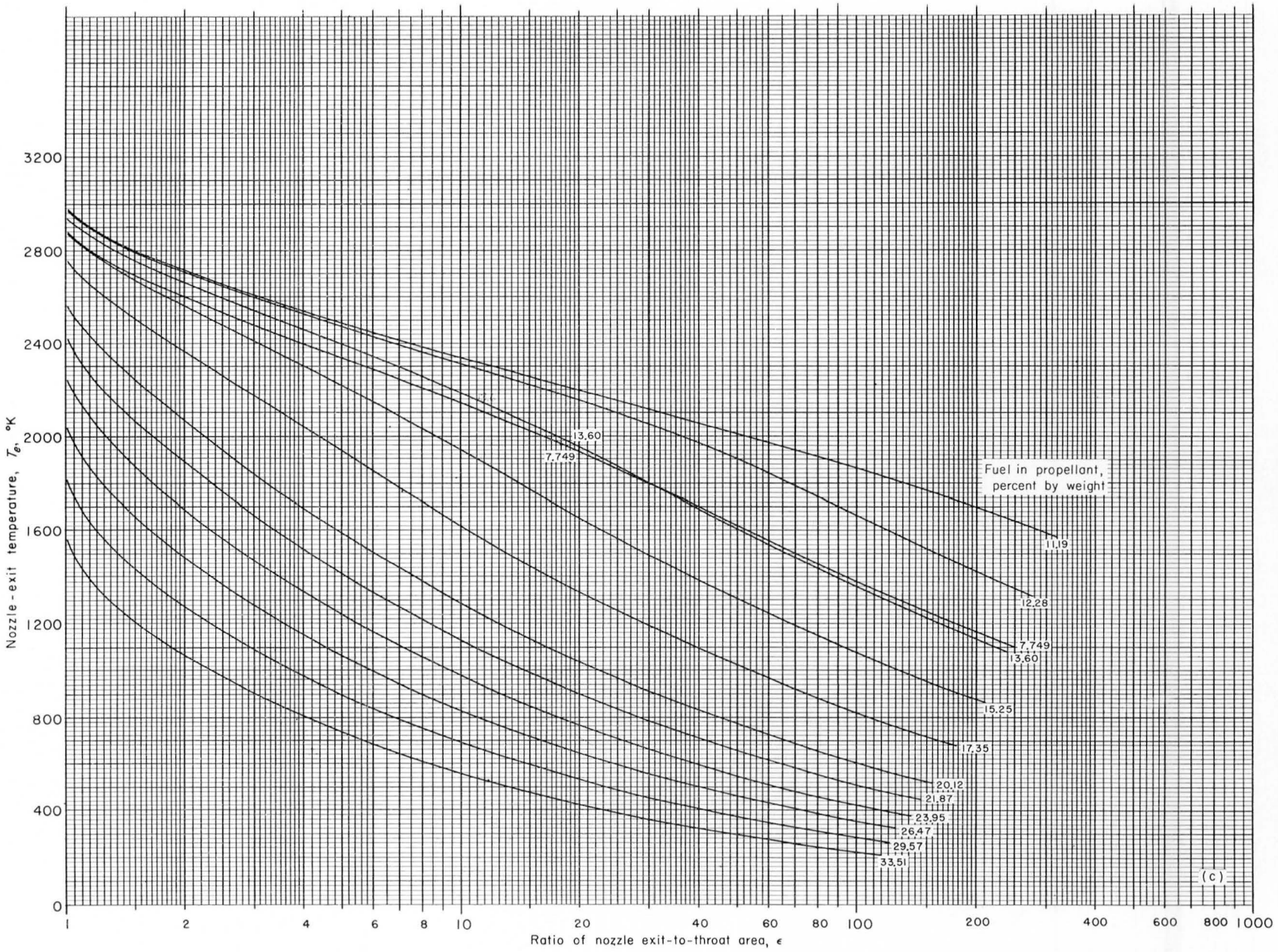

(c) Chamber pressure, 30 pounds per square inch absolute; equilibrium composition during isentropic expansion to area ratio indicated.

FIGURE 4.—Continued. Theoretical nozzle-exit temperatures of liquid hydrogen and liquid oxygen.

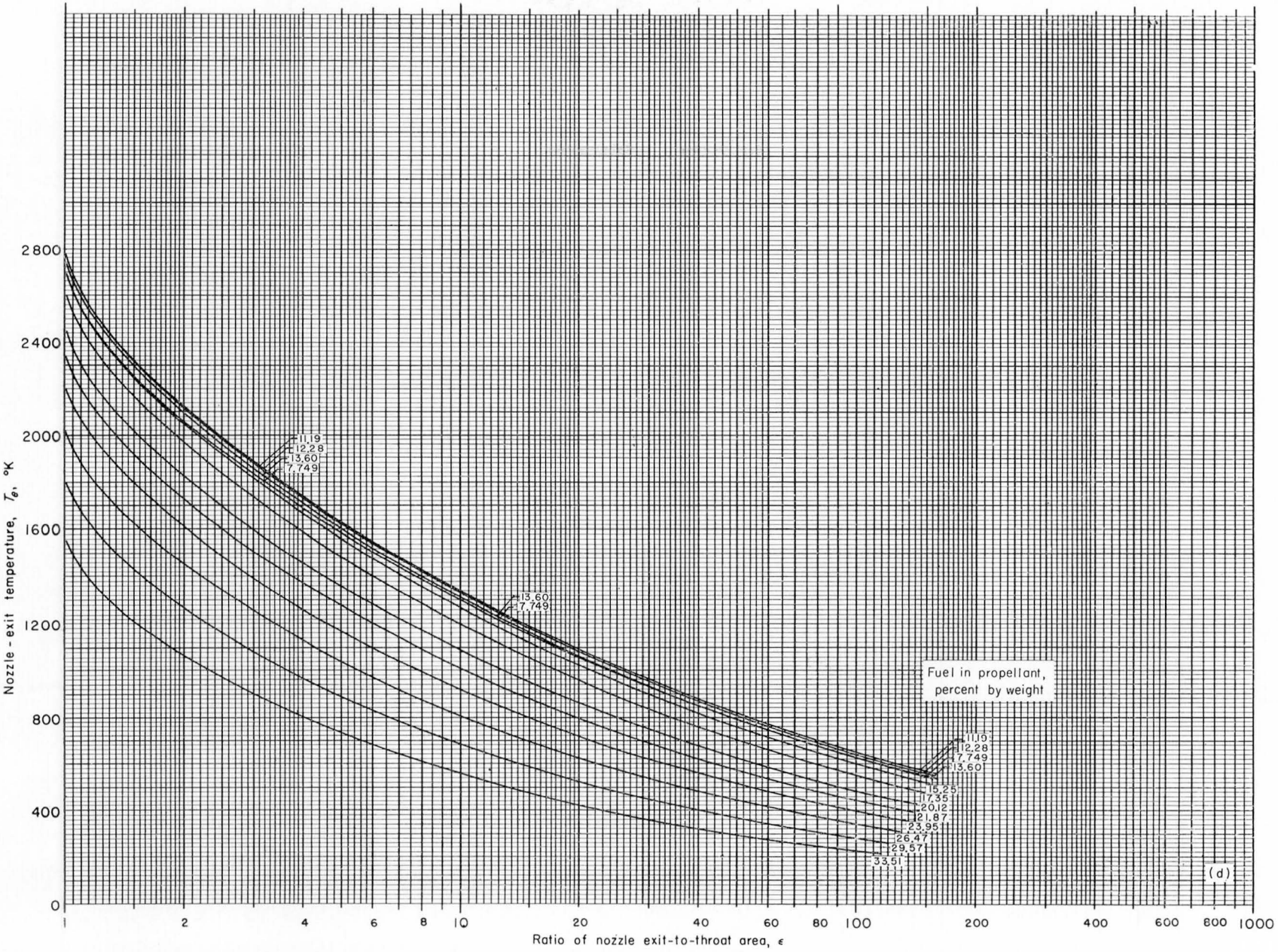

(d) Chamber pressure, 30 pounds per square inch absolute; frozen composition during isentropic expansion to area ratio indicated.

FIGURE 4.—Continued. Theoretical nozzle-exit temperatures of liquid hydrogen and liquid oxygen.

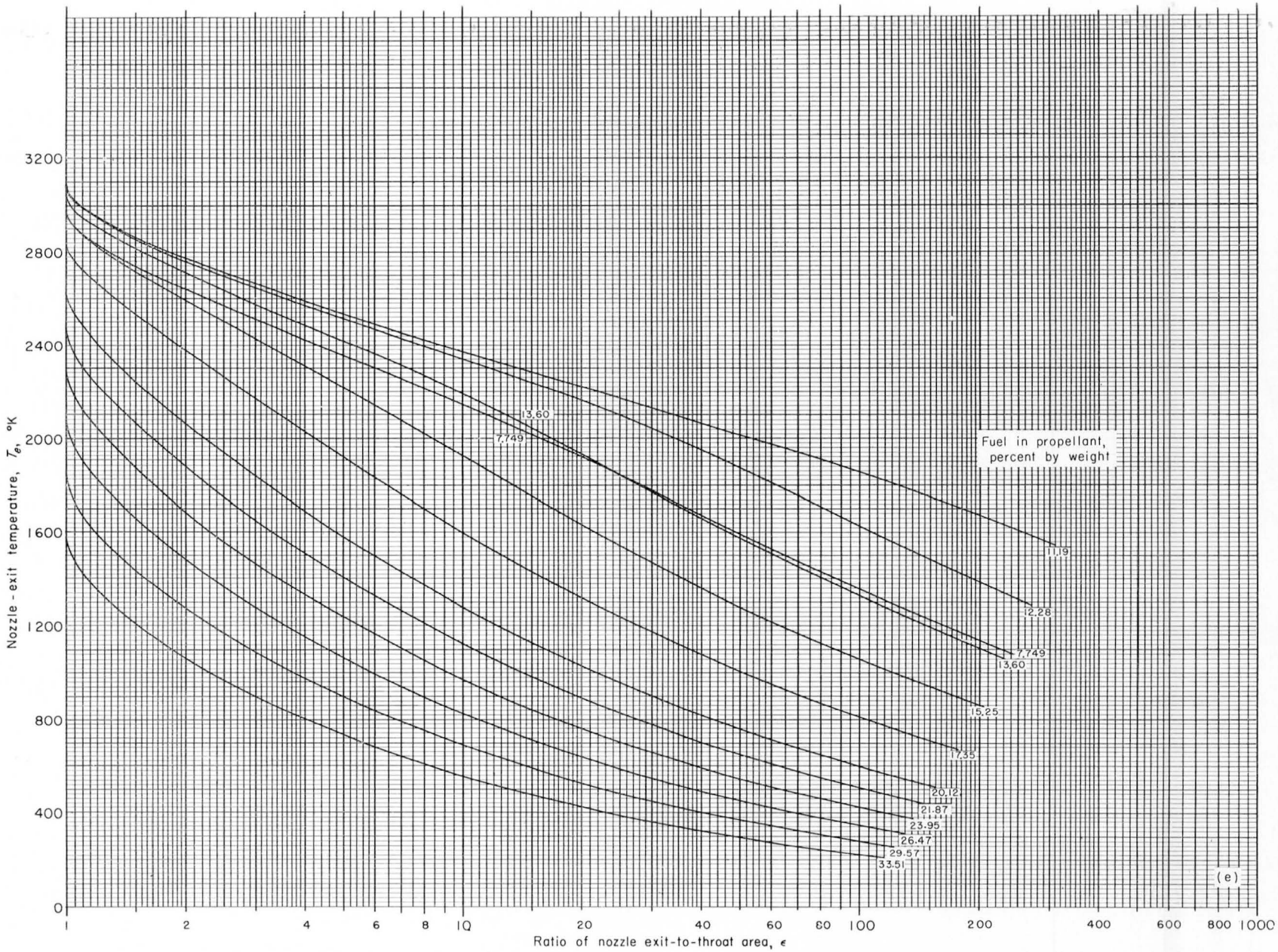

(e) Chamber pressure, 60 pounds per square inch absolute; equilibrium composition during isentropic expansion to area ratio indicated.

FIGURE 4.—Continued. Theoretical nozzle-exit temperatures of liquid hydrogen and liquid oxygen.

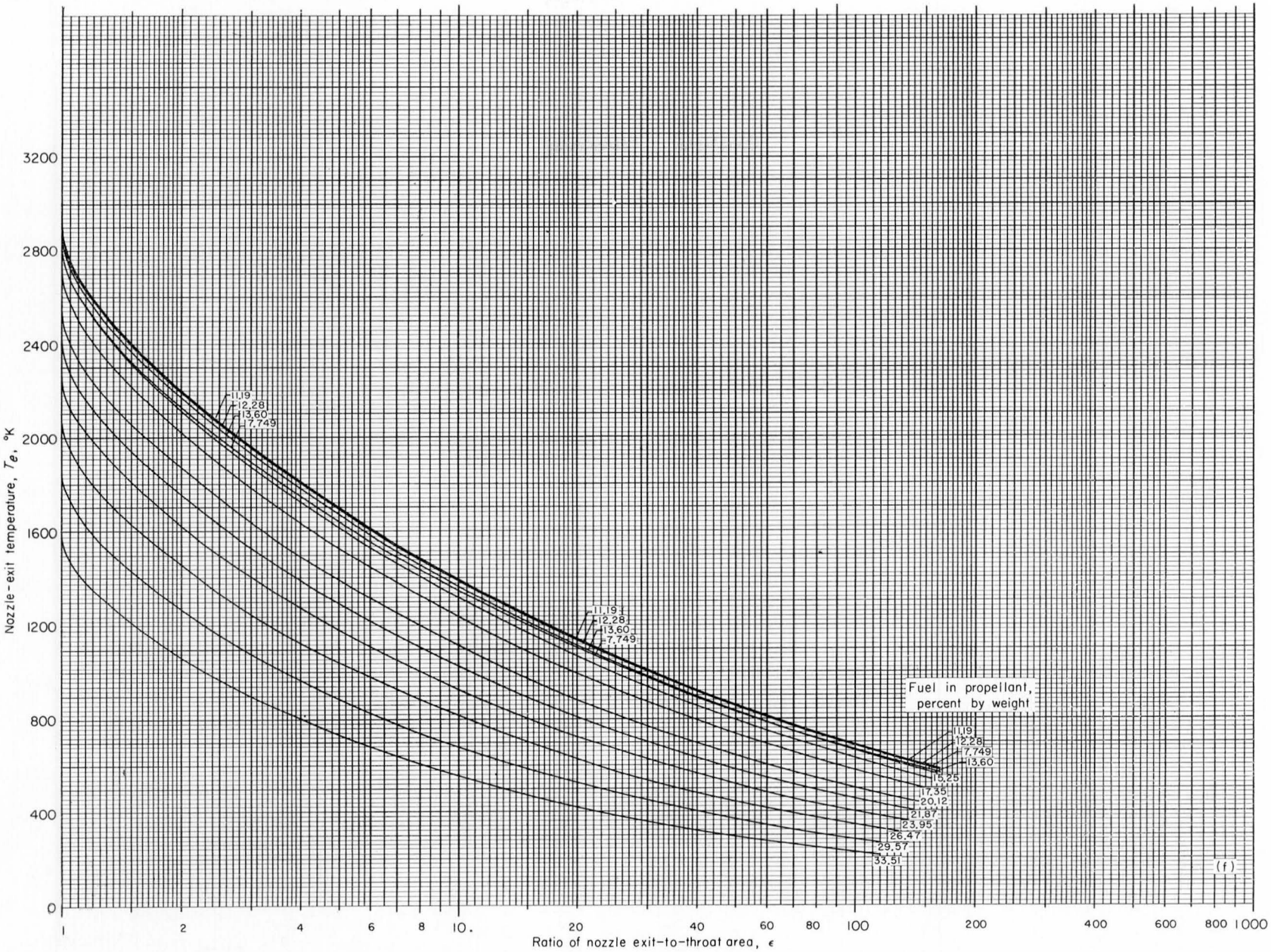

(f) Chamber pressure, 60 pounds per square inch absolute; frozen composition during isentropic expansion to area ratio indicated.

FIGURE 4.—Continued. Theoretical nozzle-exit temperatures of liquid hydrogen and liquid oxygen.

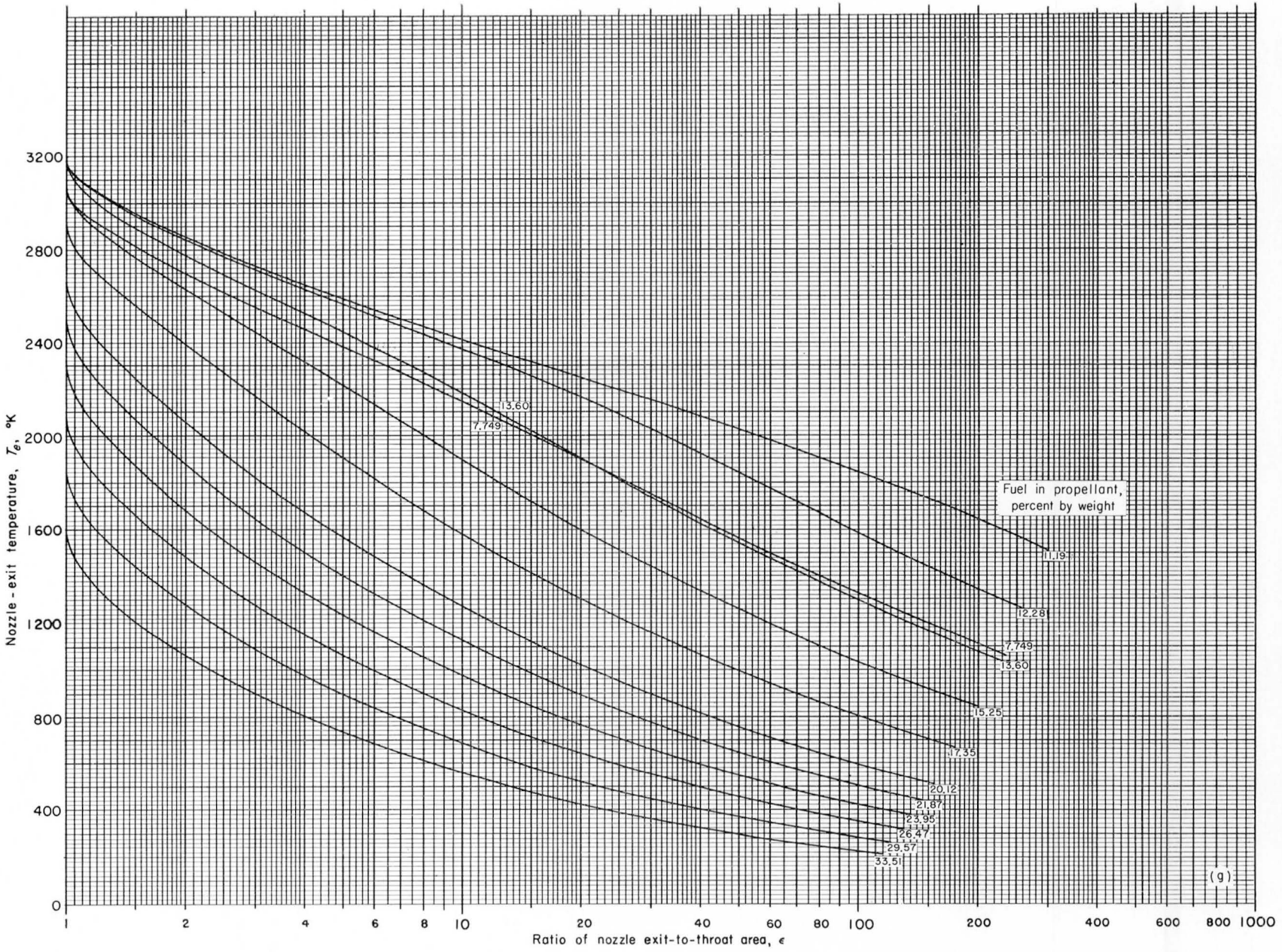

(g) Chamber pressure, 150 pounds per square inch absolute; equilibrium composition during isentropic expansion to area ratio indicated.

FIGURE 4.—Continued. Theoretical nozzle-exit temperatures of liquid hydrogen and liquid oxygen.

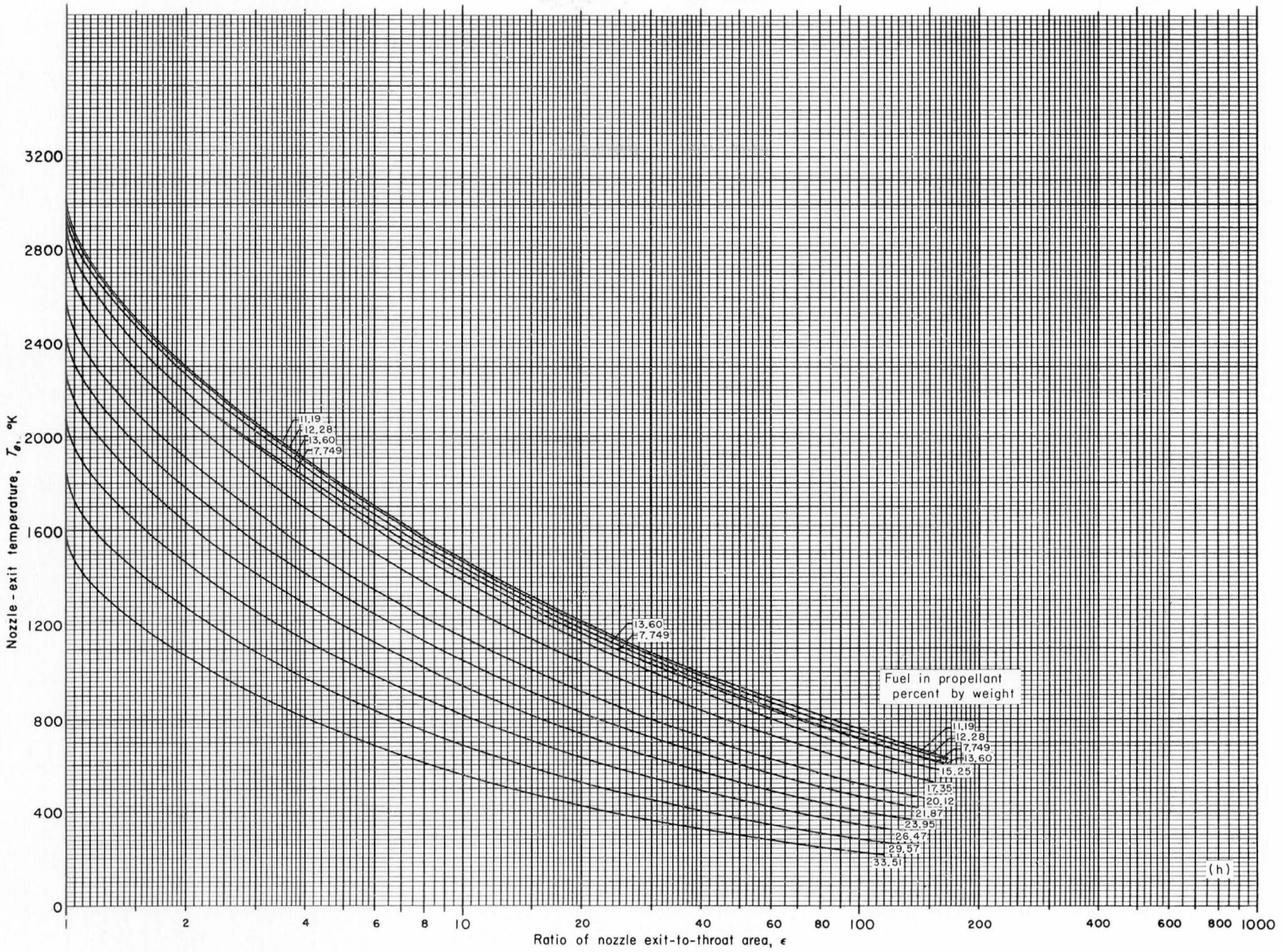

(h) Chamber pressure, 150 pounds per square inch absolute; frozen composition during isentropic expansion to area ratio indicated.

FIGURE 4.—Continued. Theoretical nozzle-exit temperatures of liquid hydrogen and liquid oxygen.

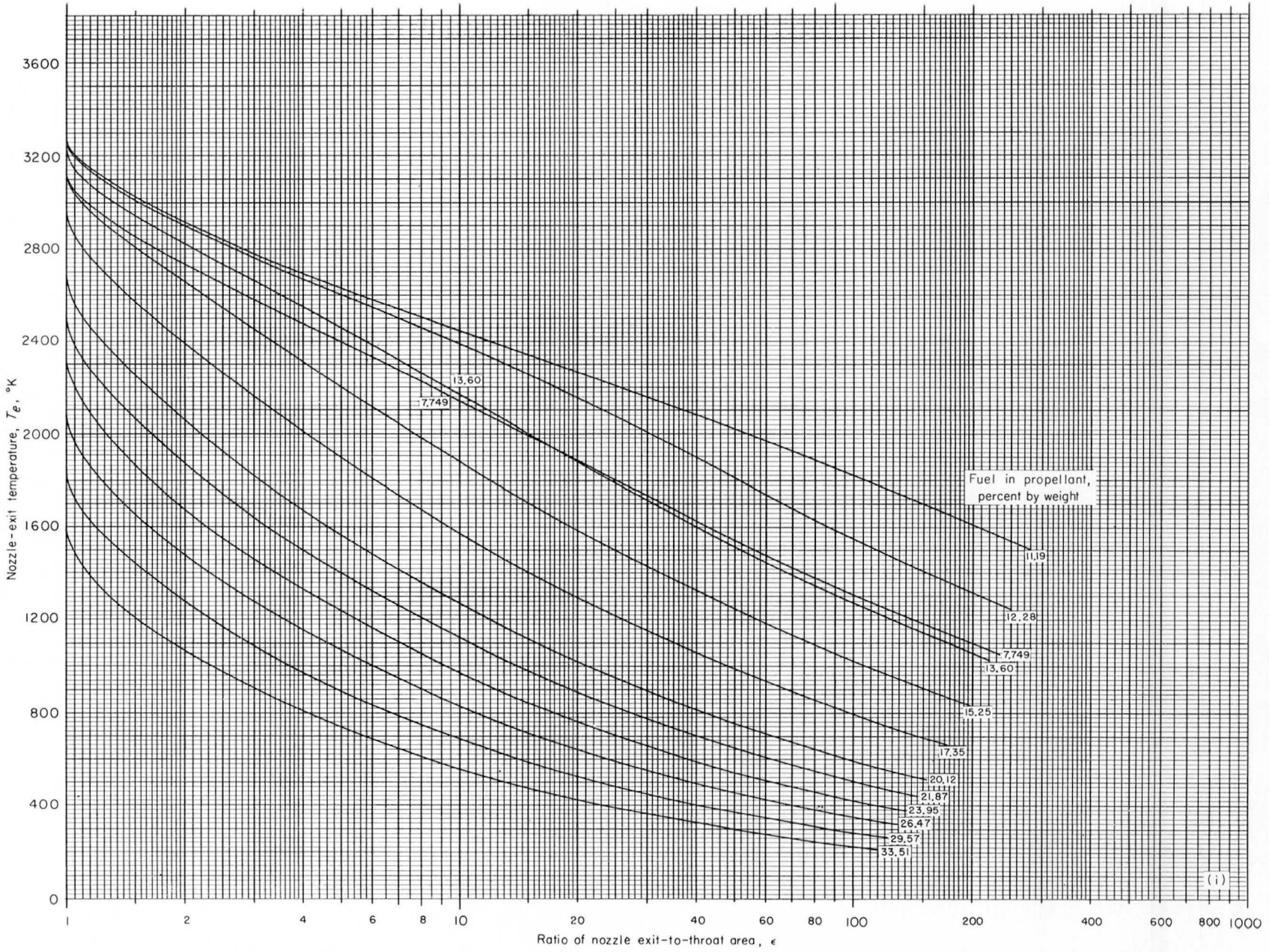

(i) Chamber pressure, 300 pounds per square inch absolute; equilibrium composition during isentropic expansion to area ratio indicated.

FIGURE 4.—Continued. Theoretical nozzle-exit temperatures of liquid hydrogen and liquid oxygen.

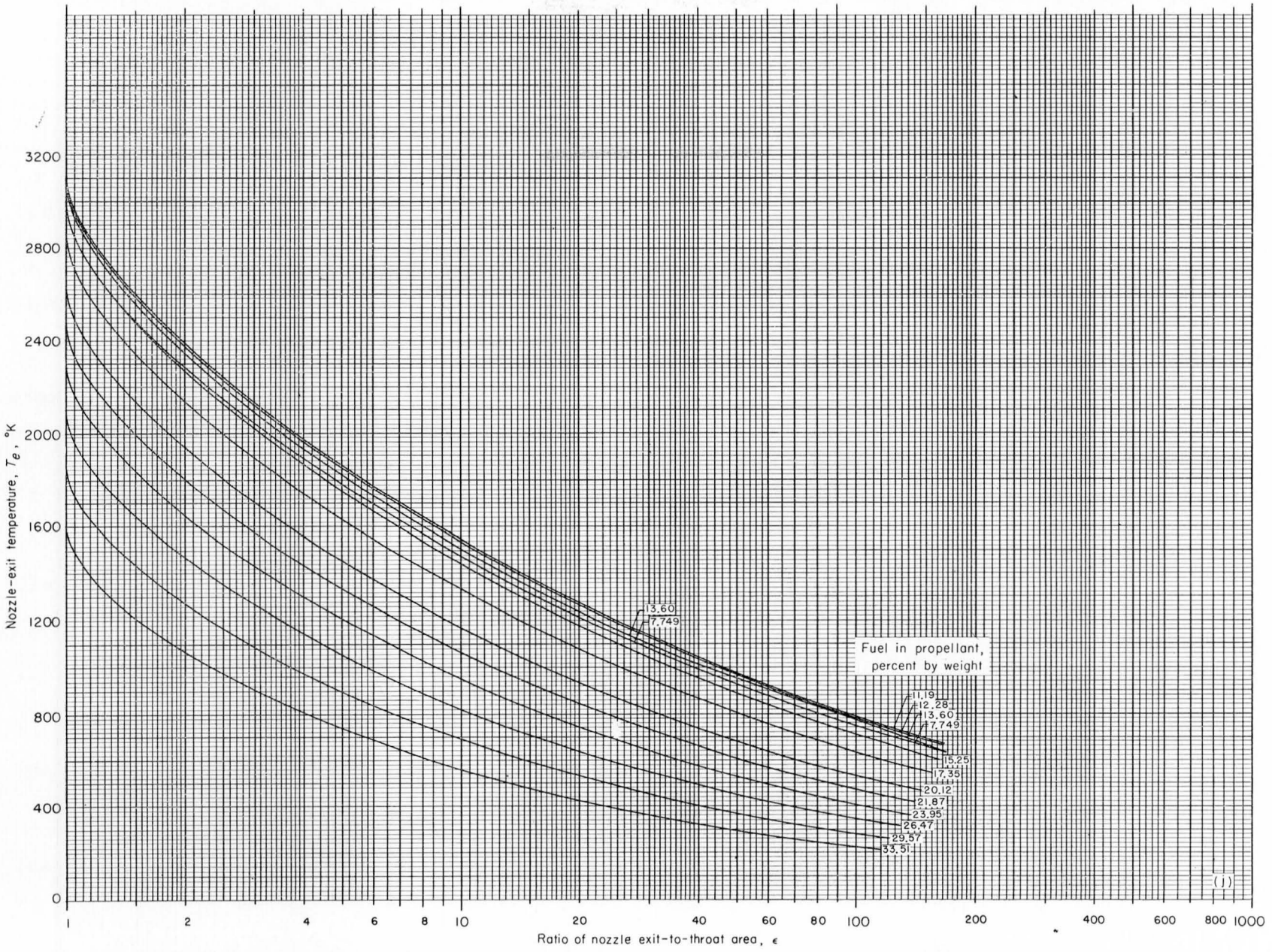

(j) Chamber pressure, 300 pounds per square inch absolute; frozen composition during isentropic expansion to area ratio indicated.

FIGURE 4.—Continued. Theoretical nozzle-exit temperatures of liquid hydrogen and liquid oxygen.

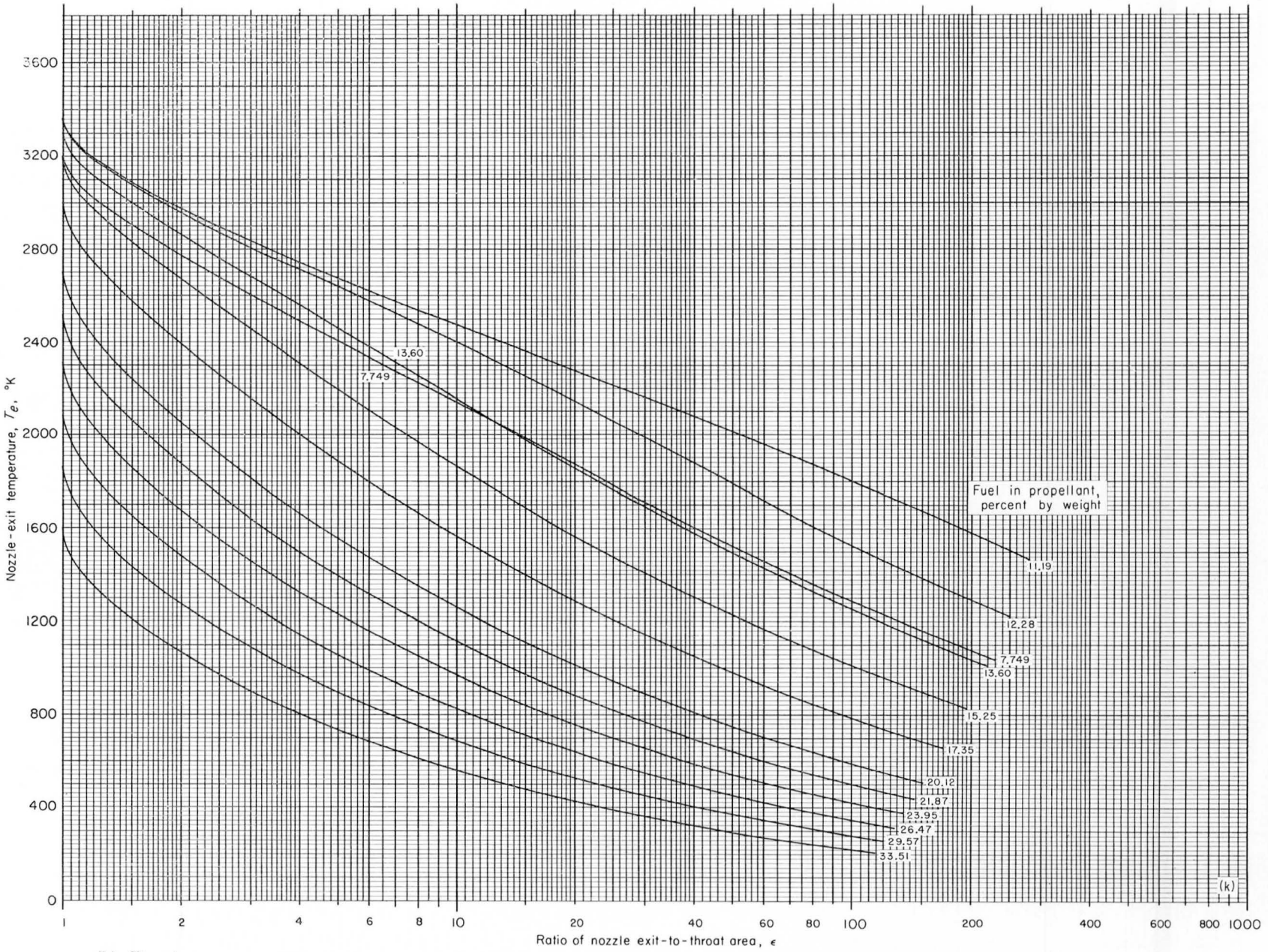

(k) Chamber pressure, 600 pounds per square inch absolute; equilibrium composition during isentropic expansion to area ratio indicated.

FIGURE 4.—Continued. Theoretical nozzle-exit temperatures of liquid hydrogen and liquid oxygen.

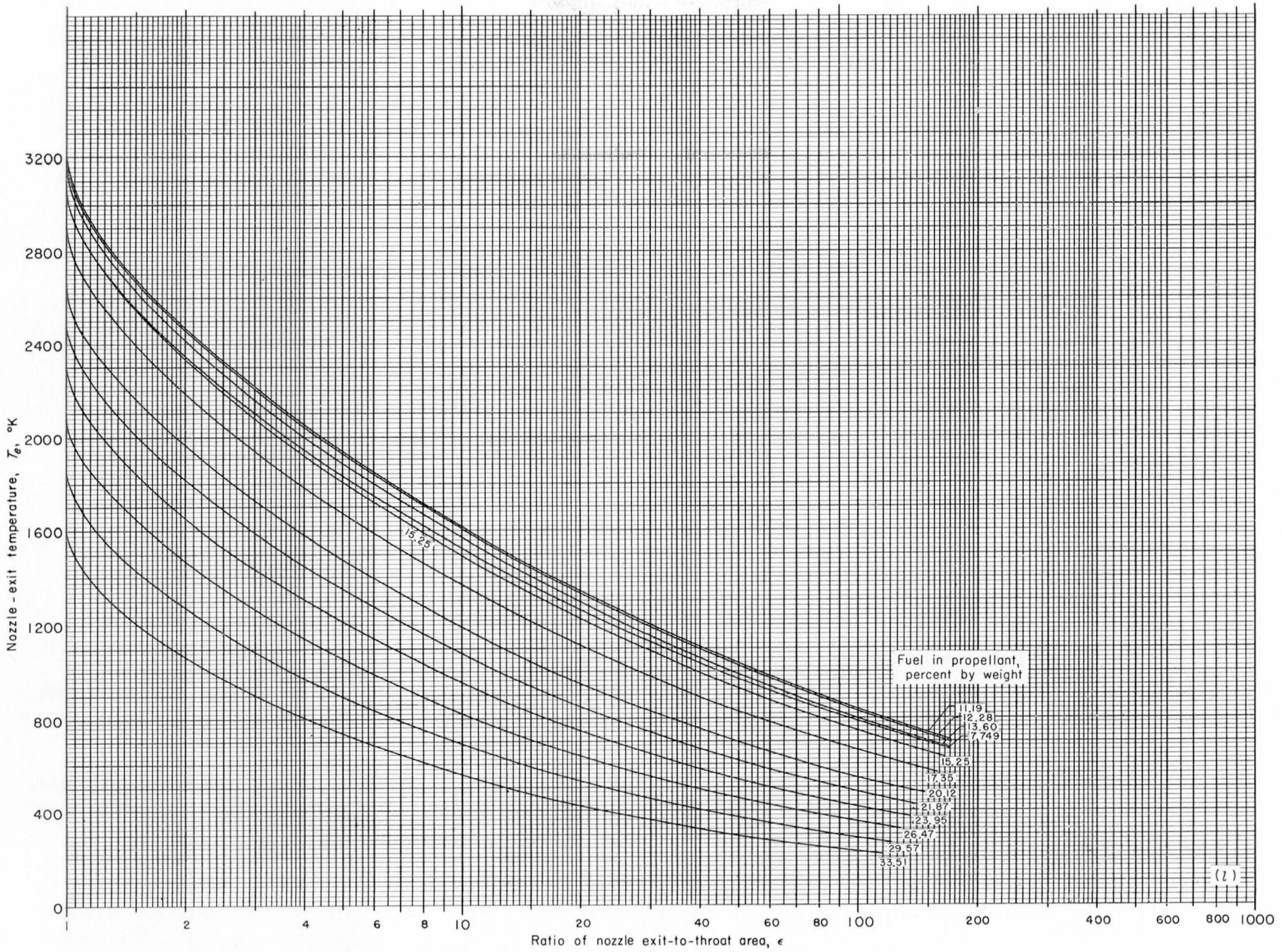

(l) Chamber pressure, 600 pounds per square inch absolute; frozen composition during isentropic expansion to area ratio indicated.

FIGURE 4.—Continued. Theoretical nozzle-exit temperatures of liquid hydrogen and liquid oxygen.

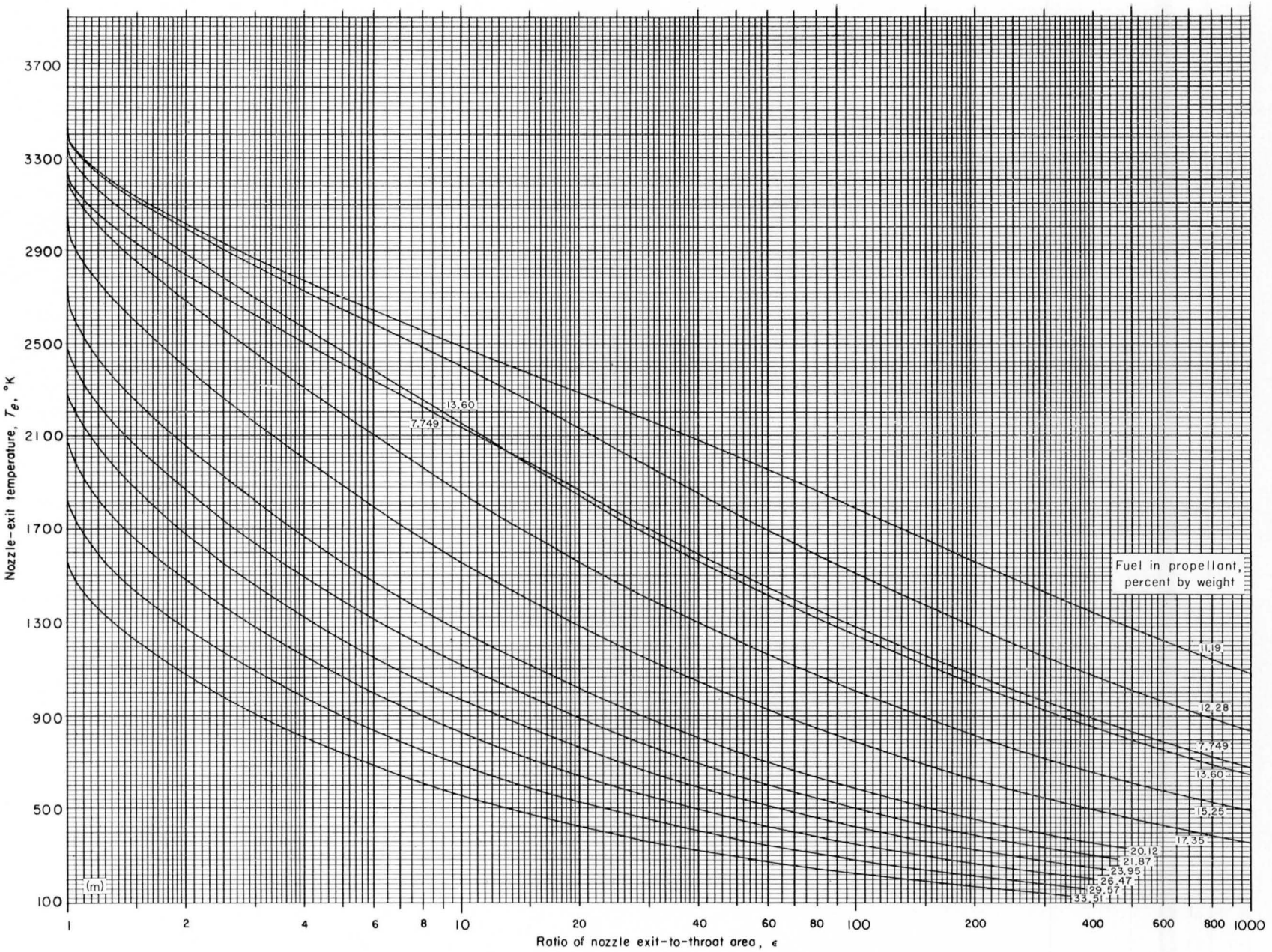

(m) Chamber pressure, 900 pounds per square inch absolute; equilibrium composition during isentropic expansion to area ratio indicated.

FIGURE 4.—Continued. Theoretical nozzle-exit temperatures of liquid hydrogen and liquid oxygen.

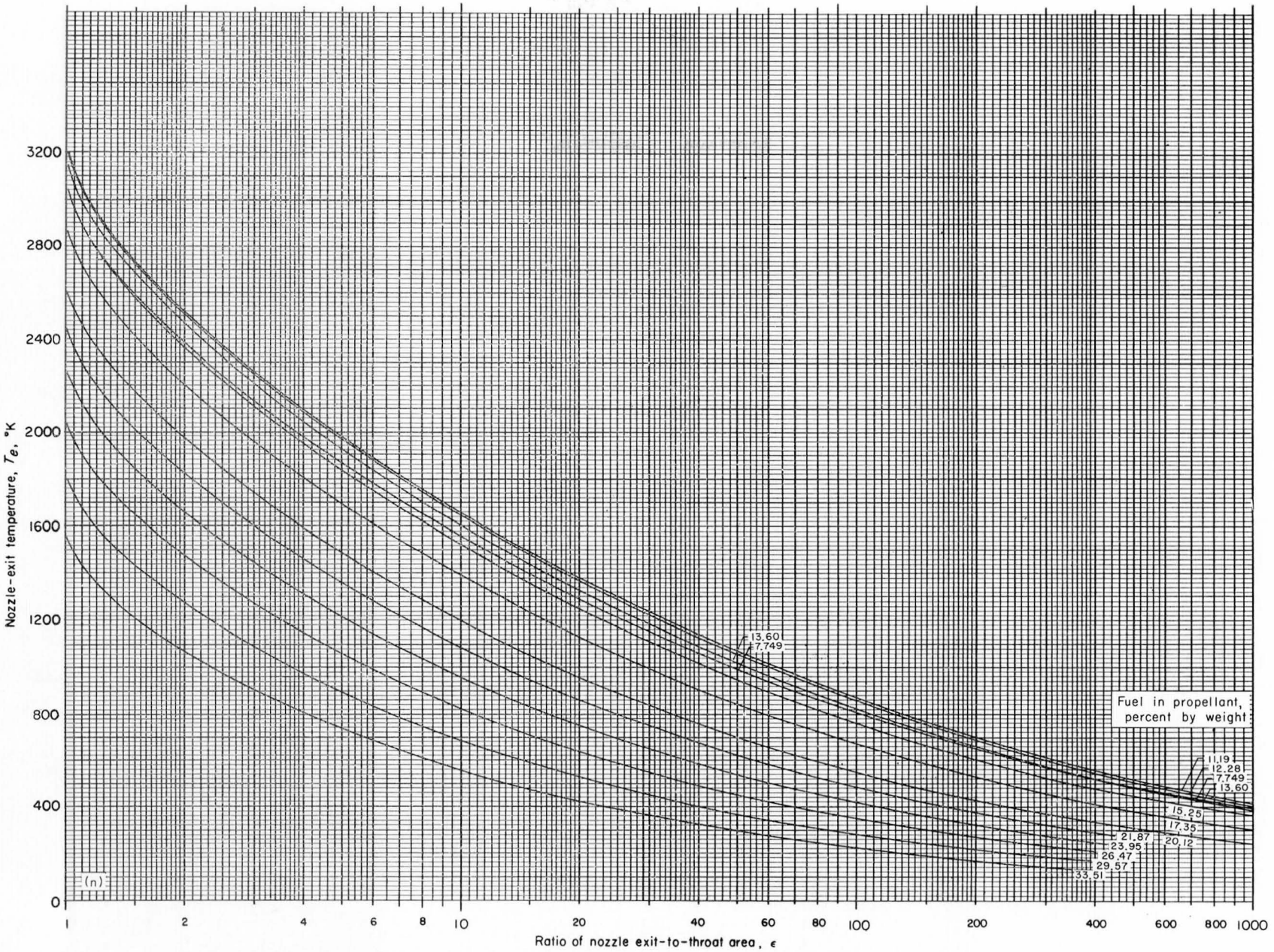

(n) Chamber pressure, 900 pounds per square inch absolute; frozen composition during isentropic expansion to area ratio indicated.

FIGURE 4.—Continued. Theoretical nozzle-exit temperatures of liquid hydrogen and liquid oxygen.

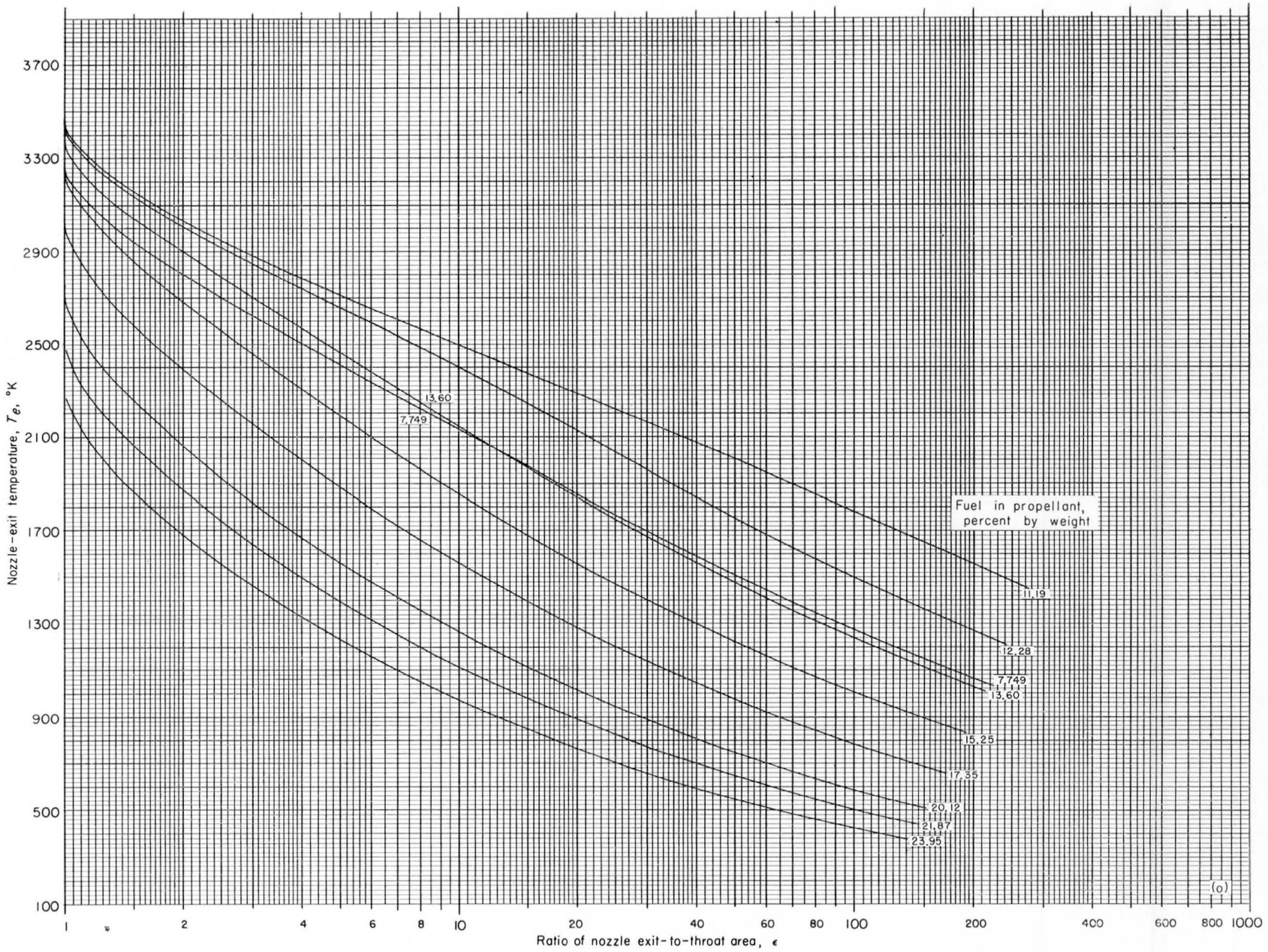

(o) Chamber pressure, 1200 pounds per square inch absolute; equilibrium composition during isentropic expansion to area ratio indicated.

FIGURE 4.—Continued. Theoretical nozzle-exit temperatures of liquid hydrogen and liquid oxygen.

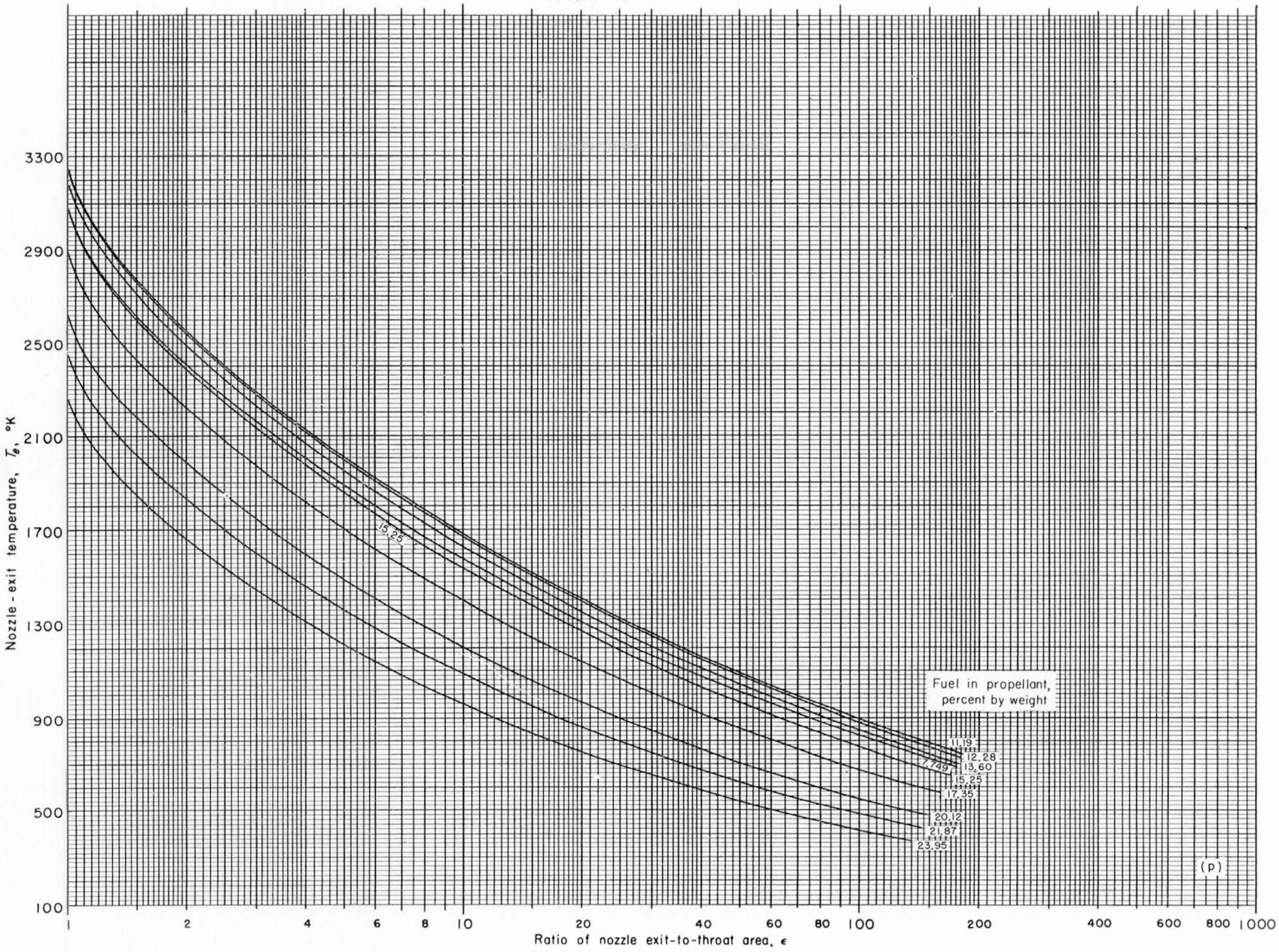

(p) Chamber pressure, 1200 pounds per square inch absolute; frozen composition during isentropic expansion to area ratio indicated.

FIGURE 4.—Concluded. Theoretical nozzle-exit temperatures of liquid hydrogen and liquid oxygen.

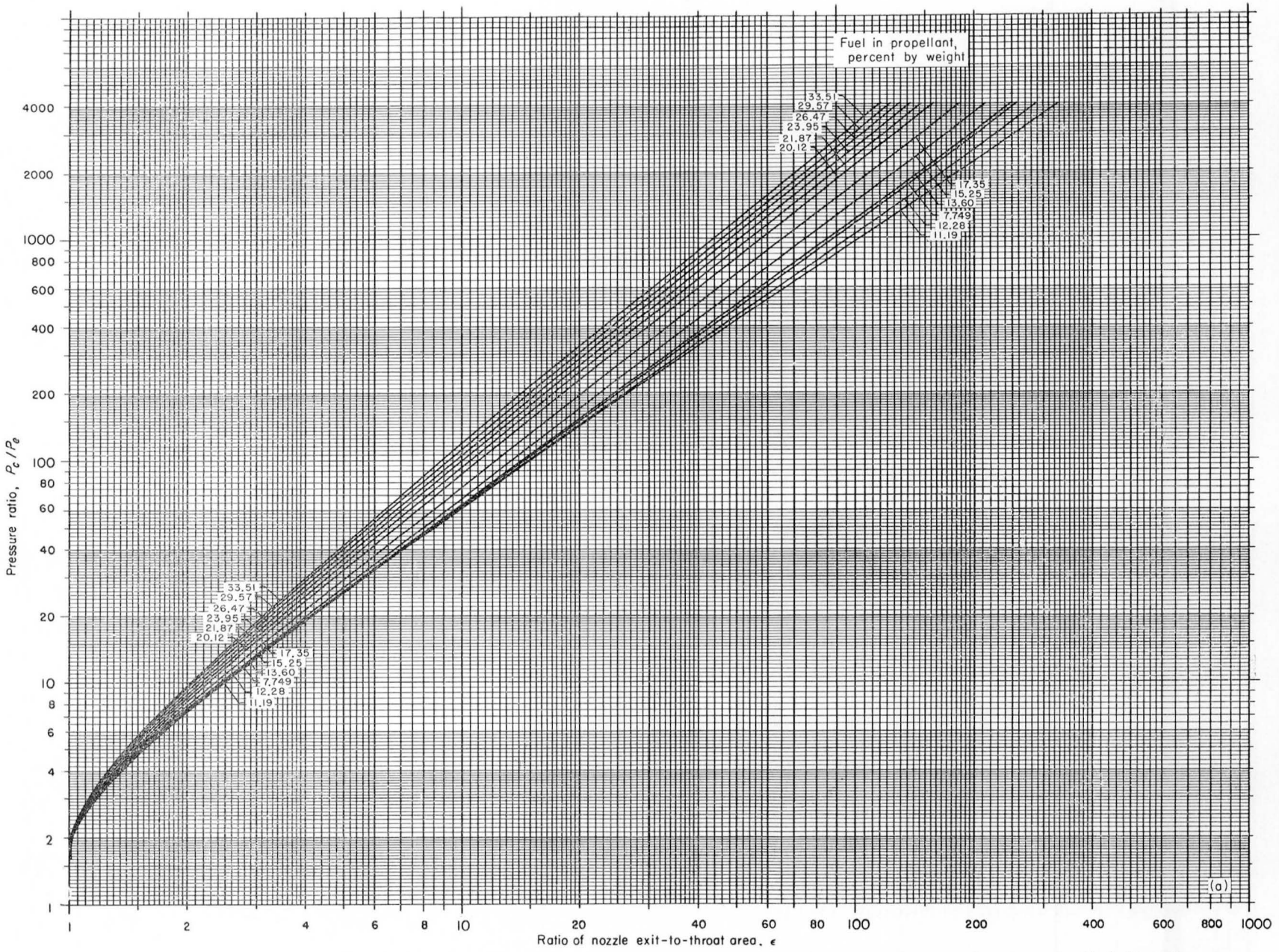

(a) Chamber pressure, 15 pounds per square inch absolute; equilibrium composition during isentropic expansion to area ratio indicated.

FIGURE 5.—Theoretical ratio of combustion-chamber to nozzle-exit pressure of liquid hydrogen and liquid oxygen.

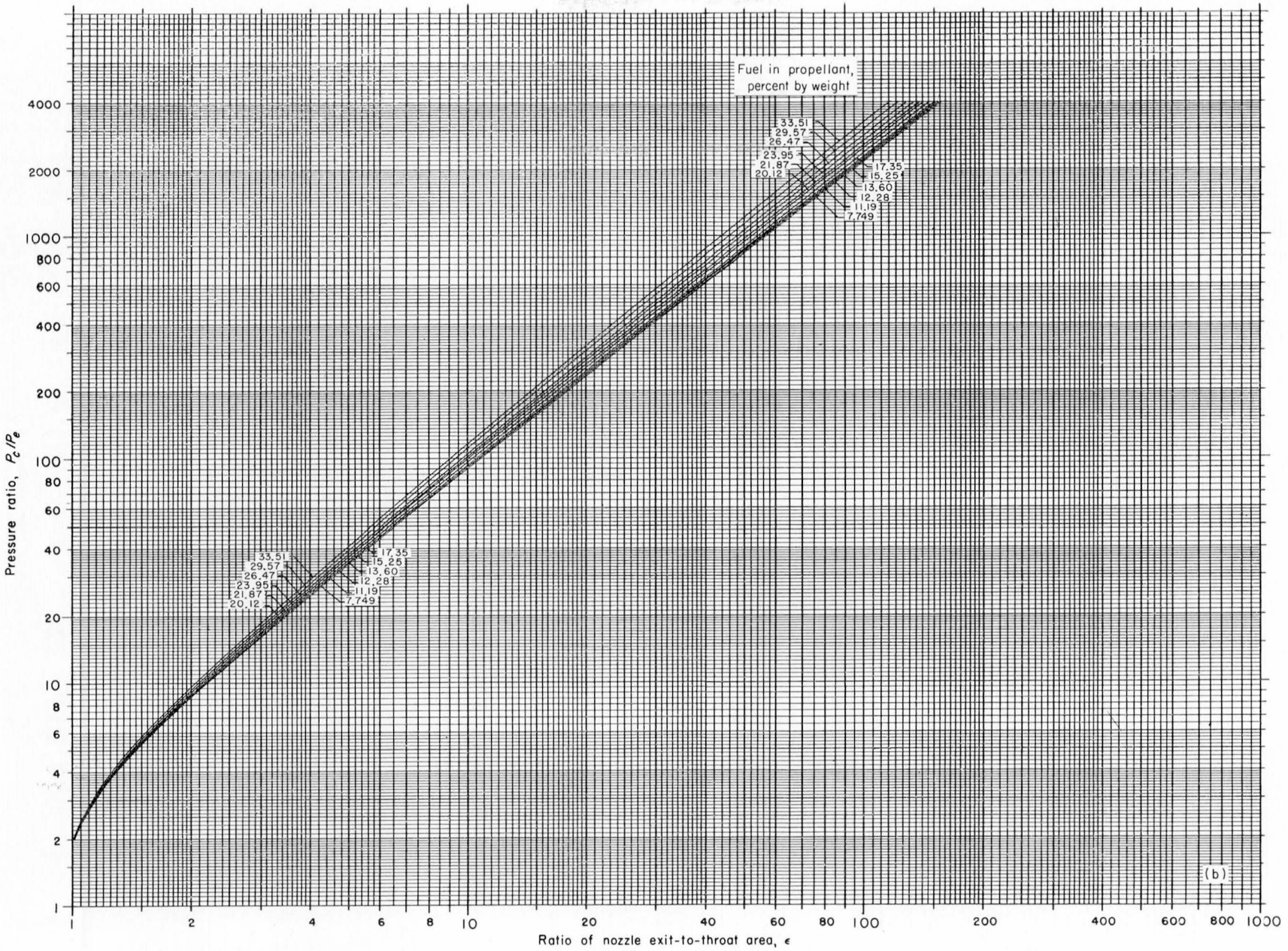

(b) Chamber pressure, 15 pounds per square inch absolute; frozen composition during isentropic expansion to area ratio indicated.

FIGURE 5.—Continued. Theoretical ratio of combustion-chamber to nozzle-exit pressure of liquid hydrogen and liquid oxygen.

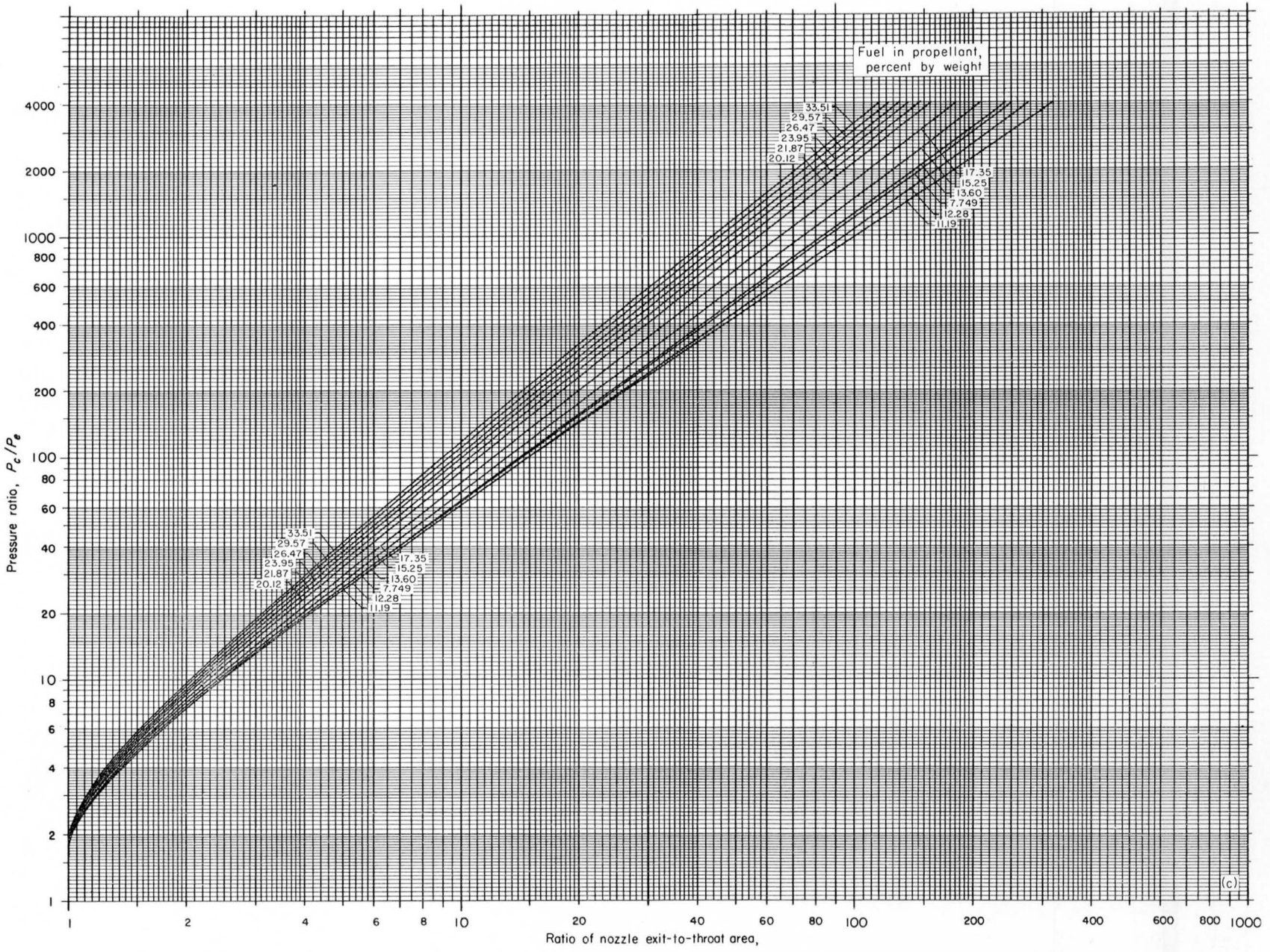

(c) Chamber pressure, 30 pounds per square inch absolute; equilibrium composition during isentropic expansion to area ratio indicated.

FIGURE 5.—Continued. Theoretical ratio of combustion-chamber to nozzle-exit pressure of liquid hydrogen and liquid oxygen.

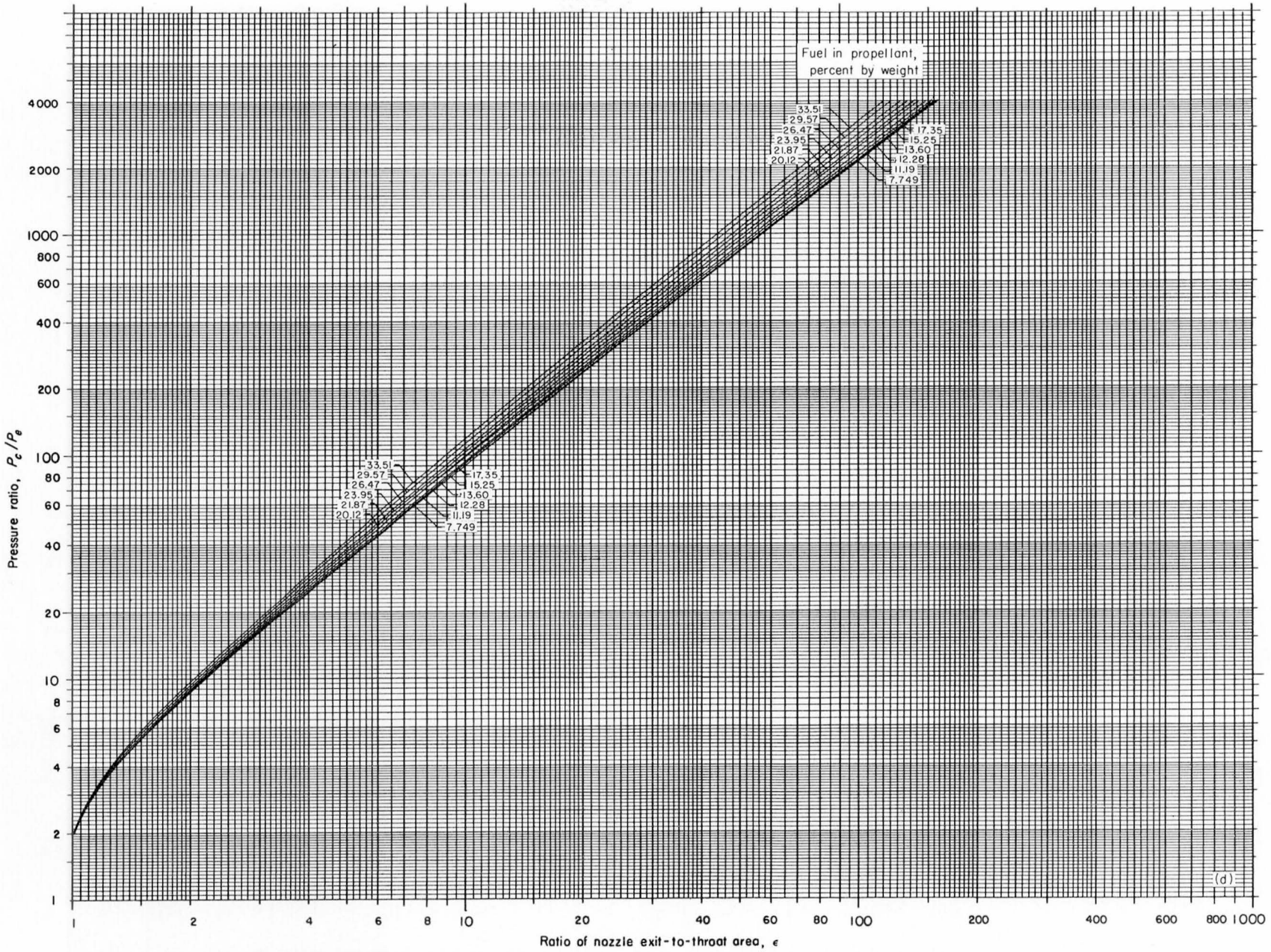

(d) Chamber pressure, 30 pounds per square inch absolute; frozen composition during isentropic expansion to area ratio indicated.

FIGURE 5.—Continued. Theoretical ratio of combustion-chamber to nozzle-exit pressure of liquid hydrogen and liquid oxygen.

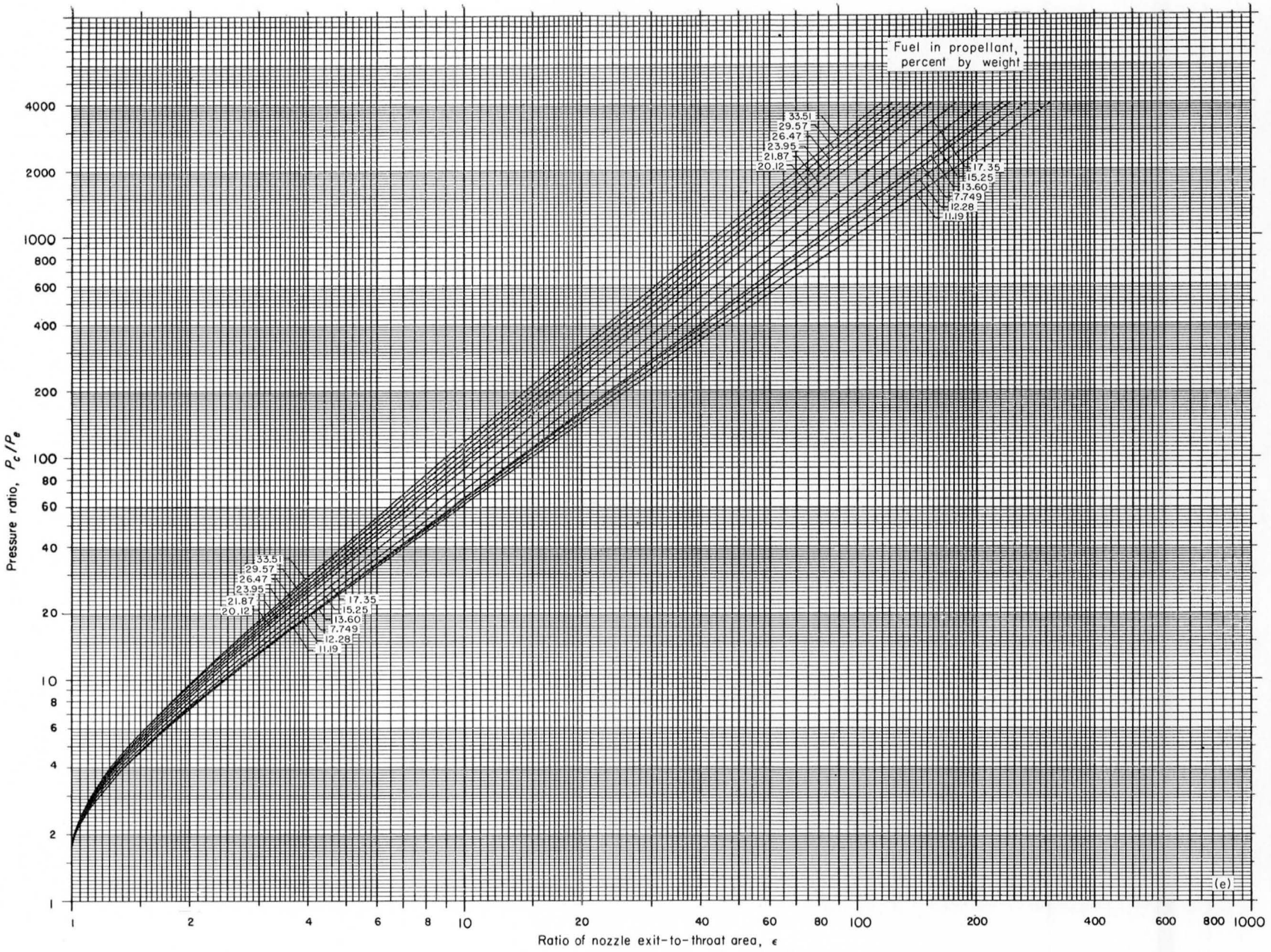

(e) Chamber pressure, 60 pounds per square inch absolute; equilibrium composition during isentropic expansion to area ratio indicated.

FIGURE 5.—Continued. Theoretical ratio of combustion-chamber to nozzle-exit pressure of liquid hydrogen and liquid oxygen.

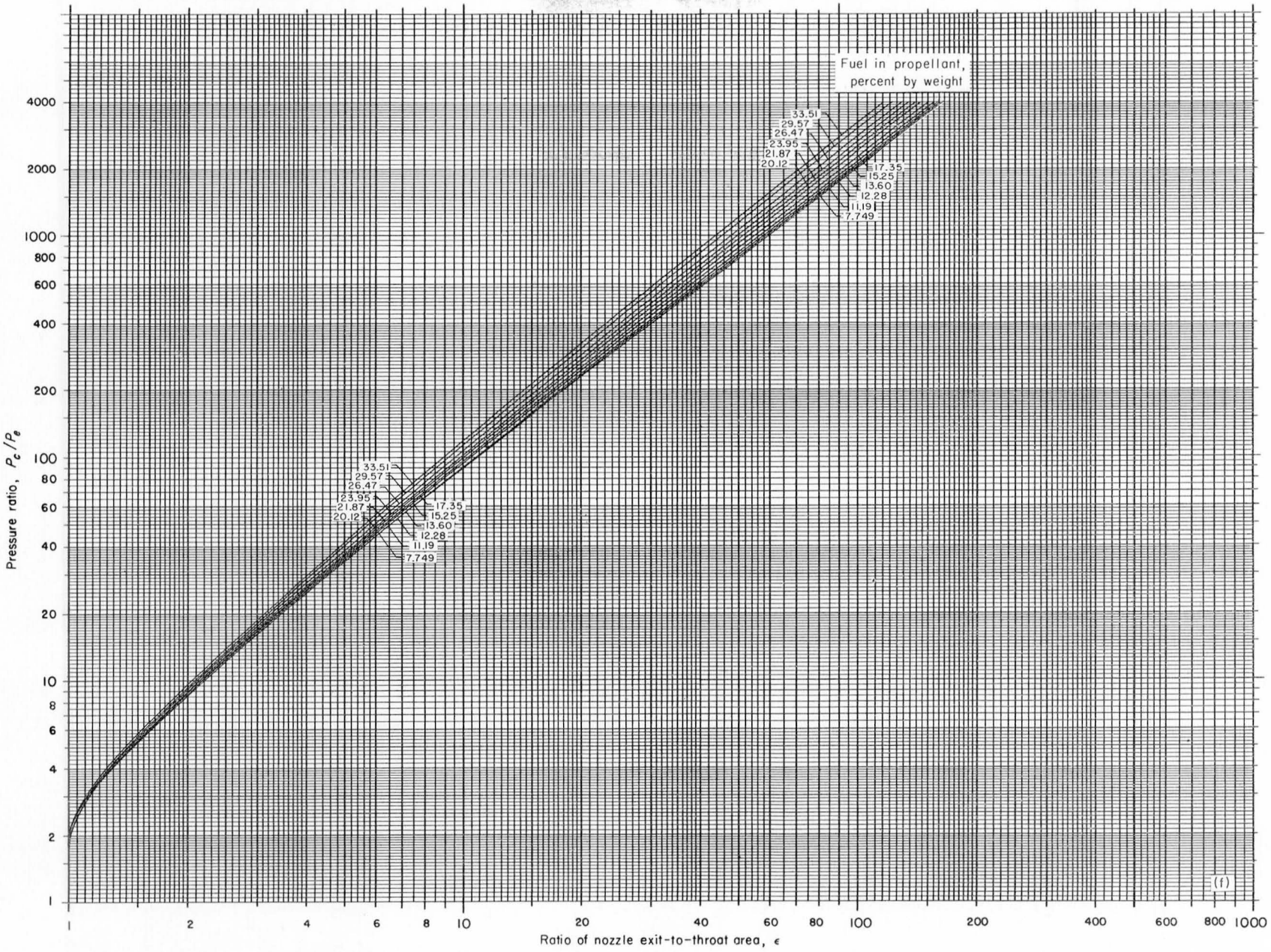

(f) Chamber pressure, 60 pounds per square inch absolute; frozen composition during isentropic expansion to area ratio indicated.

FIGURE 5.—Continued. Theoretical ratio of combustion-chamber to nozzle-exit pressure of liquid hydrogen and liquid oxygen.

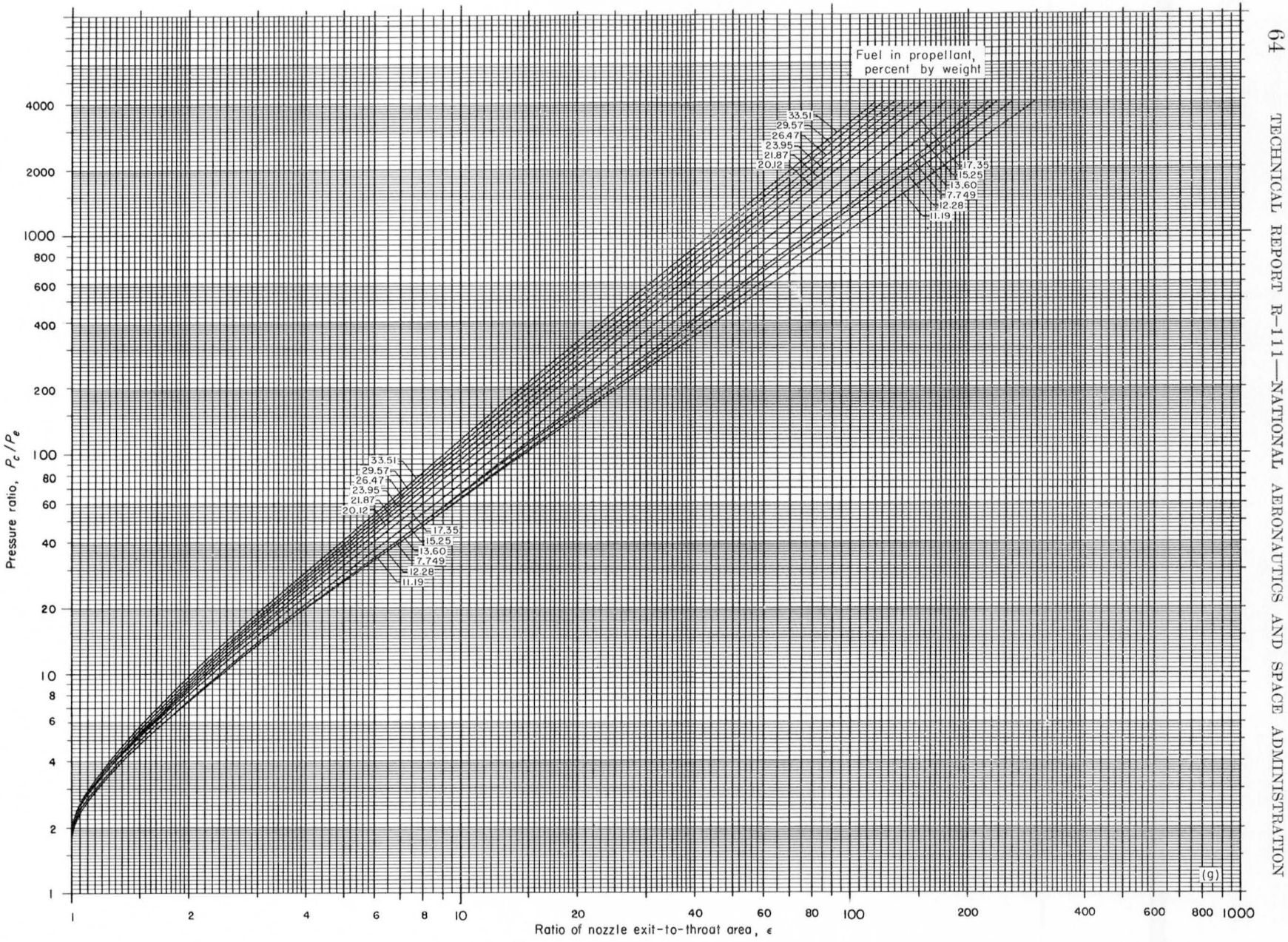

(g) Chamber pressure, 150 pounds per square inch absolute; equilibrium composition during isentropic expansion to area ratio indicated.

FIGURE 5.—Continued. Theoretical ratio of combustion-chamber to nozzle-exit pressure of liquid hydrogen and liquid oxygen.

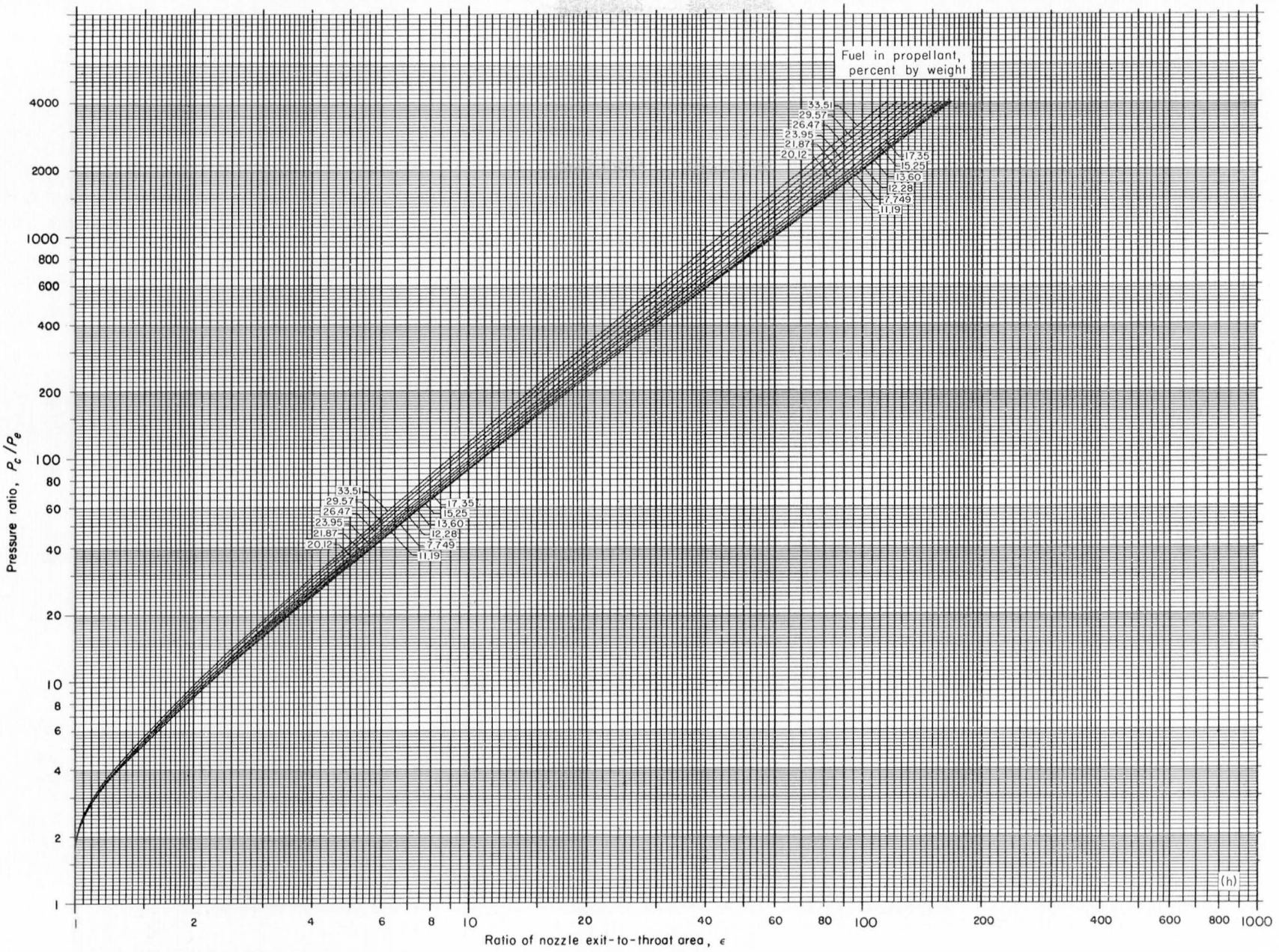

(h) Chamber pressure, 150 pounds per square inch absolute; frozen composition during isentropic expansion to area ratio indicated.

FIGURE 5.—Continued. Theoretical ratio of combustion-chamber to nozzle-exit pressure of liquid hydrogen and liquid oxygen.

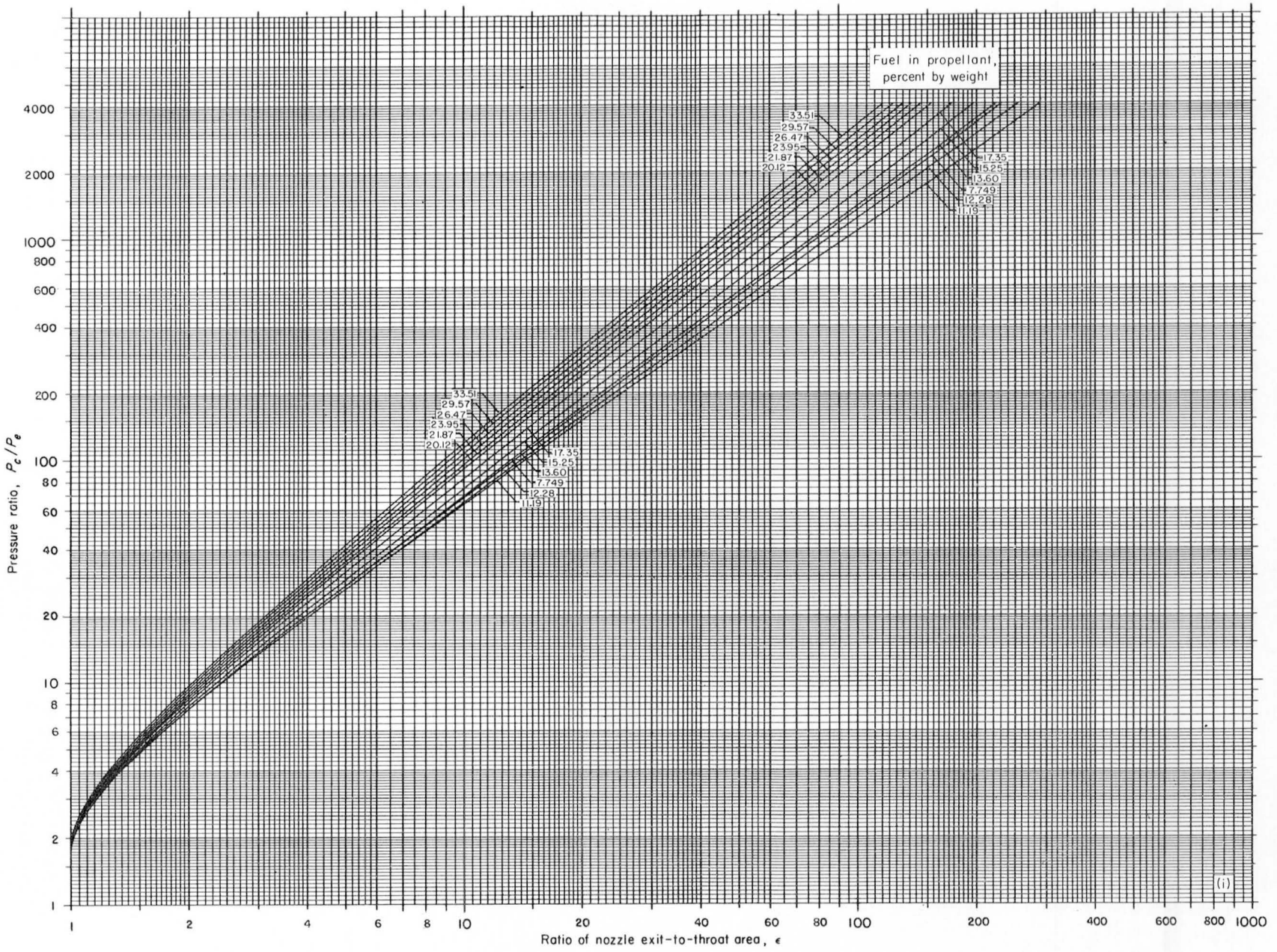

(i) Chamber pressure, 300 pounds per square inch absolute; equilibrium composition during isentropic expansion to area ratio indicated.

FIGURE 5.—Continued. Theoretical ratio of combustion-chamber to nozzle-exit pressure of liquid hydrogen and liquid oxygen.

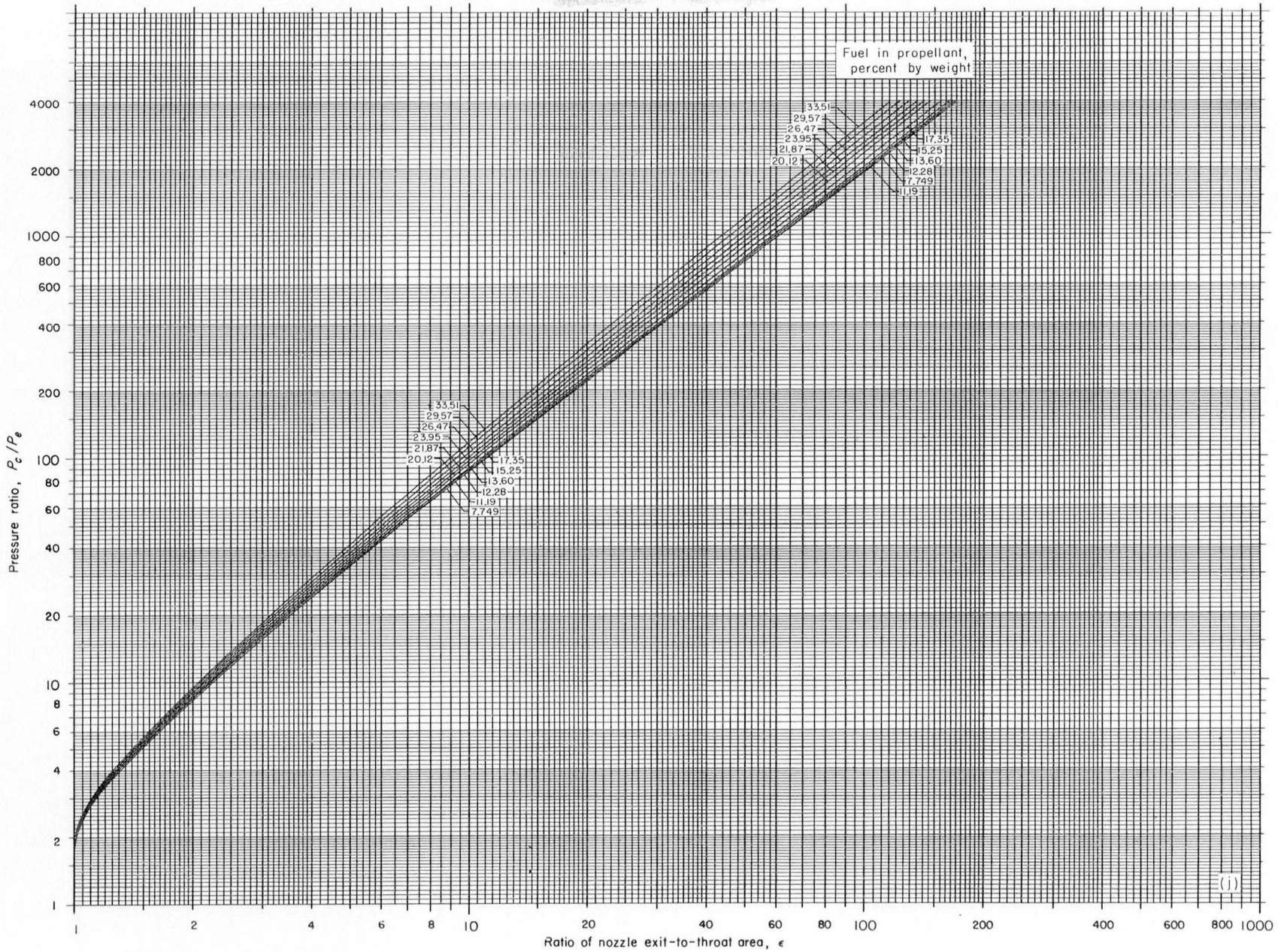

(j) Chamber pressure, 300 pounds per square inch absolute; frozen composition during isentropic expansion to area ratio indicated.

FIGURE 5.—Continued. Theoretical ratio of combustion-chamber to nozzle-exit pressure of liquid hydrogen and liquid oxygen.

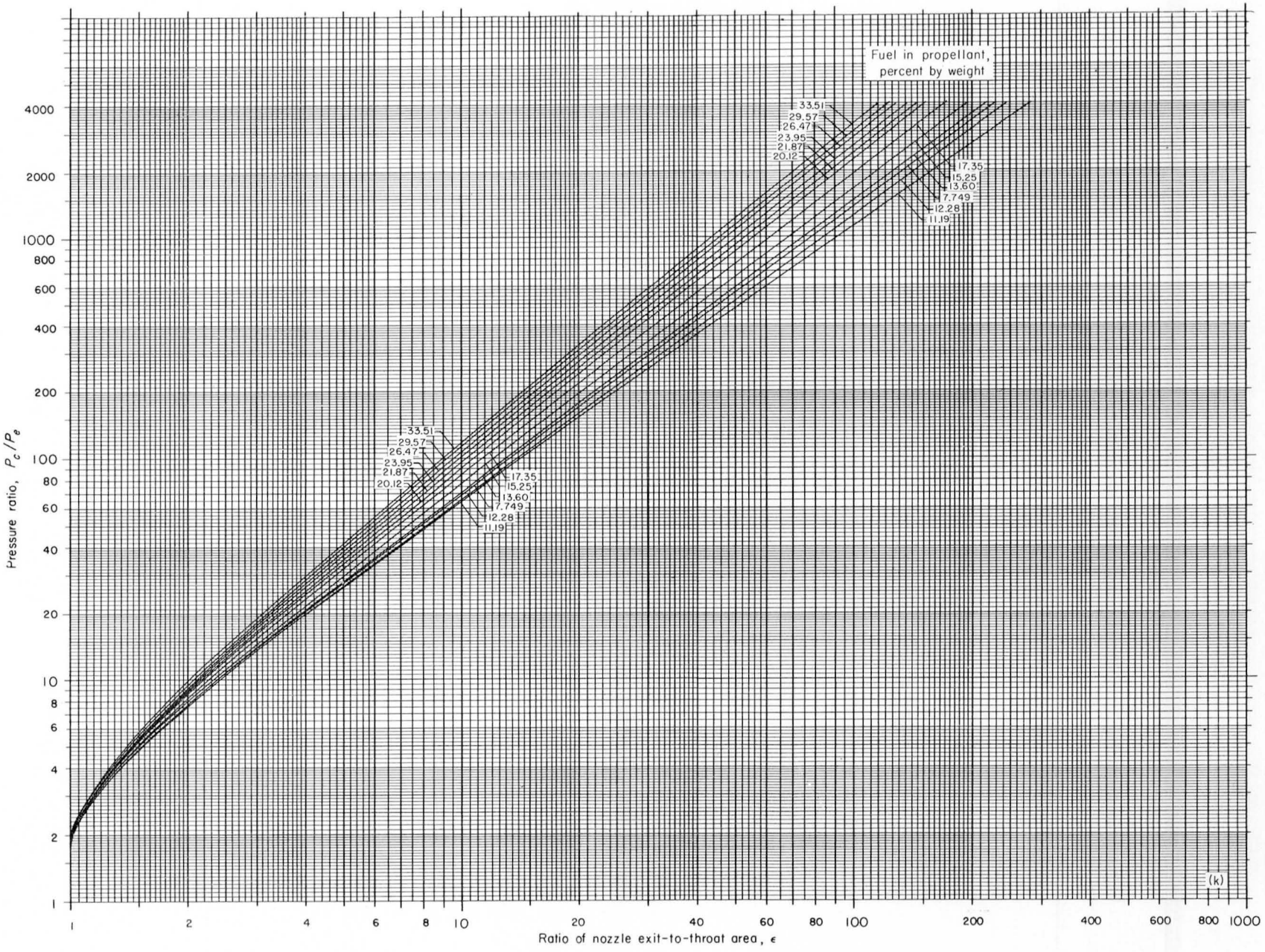

(k) Chamber pressure, 600 pounds per square inch absolute; equilibrium composition during isentropic expansion to area ratio indicated.

FIGURE 5.—Continued. Theoretical ratio of combustion-chamber to nozzle-exit pressure of liquid hydrogen and liquid oxygen.

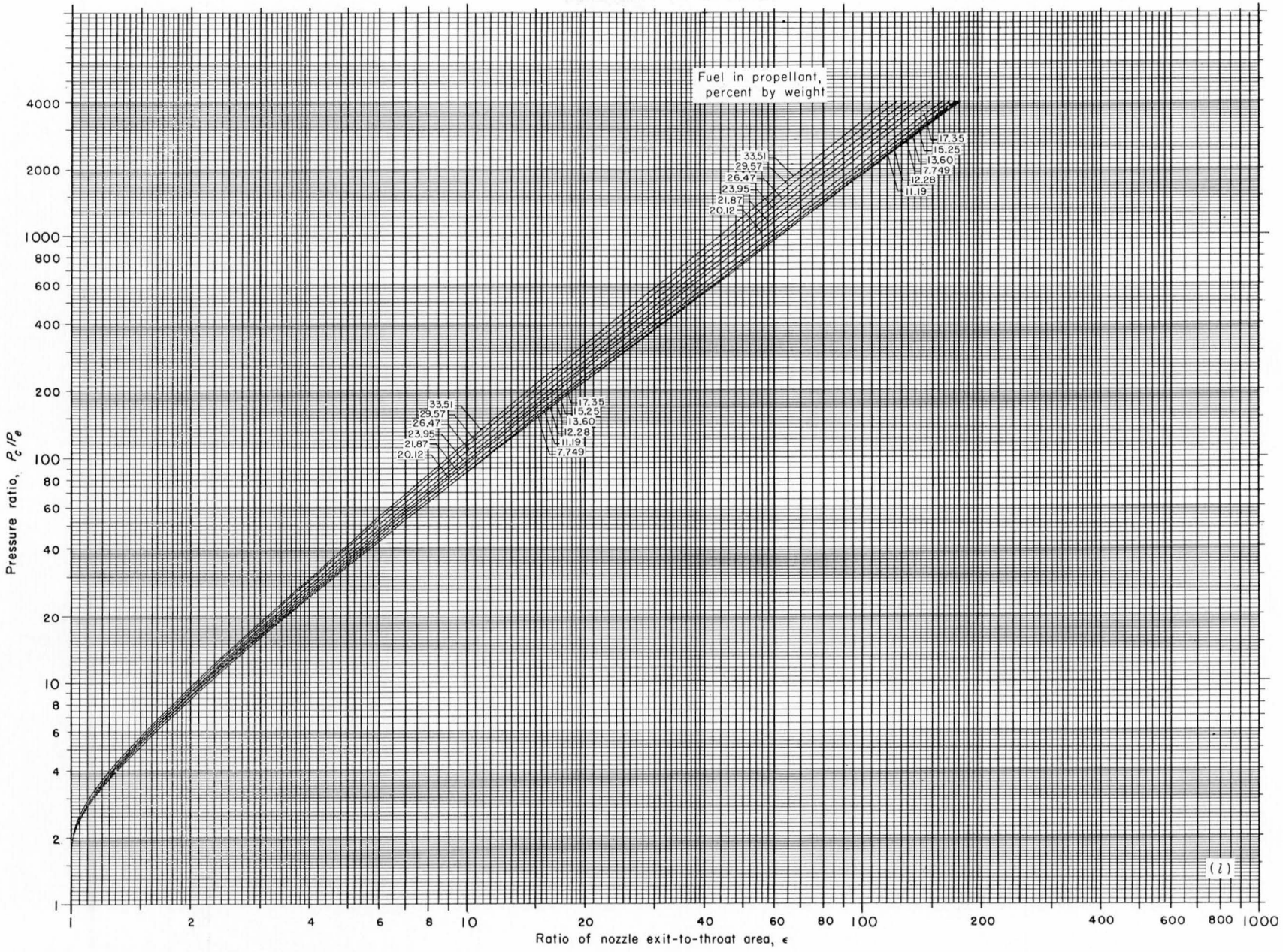

(l) Chamber pressure, 600 pounds per square inch absolute; frozen composition during isentropic expansion to area ratio indicated.

FIGURE 5.—Continued. Theoretical ratio of combustion-chamber to nozzle-exit pressure of liquid hydrogen and liquid oxygen.

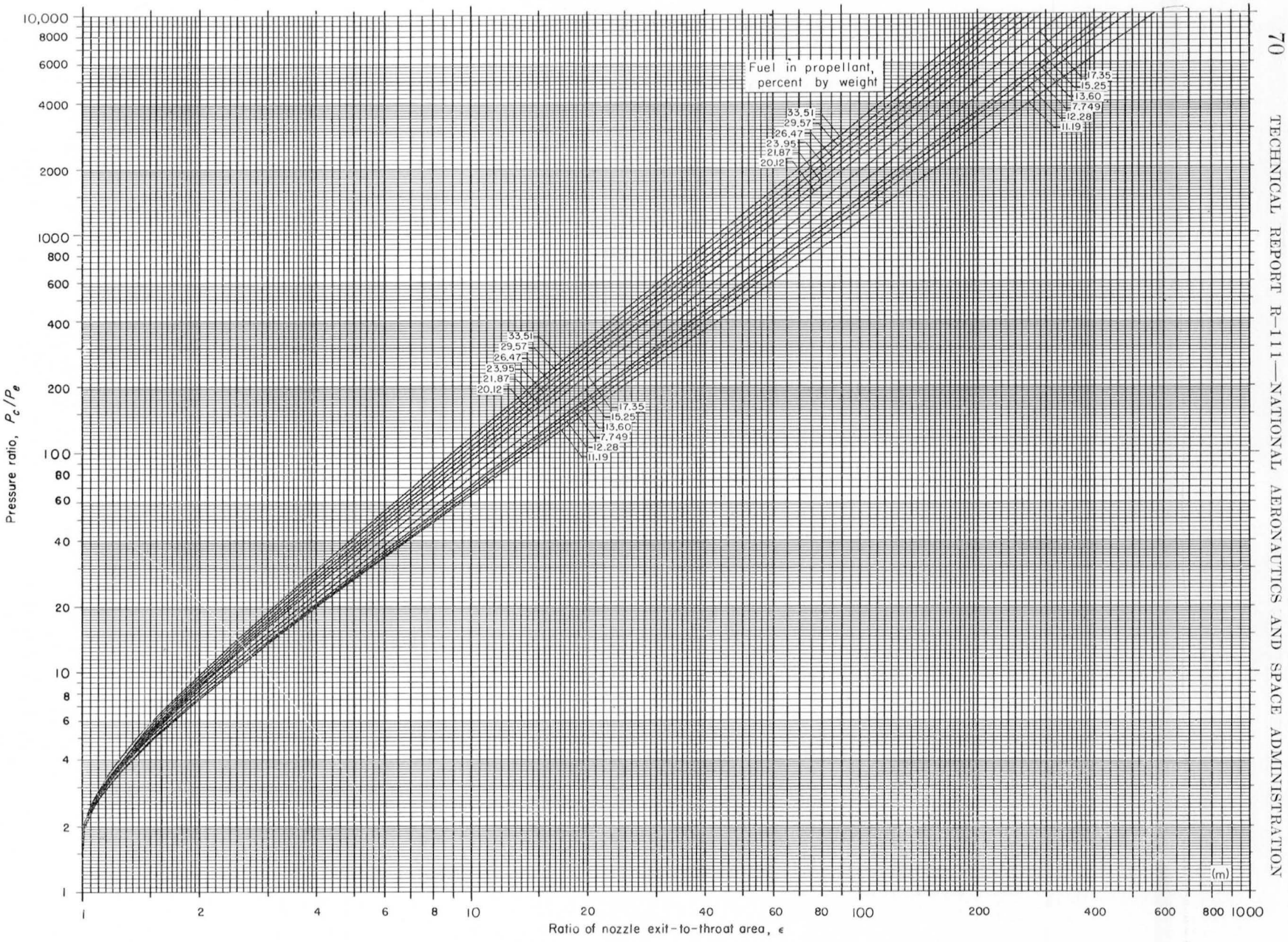

(m) Chamber pressure, 900 pounds per square inch absolute; equilibrium composition during isentropic expansion to area ratio indicated.

FIGURE 5.—Continued. Theoretical ratio of combustion-chamber to nozzle-exit pressure of liquid hydrogen and liquid oxygen.

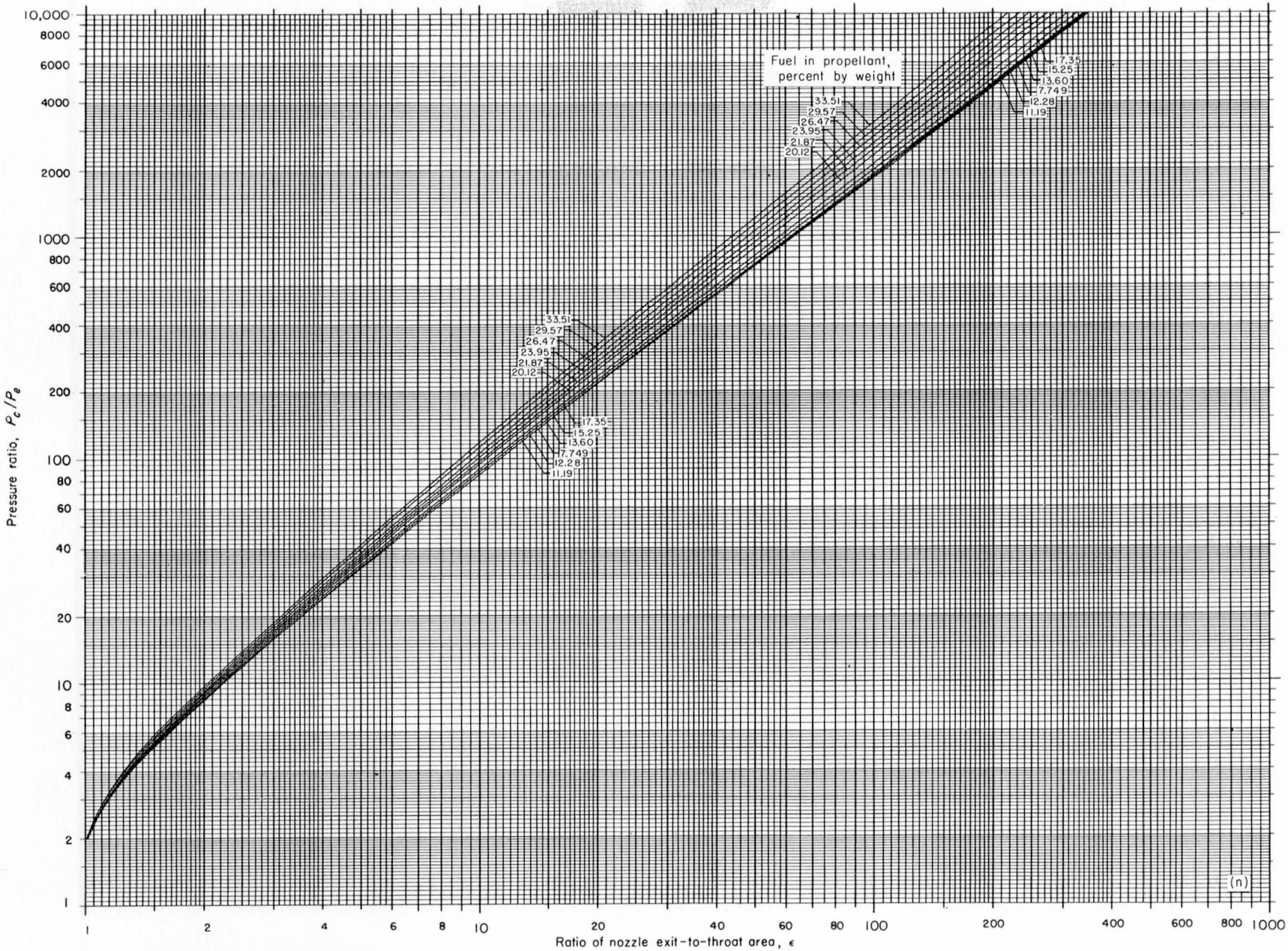

(n) Chamber pressure, 900 pounds per square inch absolute; frozen composition during isentropic expansion to area ratio indicated.

FIGURE 5.—Continued. Theoretical ratio of combustion-chamber to nozzle-exit pressure of liquid hydrogen and liquid oxygen.

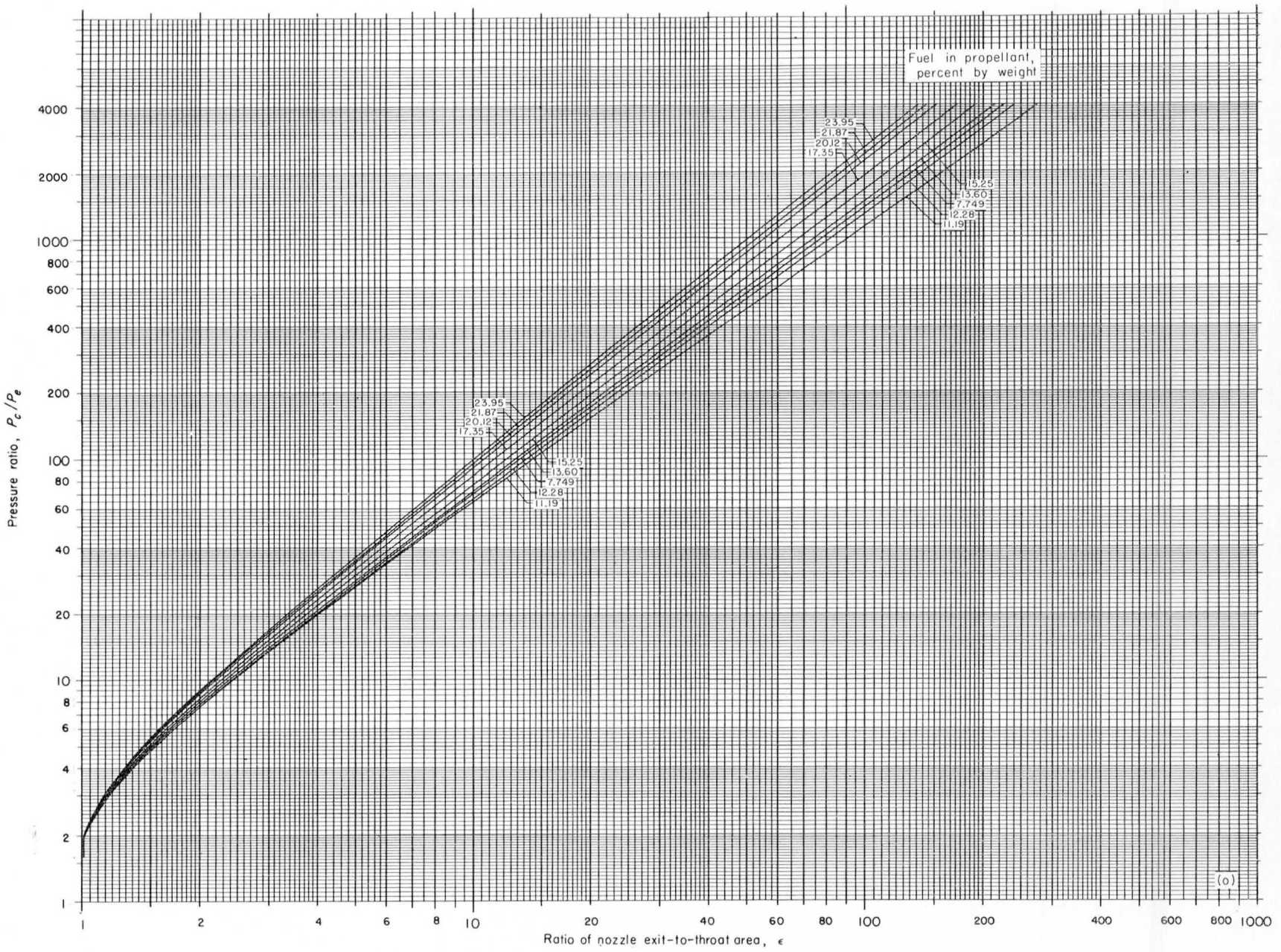

(o) Chamber pressure, 1200 pounds per square inch absolute; equilibrium composition during isentropic expansion to area ratio indicated.

FIGURE 5.—Continued. Theoretical ratio of combustion-chamber to nozzle-exit pressure of liquid hydrogen and liquid oxygen.

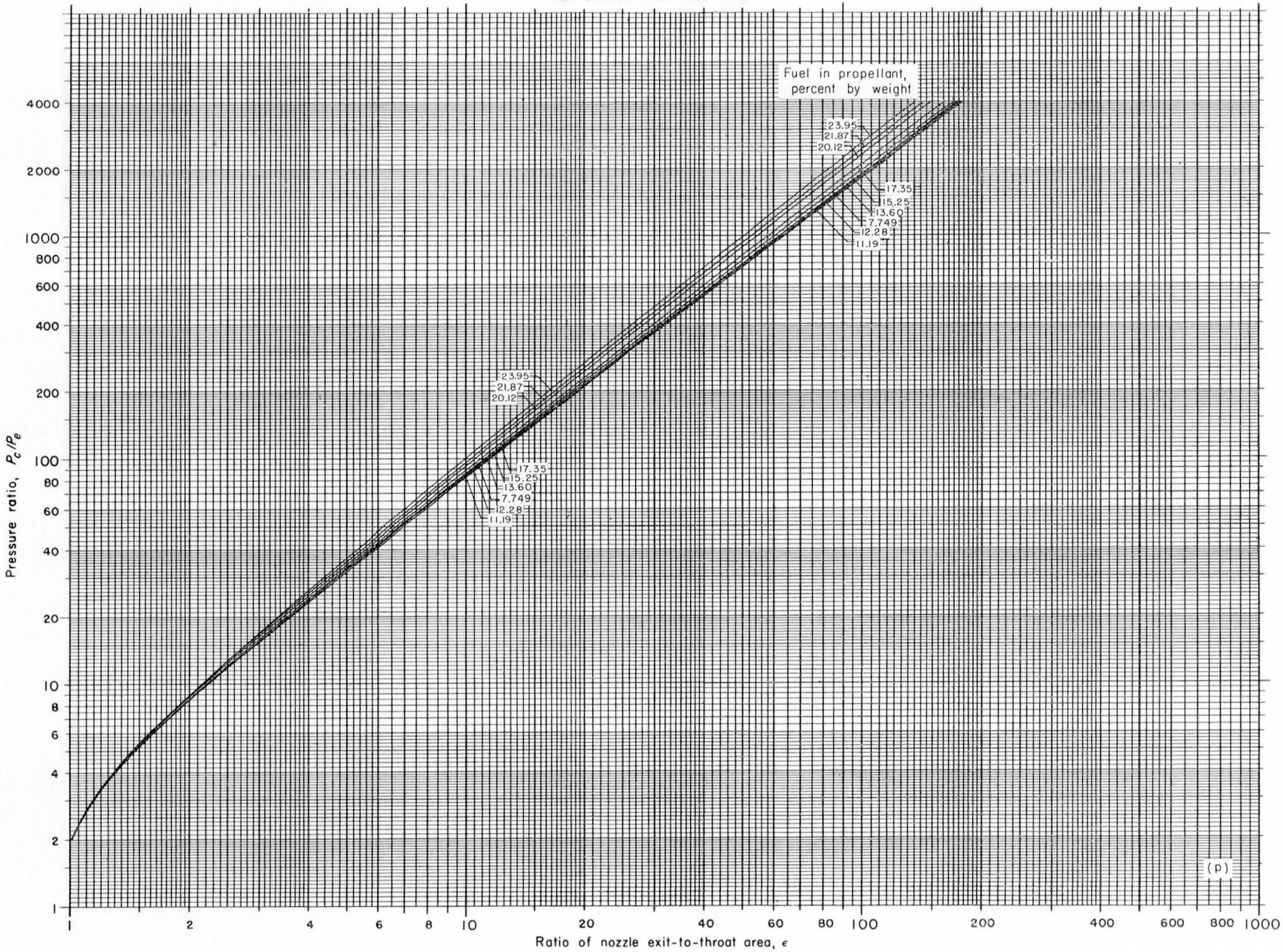

(p) Chamber pressure, 1200 pounds per square inch absolute; frozen composition during isentropic expansion to area ratio indicated.

FIGURE 5.—Concluded. Theoretical ratio of combustion-chamber to nozzle-exit pressure of liquid hydrogen and liquid oxygen.

Request Form

Please send the complete set of 66 working charts for figures 1 to 5 from NASA TR R–111.

(Name of organization)

(Street number)

(City and State)

Attention: Mr. ----------

Title ----------

(Address the request form to—

Office of Scientific and Technical Information—Code AFS

National Aeronautics and Space Administration

1520 H Street NW., Washington 25, D.C.)

U.S. GOVERNMENT PRINTING OFFICE: 1962

NASA TR R-111
National Aeronautics and Space Administration.
THEORETICAL PERFORMANCE OF HYDROGEN-OXYGEN ROCKET THRUST CHAMBERS. Gilbert K. Sievers, William A. Tomazic, and George R. Kinney. 1961. i, 75 p. diagrs., tabs. GPO price 65 cents. (NASA TECHNICAL REPORT R-111.)

Data are presented for liquid-hydrogen—liquid-oxygen thrust chambers at chamber pressures from 15 to 1200 pounds per square inch absolute, area ratios to approximately 300, and percent fuel from about 8 to 34 for both equilibrium and frozen composition during expansion. Specific impulse in vacuum, specific impulse, combustion-chamber temperature, nozzle-exit temperature, characteristic velocity, and the ratio of chamber-to-nozzle-exit pressure are included. The data are presented in convenient graphical forms to allow quick calculation of theoretical nozzle performance with over- or underexpansion, flow separation, and introduction of the propellants at various initial conditions or heat loss from the combustion chamber.

(Initial NASA distribution: 39, Propulsion systems, liquid-fuel rockets; 44, Propulsion systems, theory.)
Copies obtainable from Supt. of Docs., GPO, Washington

I. Sievers, Gilbert K.
II. Tomazic, William A.
III. Kinney, George R.
IV. NASA TR R-111

NASA

NASA TR R-111
National Aeronautics and Space Administration.
THEORETICAL PERFORMANCE OF HYDROGEN-OXYGEN ROCKET THRUST CHAMBERS. Gilbert K. Sievers, William A. Tomazic, and George R. Kinney. 1961. i, 75 p. diagrs., tabs. GPO price 65 cents. (NASA TECHNICAL REPORT R-111.)

Data are presented for liquid-hydrogen—liquid-oxygen thrust chambers at chamber pressures from 15 to 1200 pounds per square inch absolute, area ratios to approximately 300, and percent fuel from about 8 to 34 for both equilibrium and frozen composition during expansion. Specific impulse in vacuum, specific impulse, combustion-chamber temperature, nozzle-exit temperature, characteristic velocity, and the ratio of chamber-to-nozzle-exit pressure are included. The data are presented in convenient graphical forms to allow quick calculation of theoretical nozzle performance with over- or underexpansion, flow separation, and introduction of the propellants at various initial conditions or heat loss from the combustion chamber.

(Initial NASA distribution: 39, Propulsion systems, liquid-fuel rockets; 44, Propulsion systems, theory.)
Copies obtainable from Supt. of Docs., GPO, Washington

I. Sievers, Gilbert K.
II. Tomazic, William A.
III. Kinney, George R.
IV. NASA TR R-111

NASA

NASA TR R-111
National Aeronautics and Space Administration.
THEORETICAL PERFORMANCE OF HYDROGEN-OXYGEN ROCKET THRUST CHAMBERS. Gilbert K. Sievers, William A. Tomazic, and George R. Kinney. 1961. i, 75 p. diagrs., tabs. GPO price 65 cents. (NASA TECHNICAL REPORT R-111.)

Data are presented for liquid-hydrogen—liquid-oxygen thrust chambers at chamber pressures from 15 to 1200 pounds per square inch absolute, area ratios to approximately 300, and percent fuel from about 8 to 34 for both equilibrium and frozen composition during expansion. Specific impulse in vacuum, specific impulse, combustion-chamber temperature, nozzle-exit temperature, characteristic velocity, and the ratio of chamber-to-nozzle-exit pressure are included. The data are presented in convenient graphical forms to allow quick calculation of theoretical nozzle performance with over- or underexpansion, flow separation, and introduction of the propellants at various initial conditions or heat loss from the combustion chamber.

(Initial NASA distribution: 39, Propulsion systems, liquid-fuel rockets; 44, Propulsion systems, theory.)
Copies obtainable from Supt. of Docs., GPO, Washington

I. Sievers, Gilbert K.
II. Tomazic, William A.
III. Kinney, George R.
IV. NASA TR R-111

NASA